AFML-TR-71-237

FINAL REPORT ON JOINING TECHNIQUES FOR FABRICATION OF HIGH-TEMPERATURE SUPERALLOY BLADES

C. G. NESSLER
Pratt & Whitney Aircraft
Division of United Aircraft Corporation

TECHNICAL REPORT AFML-TR-71-237
DECEMBER 1971

APPROVED FOR PUBLIC RELEASE; DISTRIBUTION UNLIMITED

AIR FORCE MATERIALS LABORATORY
AIR FORCE SYSTEMS COMMAND
WRIGHT-PATTERSON AIR FORCE BASE, OHIO

NOTICE

When Government drawings, specifications, or other data are used for any purpose other than in connection with a definitely related Government procurement operation, the United States Government thereby incurs no responsibility nor any obligation whatsoever; and the fact that the government may have formulated, furnished, or in any way supplied the said drawings, specifications, or other data, is not to be regarded by implication or otherwise as in any manner licensing the holder or any other person or corporation, or conveying any rights or permission to manufacture, use, or sell any patented invention that may in any way be related thereto.

Copies of this report should not be returned unless return is required by security considerations, contractual obligations, or notice on a specific document.

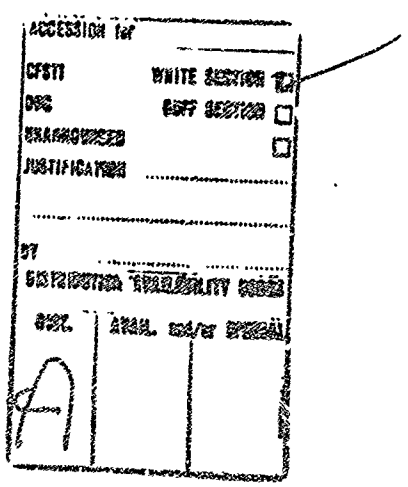

UNCLASSIFIED

Security Classification

DOCUMENT CONTROL DATA - R & D

(Security classification of title, body of abstract and indexing annotation must be entered when the overall report is classified)

1. ORIGINATING ACTIVITY (Corporate author) Pratt & Whitney Aircraft Division of United Aircraft Corporation East Hartford, Connecticut 06108	2a. REPORT SECURITY CLASSIFICATION UNCLASSIFIED 2b. GROUP

3. REPORT TITLE

FINAL REPORT ON JOINING TECHNIQUES FOR FABRICATION OF HIGH-TEMPERATURE SUPERALLOY BLADES

4. DESCRIPTIVE NOTES (Type of report and inclusive dates)

Final Report

5. AUTHOR(S) (First name, middle initial, last name)

C. G. Nessler

6. REPORT DATE	7a. TOTAL NO. OF PAGES	7b. NO. OF REFS
December 1971	126	2

8a. CONTRACT OR GRANT NO	9a. ORIGINATOR'S REPORT NUMBER(S)
F33615-70-C-1784 b. PROJECT NO. OM-1505/7351 c. d.	PWA-4333 9b. OTHER REPORT NO(S) (Any other numbers that may be assigned this report) AFML-TR-71-237

10. DISTRIBUTION STATEMENT

Approved for public release; distribution unlimited.

11. SUPPLEMENTARY NOTES	12. SPONSORING MILITARY ACTIVITY
Copies of this report should not be returned unless return is required by security considerations, contractual obligations, or notice on a specific document.	Air Force Materials Laboratory Wright-Patterson Air Force Base, Ohio 45433

13. ABSTRACT

Three diffusion welding systems were evaluated for applicability to the fabrication of advanced design air-cooled gas turbine blades from split halves. The joining systems evaluated were based upon the use of interlayers to promote and enhance diffusion welding of the directionally solidified superalloy (modification of MARM-200) used for this program. Particular emphasis was placed on increasing the ability of the joining systems to accommodate lack of fit which is a major concern in diffusion welding complex-shaped hollow parts.

The three systems, an electroplated nickel-cobalt alloy interlayer, a nickel-cobalt-tungsten-chromium dispersion electroplated interlayer, and thin foil intermediaries were first evaluated on test specimens using metallography, microprobe analysis, and selective shear testing. Typically, parts were welded under pressure of 1000 psi or greater at 2200°F for up to four hours. It was found that nickel-cobalt interlayers up to 0.5 mils thick per side were usable, with the most successful interlayer composition being nickel 20 percent cobalt. Dispersion electroplated interlayers resulted in inferior joints due to the inherent inclusion of electrolyte in the plating. Thick nickel-cobalt interlayers and foil intermediaries were found to be effective in accommodating lack of fit between faying surfaces.

Tensile testing at 1400°F and 1800°F indicated properties in the range of 80-90 percent of base metal for 0.2 and 0.5 mil interlayer and foil intermediary joints. Stress rupture testing indicated that the former two systems were above 70 percent of the base metal minimum. Foil intermediary joint stress rupture properties were poor due to the choice of foil composition. Specimen cycling between 1800°F and 70°F indicated that the thermal fatigue strength of 0.2 mil interlayer joints was good; 0.5 mil interlayer joints were somewhat inferior.

To broadly demonstrate the applicability of the diffusion welding method to actual hardware, thirteen blades were fabricated in the third phase of the program. Un-machined as-cast blade halves prepared by grit blasting and electroplating were joined with and without foil intermediaries using cast ceramic dies. Selected airfoil segments were thermal fatigue tested. The results indicated that blades could be fabricated from split halves, however further work to refine joint and die design to avoid misalignment and parameter deviations are needed to reproducibly manufacture parts

DD FORM 1 NOV 68 1473 REPLACES DD FORM 1473, 1 JAN 64, WHICH IS OBSOLETE FOR ARMY USE.

UNCLASSIFIED

Security Classification

14. KEY WORDS	LINK A		LINK B		LINK C	
	ROLE	WT	ROLE	WT	ROLE	WT
Diffusion Welding						
Air-Cooled Gas Turbine Blades						
Joining Techniques						
Superalloy Split-Blade Fabrication						

AFML-TR-71-237

FINAL REPORT ON JOINING TECHNIQUES FOR FABRICATION OF HIGH-TEMPERATURE SUPERALLOY BLADES

C. G. NESSLER
Pratt & Whitney Aircraft
Division of United Aircraft Corporation

TECHNICAL REPORT AFML-TR-71-237
DECEMBER 1971

AIR FORCE MATERIALS LABORATORY
AIR FORCE SYSTEMS COMMAND
WRIGHT-PATTERSON AIR FORCE BASE, OHIO

FOREWORD

This Final Report, designated by the contractor as Report PWA-4333, describes the work conducted during the period 1 July 1971 through 30 September 1971 by Pratt & Whitney Aircraft, East Hartford, Connecticut, under Contract No. F33615-70-C-1784, Project Number 7351, with the Air Force Systems Command, Aeronautical Systems Division, Wright-Patterson Air Force Base, Ohio.

The program was conducted under the technical direction of Dr. G. E. Metzger and Mr. L. D. Parsons, LLP, Air Force Materials Laboratory, Wright-Patterson Air Force Base. Mr. C. G. Nessler was program manager for Pratt & Whitney Aircraft. Pratt & Whitney personnel included Mr. G. P. Putnam who developed the electrochemical processes, Messrs. R. D. Eng and D. F. Paulonis who were responsible for metallurgical development and evaluation, and Mr. J. Scutnick who prepared and welded the parts.

This report is submitted 31 October 1971 and is in compliance with the requirements of Sequence Number B003 of the Contract Data Requirements List, DD Form 1423, attached to the above contract.

This technical report has been reviewed and is approved

I. Perlmutter
Chief, Metals Branch

ABSTRACT

Three diffusion welding systems were evaluated for applicability to the fabrication of advanced design air-cooled gas turbine blades from split halves. The joining systems evaluated were based upon the use of interlayers to promote and enhance diffusion welding of the directionally solidified superalloy (modification of MARM-200) used for this program. Particular emphasis was placed on increasing the ability of the joining systems to accommodate lack of fit which is a major concern in diffusion welding complex-shaped hollow parts.

The three systems, an electroplated nickel-cobalt alloy interlayer, a nickel-cobalt-tungsten-chromium dispersion electroplated interlayer, and thin foil intermediaries were first evaluated on test specimens using metallography, microprobe analysis, and selective shear testing. Typically, parts were welded under pressure of 1000 psi or greater at 2200°F for up to four hours. It was found that nickel-cobalt interlayers up to 0.5 mils thick per side were usable, with the most successful interlayer composition being nickel 20 percent cobalt. Dispersion electroplated interlayers resulted in inferior joints due to the inherent inclusion of electrolyte in the plating. Thick nickel-cobalt interlayers and foil intermediaries were found to be effective in accommodating lack of fit between faying surfaces.

Sporadic joint contamination was overcome by changes in both electroplating and surface preparation processes. There was some propensity for cracking in welded specimens made with thicker interlayers due to thermal stresses arising during heat treatment. However, through improved process control, cracking could be largely eliminated.

Tensile testing at 1400°F and 1800°F indicated properties in the range of 80-90 percent of base metal for 0.2 and 0.5 mil interlayer and foil intermediary joints. Stress rupture testing indicated that the former two systems were above 70 percent of the base metal minimum. Foil intermediary joint stress rupture properties were poor due to the choice of foil composition. Specimen cycling between 1800°F and 70°F indicated that the thermal fatigue strength of 0.2 mil interlayer joints was good; 0.5 mil interlayer joints were somewhat inferior.

To broadly demonstrate the applicability of the diffusion welding method to actual hardware, thirteen blades were fabricated in the third phase of the program. Un-machined as-cast blade halves prepared by grit blasting and electroplating were joined with and without foil intermediaries using cast ceramic dies. Selected airfoil segments were thermal fatigue tested. The results indicated that blades could be fabricated from split halves, however further work to refine joint and die design to avoid misalignment and parameter deviations are needed to reproducibly manufacture parts.

TABLE OF CONTENTS

TABLE OF CONTENTS (Cont'd)

LIST OF ILLUSTRATIONS

LIST OF ILLUSTRATIONS (Cont'd)

LIST OF ILLUSTRATIONS (Cont'd)

LIST OF ILLUSTRATIONS (Cont'd)

LIST OF ILLUSTRATIONS (Cont'd)

LIST OF ILLUSTRATIONS (Cont'd)

LIST OF TABLES

LIST OF TABLES (Cont'd)

I

INTRODUCTION

The objective of this program was to develop joining techniques for the fabrication of superalloy blades and vanes capable of operating at gas turbine inlet temperatures appreciably greater than 2500°F. Specifically, the program was oriented to the fabrication of hollow transpiration-cooled blades having cast or drilled holes in solid walls by diffusion welding cast blade halves. Emphasis was placed on the joining aspect rather than associated problems such as material development, casting, or machining.

A. SELECTION OF BLADE DESIGN

A hollow airfoil with drilled or cast holes was chosen over alternative transpiration-cooled structures such as laminated sheet or woven wire because it offers the best combination of service durability and performance. This design selection was previously made and demonstrated in advanced turbine engines. When such a blade is fabricated by mating split concave and convex blade halves parted along the leading and trailing edge, the following advantages are realized:

- Closer wall thickness control (elimination of core shift or print).
- Greater freedom in cooling passage design (no core thickness requirement).
- Elimination of core leaching and attendant grain boundary penetration hazards.
- Opportunity to improve hole drilling efficiency by laser or electron beam techniques, or development of cast holes.
- Growth opportunity to use other material forms such as forgings or powder metals.

B. SELECTION OF MATERIAL

The material selected for the fabrication of split blades was PWA 1422, a directionally-solidified cast nickel alloy exhibiting superior performance in advanced gas turbine engines. This material is currently used for hollow transpiration cooled blades in development engines having turbine inlet temperatures exceeding 2500°F. PWA 1422 has essentially the composition of MARM-200 with the addition of two percent hafnium. MARM-200, a nickel base superalloy first introduced in 1959, exhibits high elevated temperature strength but poor ductility. In 1964, Pratt & Whitney Aircraft applied directional solidification to this alloy to eliminate grain boundaries perpendicular to the direction of principal stress, providing a strong and ductile material for turbine blades and vanes. Subsequently, the addition of hafnium to the directionally solidified alloy to improve transverse ductility led to the development of PWA 1422.

C. SELECTION OF JOINING METHOD

To achieve the advantages of split blade construction the joining system selected should have the following characteristics:

- Produces physical and chemical homogeneity within the part.
- Gives reliable and reproducible properties.
- Accommodates significant lack of fit.
- Permits dimensional control.
- Applicable to varied joint geometries.
- Provides reasonable cost and processing time.

All nickel alloys similar to PWA 1422 present challenges to the development of joining systems because of the very properties which make them desirable for gas turbine applications. Among these characteristics are the ability to form stable oxides and surface compounds, complex metallurgical strengthening mechanisms, and high creep resistance. In split blades the joint contour and cross section is often irregular or discontinuous, in addition to being inaccessible from the exterior surface.

Solid state diffusion welding was chosen as the most promising method for joining PWA 1422 nickel superalloy. Fusion welding appears to inherently lead to heat-affected zone cracking, and was inapplicable to the joint design. Solid state diffusion bonding was chosen over depressed melting point interlayer systems for several reasons: the current state of the art of the former appeared to offer more promise, the need for dies to bring the complex faying surfaces into contact was seen to be implicit, and; potentially deleterious concentrations of melting point depressant (e.g. boron) in thin wall trailing edge sections was avoided.

Based on prior experience with Udimet 700, the use of thin nickel-cobalt interlayers was shown to improve the homogeneity of diffusion welds and produce good properties*. This prior success led to the investigation of the nickel-cobalt system for PWA-1422 with particular emphasis on the problems of joining real parts.

The terminology used in this report is based upon American Welding Society Terms and Definitions. However, because of the rapid current development of diffusion welding processes, it becomes necessary to utilize new terms which are more descriptive or specific. The following two terms are used:

1) *interlayer - a material applied to either or both faying surfaces.*

2) *intermediary - a separate material interposed between, but unattached to, the faying surfaces.*

---

* United States Patent Number 3,530,568

In this program all interlayers were applied by electroplating to provide a ductile surface and prevent the formation of deleterious compounds; all intermediaries were thin foils utilized to promote contact between unfitting faying surfaces.

D. APPROACH

The program was conducted in three sequential phases as shown in Figure 1. Phase IA was directed at interlayer and intermediary development and determination of welding parameters through metallography. Phase IB involved shear testing of selected joints from Phase IA. The best joints from Phase I were tested during Phase II to determine tensile, stress rupture, and thermal fatigue strengths. During Phase III the application of the better systems to an actual blade were accomplished, and the joint fit accommodation and thermal fatigue resistance were evaluated.

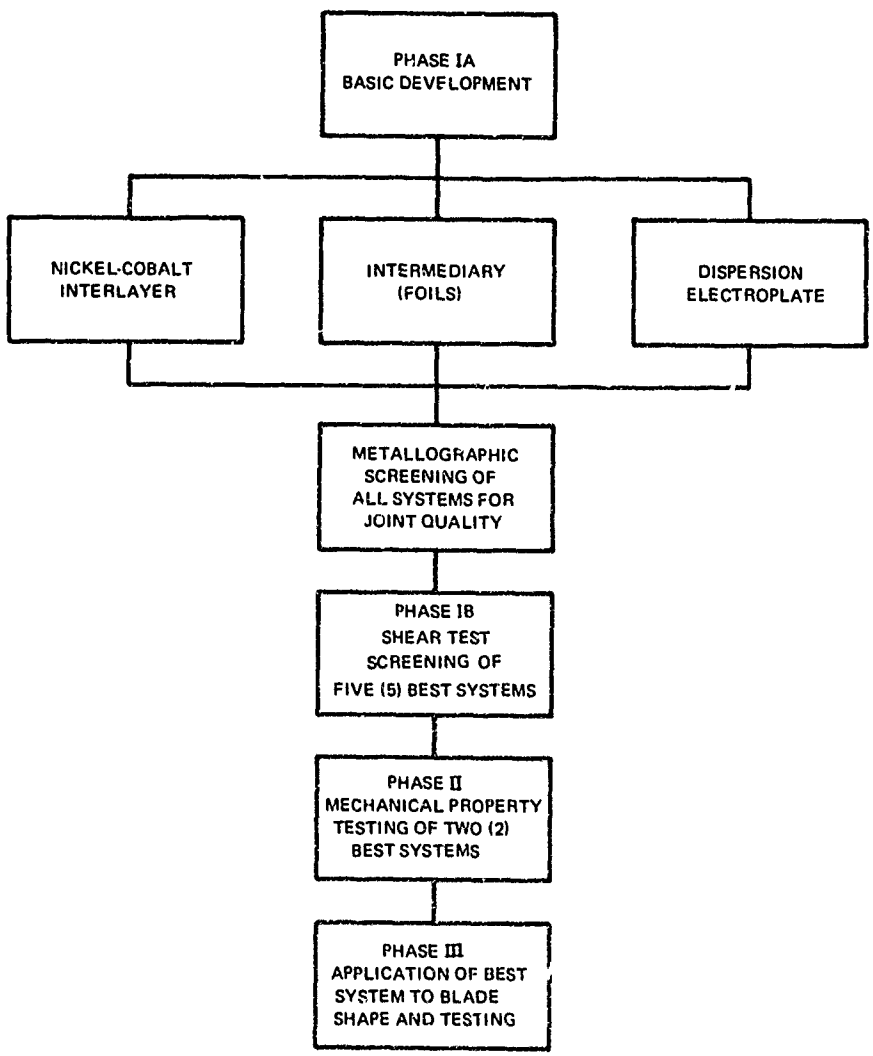

Figure 1 Summary Flow Chart of Superalloy Joining Development

II

PHASE IA – ELECTROPLATING AND INTERMEDIARY DEVELOPMENT

Previous experience in welding Udimet 700 material had shown that, if homogeneity in the joint was to be achieved, the interlayer thickness was limited to 0.1-0.2 mils. Since it was foreseeable that split halves, whether as-cast or machined, would have a lack of fit greater than this, the development program sought to determine means in which the useful interlayer thickness could be increased with the retention of good properties. To this end the following three systems were evaluated:

- Electroplated nickel-cobalt interlayers - determination of the interrelation of composition and thickness, and of welding parameters useful for the maximum thickness.
- Dispersion electroplated interlayers - incorporation of slow diffusing element particles into a nickel-cobalt interlayer to extend its useful thickness.
- Ductile metal foil intermediaries - the interposition of a third element, a thin alloy foil, between the faying surfaces in conjunction with a thin nickel-cobalt interlayer.

A. NICKEL-COBALT ELECTROPLATING

Smooth controlled-composition nickel-cobalt interlayers of varying thickness were required for the experimental program. Although sulfamate baths are commonly used for nickel-cobalt alloy plating, prior experience indicated that a sulfate bath was necessary for compatability with dispersion plating. Therefore, a sulfate bath was utilized from the outset.

The general setup for nickel-cobalt electroplating is shown schematically in Figure 2. Proportioning the total anode current between the separate nickel and cobalt anodes controls the corrosion rate of each anode which maintains the nickel-cobalt equilibrium ratios in the bath; deposition rate on the cathode is determined by the total current.

Although past experience indicated it was desirable to have relatively high metal ion concentrations which permit high current densities, when concentrations of metal ion normality 2.0 and 1.33 were tested the solutions tended to precipitate salts during room temperature storage or during use if the pH fluctuated.

Satisfactory results were obtained from a 1.0 N solution (Table I) which had proportionately increased ammonium chloride and boric acid content to improve anode corrosion and aid pH stability. The nickel-cobalt ratio of the deposit was controlled by varying the nickel-cobalt ratio in solution within the 29.4 grams per liter total metal content. The ratio in solution was maintained by splitting the anode current appropriately between the soluble nickel and cobalt anodes. Current was controlled by electronic constant current controls. Thickness was controlled by monitoring the current and time with a known deposition rate. A current density of 30 amperes per square foot gave an acceptable deposition rate with adequate uniformity of thickness and composition control.

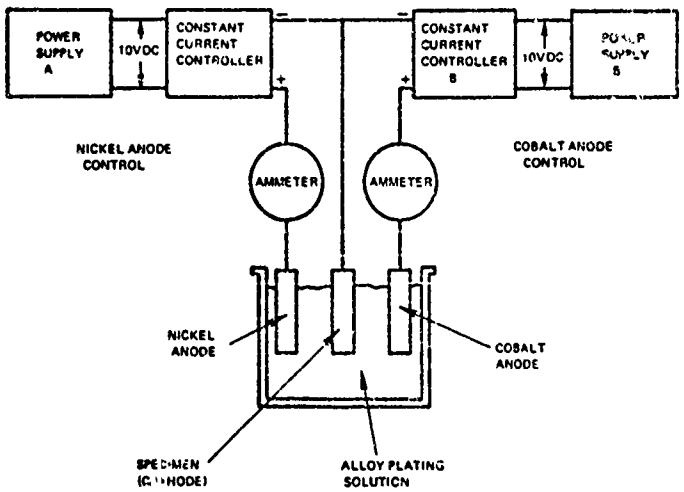

Figure 2 Electroplating Schematic Diagram

TABLE I

TYPICAL ELECTROPLATING BATH COMPOSITION

Normality (in metal content)	1.0
Nickel & Cobalt Metal (as sulfates)	29.4 grams/liter
Ammonium Chloride (NH_4Cl)	27.0 grams/liter
Boric Acid (H_3BO_3)	27.0 grams/liter
pH Range (electrometric)	4.5-5.0
Temperature Range	120 ± 2°F
Current Density	30 amps/ft^2

A three-liter bath was operated with varying nickel and cobalt ratios to establish the relation (see Figure 3) between the nickel-cobalt balance in the bath with that resulting in the electroplate. Metallic plate specimens were analyzed by atomic absorption and bath compositions by wet chemistry.

Commercial nickel anodes and cast cobalt anodes were used in the electroplating process. The conventional use of bagged electrodes was avoided since these were known to become packed with fine particles during dispersion plating. The cast cobalt anodes corroded non-uniformly and liberated undesirable particulate corrosion products into the bath. Since the contamination of the bath was a gradual process it was tolerated and easily controlled by the periodic filtration. Chloride content of the bath was increased to alleviate the problem.

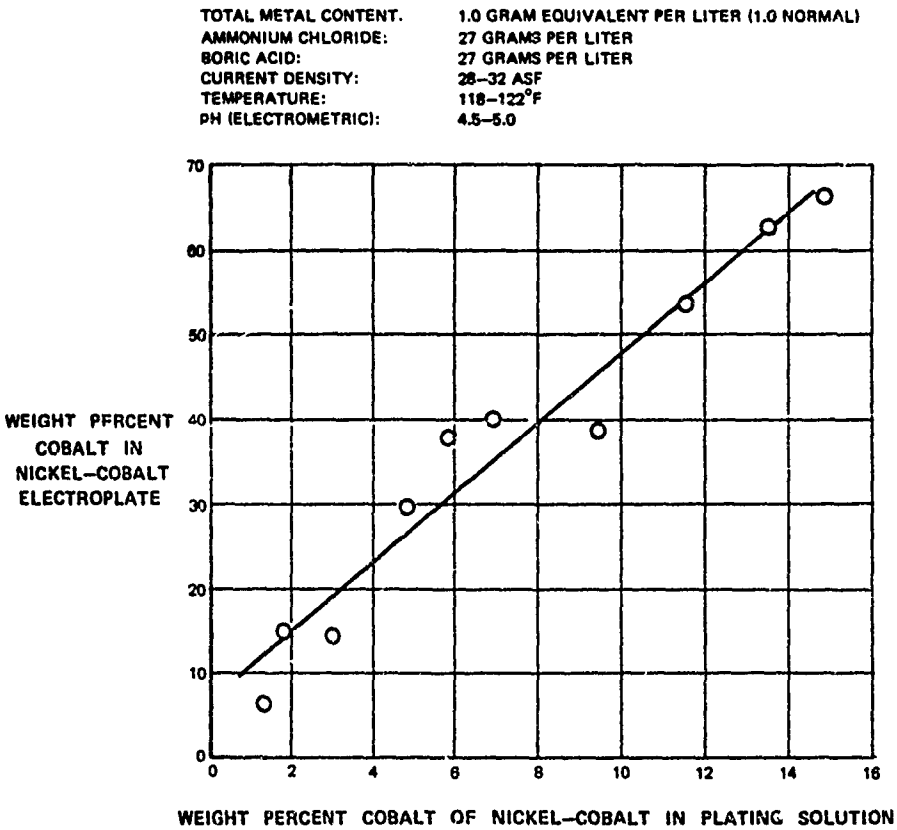

Figure 3 Electroplating Curve Showing Plating Composition as a Function of Bath Composition

1. Electroplating Procedure

The plating procedure used to deposit nickel-cobalt alloy on PWA-1422 material is shown in Figure 4. After mechanical preparation, a standard alkaline-cyanide cleaning step was used to remove minor amounts of surface contaminants from the part. The surface was activated (exposure of fresh metal) in a commercial sulfate fluoride, acid salt, anodic etch. A subsequent water-air blast was used to remove the trace amounts of dark film (smut) which formed on the etched surfaces. Approximately twenty millionths of an inch of nickel were immediately deposited on the freshly activated surface with a Wood's nickel strike to enhance the bond between the electroplating and the part. Nickel-cobalt electroplating was started within thirty seconds to avoid passivation of the nickel strike.

Preplating procedure was experimentally varied to ascertain possible causes of joint contamination. This is discussed as part of the nickel-cobalt interlayer diffusion welding results.

2. Control of Electroplating Parameters

By monitoring plating time at a constant current density of 30 amperes the thickness of the deposit was controlled; verification was through measurement of the weight change of the specimen. The average current density and deposition rate were adjusted for the area of each specimen as required, and then maintained constant during the plating process. Although the current was maintained constant (within approximately 2 percent) the current density, and consequently the deposition rate and thickness, varied across the ribbed surface as it does on any irregular shape. Figure 5 shows a typical electroplate distribution. Measurements showed that when an average current of thirty amperes per square foot was used, plating on the three rib faces deposited at the rate of 1.15 mils per hour, approximately thirty percent below the average for the whole specimen. Although the average thickness was controlled quite accurately, the deposit thickness on the bonding surfaces varied somewhat from specimen to specimen due to lack of precise reproducibility in the anode and cathode locations.

The electroplating bath was agitated and heated with a magnetic-stirrer hot plate; temperature was thermostatically maintained within ±1°F of the set temperature. A cycle-timed solenoid gave the cathode a vigorous shake every twenty seconds to minimize hydrogen gas pitting. Wetting and anti-pit agents were not used. The acidity was measured electrochemically and adjusted with dilute sulfuric acid as required. Good pH stability was achieved by sufficient buffering.

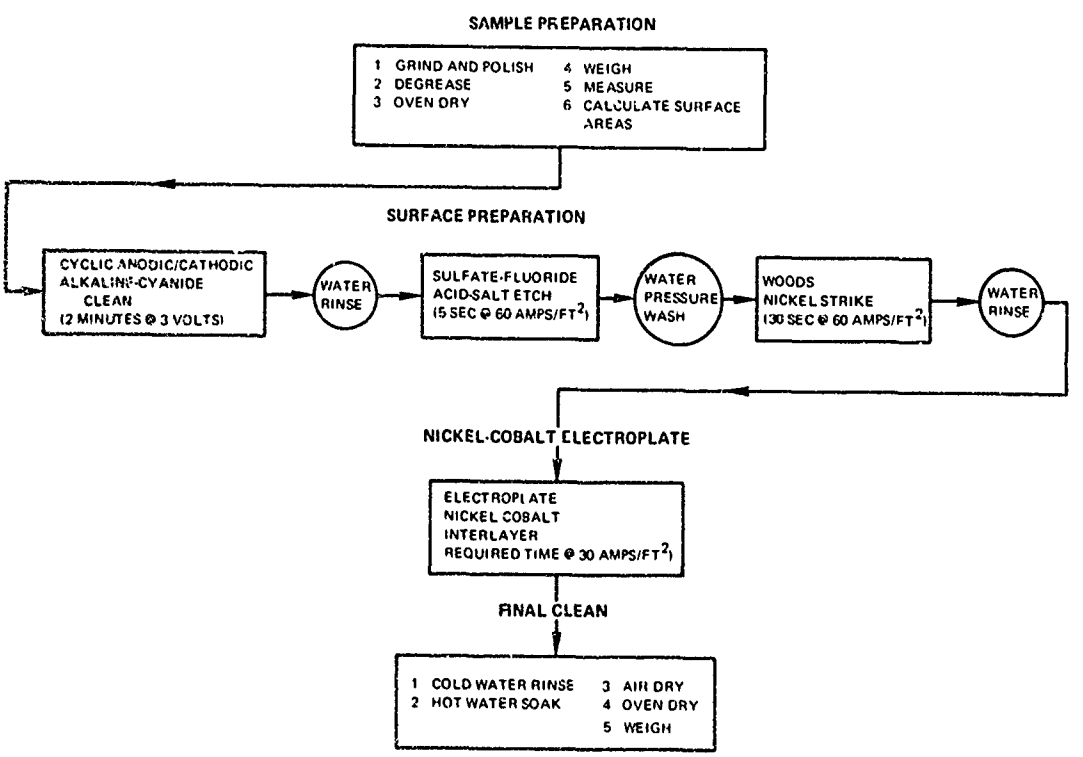

Figure 4 Plating Sequence for Electroplated Nickel-Cobalt Alloy on PWA 1422 Material

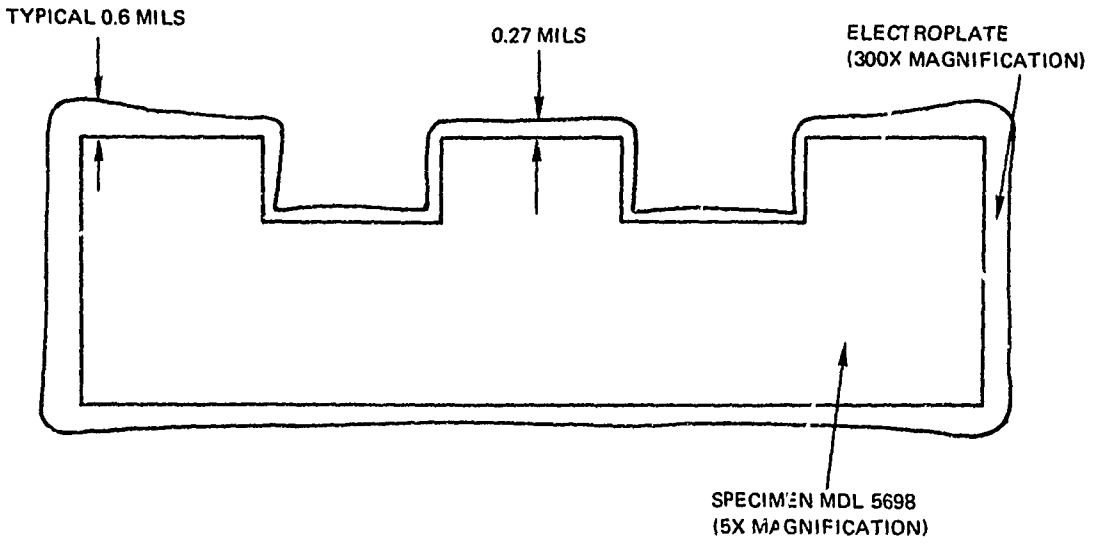

Figure 5 Typical Electroplate Distribution on a Specimen Plated With an Average of 0.38 Mils of Nickel-Cobalt

3. Chemical Analysis of Electroplates and Baths

As discussed more extensively later in this report, sporadic contamination was observed at the interface between the interlayer and base metal. Occurrence of contamination could not be influenced by systematic variations in cleaning or preparation techniques. Since there seemed to be a weak correlation between the age of the bath and frequency of contamination a spectrographic comparison of two baths was undertaken. The results, shown in Table II, did not indicate any accumulated contamination in a six-month old heavily used bath compared to a freshly prepared bath.

TABLE II

SPECTROCHEMICAL COMPARISON OF ELECTROPLATING SOLUTIONS

Solution	Major Elements	Trace Elements
No. 49 (Fresh)	Ni, Co, B	Mg, Na, Mn, Fe, Pb
No. 36 (6-Month Old)	Ni, Co, B	Mg, Na, Mn

Chemical analysis of a 5-mil, as-deposited, typical, nickel-cobalt electroplate stripped from the substrate is presented in Table III. The absence of significant sulfur indicated the oxygen was probably combined with the nascent plating surface. Whether this oxygen content was typical and persists through heating prior to welding was not determined; it is high compared to the typical base metal content of 2-10 ppm.

TABLE III

CHEMICAL ANALYSIS OF ELECTROPLATE
(BY WT PERCENT)

Specimen	Principal Composition	Oxygen	Sulfur
#289 Ni-Co	64 Ni-36 Co	0.039	0*

*Sensitivity limit was 0.001

B DISPERSION ELECTROPLATING

Dispersion electroplating is a technique whereby particles suspended in an electroplating bath are co-deposited throughout the plating as it forms on the cathode surface. In this manner multi-element deposits are readily achieved. Diffusion welding interlayer thickness is limited by the reasonable time in which base metal elements will diffuse into the joint. To extend the useful thickness of nickel-cobalt interlayers by reducing the time to reach homogeneity by diffusion, elemental tungsten and chromium–slow diffusers–were included in the electroplate by dispersion plating.

Initially it was thought that pre-alloyed powders would be desirable as dispersant particles. However, when tungsten and chromium were non-consumably arc melted under 0.8 atmospheres of argon, considerable melt instability and chromium loss were encountered at higher tungsten contents. Five melts of 200 grams each produced an alloy having an average composition of 48 percent tungsten and 52 percent chromium. This alloy was characterized by a two-phase structure as shown in Figure 6.

Since the size of these phases exceeded the required dispersant particle size of less than ten microns, attrition could be expected to produce particles consisting of almost entirely one phase or the other. If particles of one such phase were preferentially co-deposited in the plate due to some mechanical or physical property, the compositional control would be lost and reproducibility would be poor. Furthermore, initial trials at disintegration of the alloy through fluid energy mill processing indicated difficulty in the formation of fine particles.

Consequently, it was decided to utilize elemental metal powders when both tungsten and chromium were found to be basically compatible with the electrolyte. Since the deposition of the dispersant appears to be largely a mechanical phenomenon, the deposition rate for each element was determined by the initial loading of the bath. Commercially available metal powders of 99+ percent purity having the particle distributions shown in Figure 7 were added to the sulfate electroplating bath previously described. A number of dispersion plating baths were prepared, each requiring considerable processing including blending, degassing, and filtering.

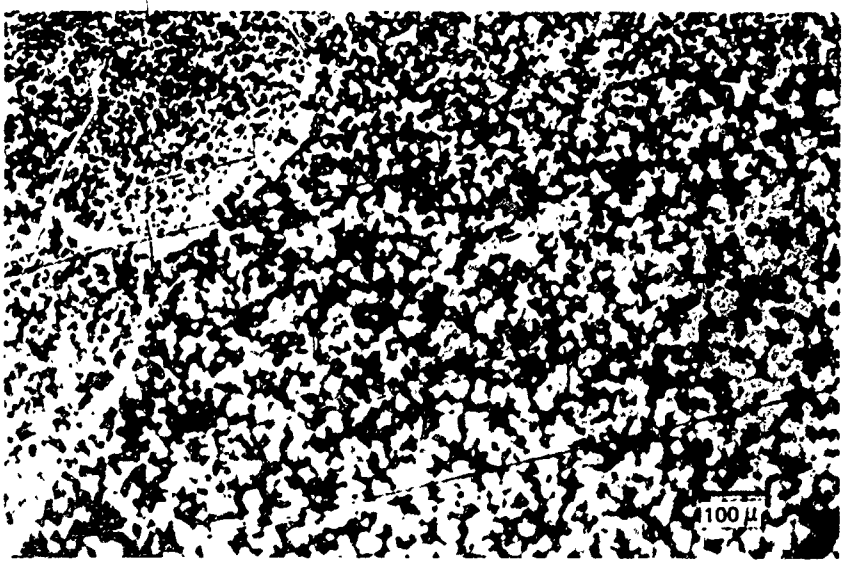

ES 3038-4. 100X

Figure 6 Typical Microstructure of 52Cr-46W Alloy Non-Consumably Arc Melted in 0.8 Atmosphere of Argon (Etchant: Phosphoric Acid Electrolytic)

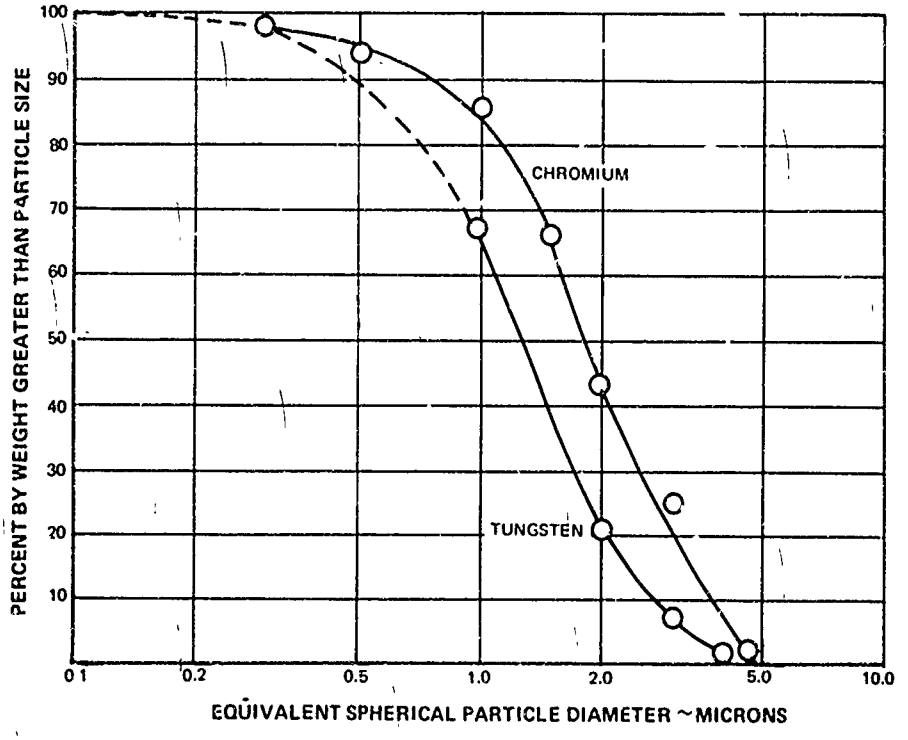

Figure 7 Particle Size Distribution of Elemental Tungsten and Chromium Dispersant Powders

The characteristic structure of as-plated interlayers is shown in Figure 8. The introduction of powders into the sulfate bath did not appear to greatly disturb the equilibrium between bath composition and electroplate composition that was determined prior to the introduction of dispersants.

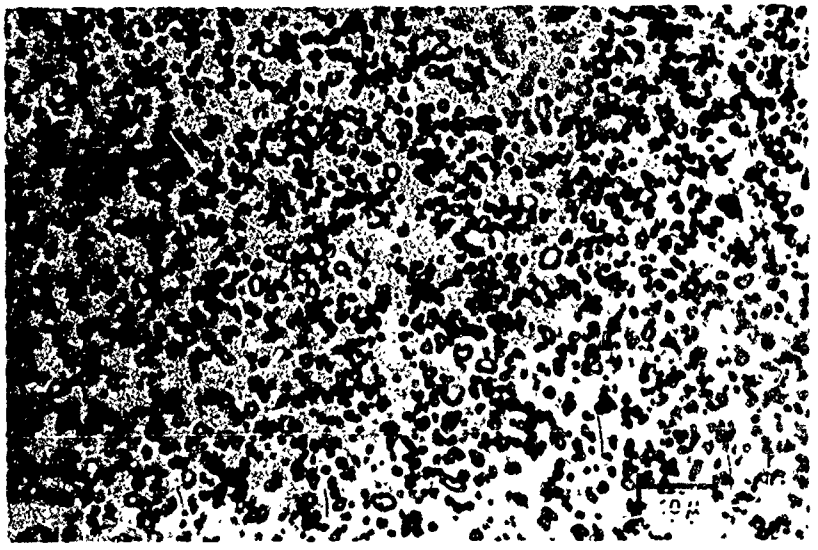

ES 3586-2 1000X

Figure 8 Typical Microstructure of Nickel-Cobalt Dispersion Electroplate. Tungsten and Chromium are Present as Particles (Etchant: 1% NaOH Electrolytic)

Table IV presents the dispersion electroplating results. The bath composition was determined by the weight of the initial ingredients and is approximate since there is some compositional change as a result of filtering and maintenance operations. The composition of the electroplate was determined by wet chemical analysis. The original target composition, 56 percent Ni, 25 percent Co, 9 percent Cr, 11 percent W, was based on the proportions in which these elements were present in the base metal. This composition was approximated by Solutions Numbers 40 and 44. Subsequent solutions were compounded based on the observed results of diffusion welding.

One item worth noting is the high total dispersant content achieved in several of the test panels. For instance, one test panel had a dispersant content of 30 percent by weight (9% Cr, 21% W). Converting to volume percentage to discount the high density of tungsten gives 23 percent total dispersant. Compared to prior experience with chromium dispersed nickel electroplate systems this is high.

TABLE IV

SUMMARY OF ELECTROPLATING RESULTS

Solution Number	Panel Number	Current Density amps/ft^2	Solution Composition ~Grams/Liter						Deposit Composition ~Percent by Weight			
			$NiSO_4$-$6H_2O$	$CoSO_4$-$7H_2O$	H_3BO_3	NH_4Cl	Chromium*	Tungsten*	Nickel	Cobalt	Chromium	Tungsten
32	EJR-11A	30	126	8.45	37.0	27	42	115	42	28	9	21
40	29[illegible]	30	124	8.02	26.9	26.9	42	13	49	32	10	9
43	306	30	124	8.02	27.0	27.0	18	48	62	21	4	13
44	307	30	124	8.02	27.0	27.0	110	97	52	21	11	15
46**	308	47	124	8.02	27.0	27.0	42	13	61	27	8	4
52	325	30	129	2.39	27.0	27.0	49	39	68	13	8	15

*Nominal
**Duplicates Solution No. 40 at higher current density

1. Dispersion Plating Compared with Nickel-Cobalt Plating

Specimen preparation for dispersion electroplating was identical to that of the simple nickel-cobalt system except for cathode agitation. Since the dispersed bath had practically no tendency to pit, auxilliary cathode agitation was dispensed with. A lower deposition rate was observed for dispersion plating compared with that expected for a nickel-cobalt based system. Longer plating times were used to compensate for this effect.

A rapid rise in the pH of the dispersion plating solution was observed during both storage and plating. Supplementary tests indicated that tungsten is soluble at a low rate in the sulfate bath; this is the probable explanation of the pH variations while the solution is standing idle. The depressed deposition rate indicated loss of cathode efficiency attributable to hydrogen gas evolution during plating which could explain the rapid rise in pH noted during plating, although not illuminating the fundamental cause. It can be theorized that exposed tungsten particles on the surface of the cathode shift the deposition potential of nickel-cobalt relative to hydrogen favoring hydrogen evolution at the expense of metal deposition. Because the anodes were dissolving at a greater current efficiency than that at which nickel-cobalt was depositing at the cathode, there was a net accumulation of metal in the bath. These related phenomena were not predicted, nor were they fully understood from an electrochemical standpoint.

The gradual accumulation with time of dissolved tungsten, nickel, and cobalt limits the useful life of the bath. However, while these aspects have been noted, they did not seriously obstruct the production of test electroplates for the program since compensation was made.

2. Chemical Analysis

Since, as described later, oxygen rich particles were observed within diffusion welds, an analysis for oxygen and sulfur was made of an as-deposited dispersion electroplated interlayer. The results, shown in Table V, indicate that the dispersion plate probably has a small quantity of electrolyte trapped within it. Presuming the sulfur to be present as the sulfate ion, it can be readily calculated that the electrolyte inclusion could account for the major part of the oxygen content. Oxygen also may be included on the surface of the dispersant particle, or combined with the nascent plating as in the regular nickel-cobalt electroplate. It is speculated that the electrolyte inclusion occurs due to entrapment within surface irregularities of the dispersant particles. Techniques for avoiding this effect were not investigated; the only obvious course would be a consideration of the effect of particle configuration.

TABLE V

CHEMICAL ANALYSIS OF ELECTROPLATE
(BY WEIGHT PERCENT)

Panel	Principal Composition	Oxygen	Sulfur
No. 289 Ni-Co	64 Ni, 36 Co	0.039	~ 0*
No. 325 Dispersion	64 Ni, 13 Co, 8 Cr, 15 W	0.112	0.005

*Sensitivity limit was 0.001

C. FOIL INTERMEDIARIES

In this program foils fabricated from a modified parent metal alloy (depleted PWA 1422) were expected to have lower strength and creep resistance than the base metal. Therefore, most of the deformation necessary for good fit would take place within the intermediary, promoting good joint continuity while avoiding base metal distortion. Although thick (~10 mils) intermediaries would preclude homogenization through diffusion and optimum properties, the mechanical aspects of the system would be demonstrated. A logical future extension of the system would be the use of an intermediary of parent metal composition but having a structure which, while ductile during the initial welding cycle, would become strengthened during subsequent thermal exposure.

Two modified foils (Table VI) were evaluated: Foil A was similar to the base metal but without the aluminum and titanium strengtheners; Foil B more nearly approximated the composition of the base metal, but lacked hafnium and carbon. Foil B was selected based on examination of diffusion welds made with Foil A; these indicated an aluminum and titanium content might produce a more homogeneous structure.

TABLE VI

FOIL INTERMEDIARY COMPOSITIONS
(BY WEIGHT PERCENT)

	Foil A		Foil B	
	Target	Actual	Target	Actual
Chromium	9	8.76	8	8.37
Cobalt	10	10.56	10	9.91
Tungsten	12.5	12.30	12.5	11.75
Columbium	1	0.93	1.0	0.85
Nickel	Bal	Bal	Bal	Bal
Titanium	–	–	2.6	2.45
Aluminum	–	–	6.5	5.00
Carbon	–	–	–	.01

Both materials were cast into 0.030 x 1 x 3 inch flats, and cold rolled to the thinnest foil attainable on a conventional four-high laboratory mill. Cold rolling instead of hot rolling was used for simplicity and to avoid the formation of oxides which embrittle the surface grain boundaries. As might be expected, Foil A rolled to 4 mils fairly readily. In contrast, Foil B presented great resistance to being rolled below 8 mils, even with intermediate anneal or stack rolling.

A limited quantity of 8 mil foil was also made from directionally solidified PWA 1422 base metal. Usable material for making specimen joints was obtained, although tearing at the edges and fragmenting was prevalent. Chemical milling was not utilized due to evident preferential attack during a trial. Commercially available 4.5 mil Hastelloy-X foil was used in Phase III when Foil B of satisfactory integrity and thinness could not be made. The cold rolled foil was prepared for joining in the as-rolled condition by fine grit alumina blasting, mechanical polishing, and electroplating.

III

PHASE IA – DIFFUSION WELDING OF SPECIMENS

The use of interlayers as aids for joining nickel-base superalloys is well known. They serve the dual function in high aluminum and titanium bearing alloys of providing a more ductile surface which promotes intimate contact, and of preventing the formation of deleterious interfacial precipitates in the joint.

Prior work systematically determined the advantage of nickel and nickel-cobalt interlayers for Udimet 700 (described in U.S. Patent 3,530,568). It was indicated that interlayers less than 0.1 mils were ineffective in preventing the formation of surface compounds, while interlayers thicker than 0.2 mils did not yield homogeneity in the joint region. It was also found that pure nickel interlayers resulted in excess gamma prime (Ni, Al, Ti) in the joint after full heat treatment. The addition of controlled amounts of cobalt in the interlayer effectively eliminated this effect and promoted chemical and microstructural homogeneity.

The initial diffusion welding development under this program ascertained the applicability of the nickel-cobalt interlayer system to PWA 1422 alloy and determined the criticality of composition, thickness, and welding parameters. As previously described some variability in the percentage cobalt and thickness of the interlayer was anticipated. Also, it is commonly known that cast metals have localized chemical heterogeneity which will affect diffusion gradients and final joint composition. Considering these factors, the initial goal was to observe strong differences in interlayer composition, thickness, pressure, and temperature as they affected joint quality. After soundness, the primary criterion was the amount of gamma prime formed within the joint region. Further evaluation was made of contamination, accommodation of lack of fit, surface preparation, and base metal deformation.

Using conventional light metallography, the dominant microstructural feature of PWA 1422 is a uniform array of coarse gamma prime precipitate (the compound Ni_3 (Al, Ti) - See Figure 14). Gamma prime normally exists in two other forms: eutectic gamma prime, islands of large cellular-appearing colonies formed as an interdendritic phase during solidification; and a fine submicroscopic array, visible only by electron metallography. In this report the term "gamma prime" used alone refers to the optically visible coarse uniform array.

Since gamma prime is formed by a precipitation process, its presence is indicative of both the chemical composition and thermal history of the specimen. If, as in this program, the thermal history is uniform for a group of specimens, experience has shown that the appearance of gamma prime in base metal (and diffusion welds approximating base metal composition) will indicate the chemistry variations within the specimens. It is apparent that the nearer a diffusion weld region approaches base metal composition, the better will be its properties.

The exact volume percent gamma prime for PWA 1422 can be determined by chemical extraction techniques if needed. However, in this program it was more practical to metallogra-

phically compare the amount of gamma prime in a diffusion weld zone with the adjacent base metal or typical PWA 1422 structures. The following descriptive terminology is used:

- Depleted of gamma prime - less quantity of precipitate visible in the joint region (e. g. Figures 16B and 18).
- Excess gamma prime - greater quantity, usually enlarged, of precipitate in the joint than the base metal (e. g. Figures 13 and 14).
- Homogeneous - structure looks much like base metal or is typical of the range of PWA 1422 appearance (Figures 15, 16c, and 20).
- Heterogeneous or inhomogeneous - either excess or depleted of gamma prime; in either case indicating that the joint region implicitly is inferior to the base metal.

The normal specification heat treatment for PWA 1422 is 2200°F/2hr + 1975°F/4 hr + 1600°F/32 hr. Prolonged holding at the lower (aging) temperature precipitates gamma prime as well as carbides from the matrix. However, a significant amount of gamma prime is precipitated during cooling from the 2200°F solutioning step.

Therefore, in diffusion welding PWA 1422, as-cast base metal specimens are joined and subsequently heat treated at 2200°F to achieve homogeneity. Metallographic observations of joints have been made without the aging step since heavy concentrations of gamma prime can obscure other aspects, e.g., contamination. Joints which are depleted of gamma prime have remained comparatively so when subsequently aged at the lower temperature. When mechanical properties were to be measured, parts were subjected to the aging cycle; i.e., they received the full heat treatment. All specimens pictured in this report were etched with Kallings reagent (33 ml H_2O_2, 33 ml HCl, 33 ml alcohol, 1.5g $CuCl_2$).

A. SELECTION OF DIFFUSION WELDING SPECIMEN

Since this program was intended to develop joining systems for a specific end product, a split superalloy turbine blade, it was appropriate to deviate from the conventional use of a flat specimen to the choice of a ribbed specimen which somewhat simulates the construction of an airfoil (see Figure 9). This choice introduced the following variables and restraints: (1) as-cast dimensional variables in un-machined areas, (2) variation in electroplating thickness across the ribs, (3) cracking and collapse of the specimen in areas away from the joint, limiting the applied pressure and deformation, and, (4) edge and notch effects were readily visible.

Since the joint design was considerably different from that of a plain flat specimen, the stress distribution and deformation within the ribbed specimen were analyzed by a finite element plastic stress analysis. The graphic mathematical model output is shown in Figure 10.

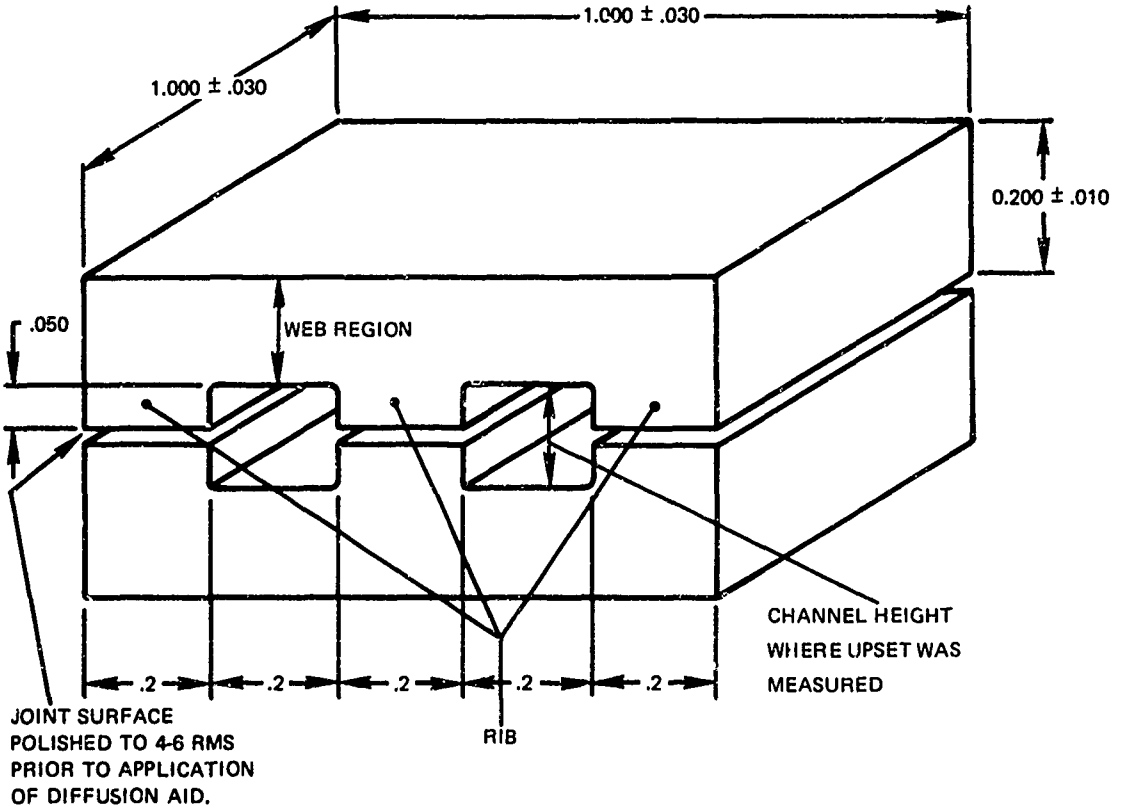

Figure 9 Sketch of 1 x 1 Inch Diffusion Welding Specimen

In the example shown (Figure 10), the specimen was subjected to constant deformation of the external surfaces, thereby simulating the condition encountered in this program when static pressure dies were used. (Similar results occur when isostatic pressure is simulated.) The stress distribution within the joint varied significantly from the calculated average value based on area and applied force. In real parts, inevitable asymmetry and misalignment can further accentuate the variation in both stress and deformation. Although not represented here, significant stresses were also existent in the base metal over the internal channels. This cursory analysis indicated that since specimen and joint design are consequential factors, diffusion welding parameters developed on flat specimens may not be readily transferrable to real parts. It also indicated that joining systems which are overly sensitive to joint stress and deformation will not be reliable.

The choice of specimen in this case acted constructively as a restraint on the choice and accuracy of welding parameters compared to a flat piece; functioning as a screen for impractical parameters and systems. Consistent with this rationale, welding conditions were allowed to vary somewhat within a range which would be practically encountered in real parts.

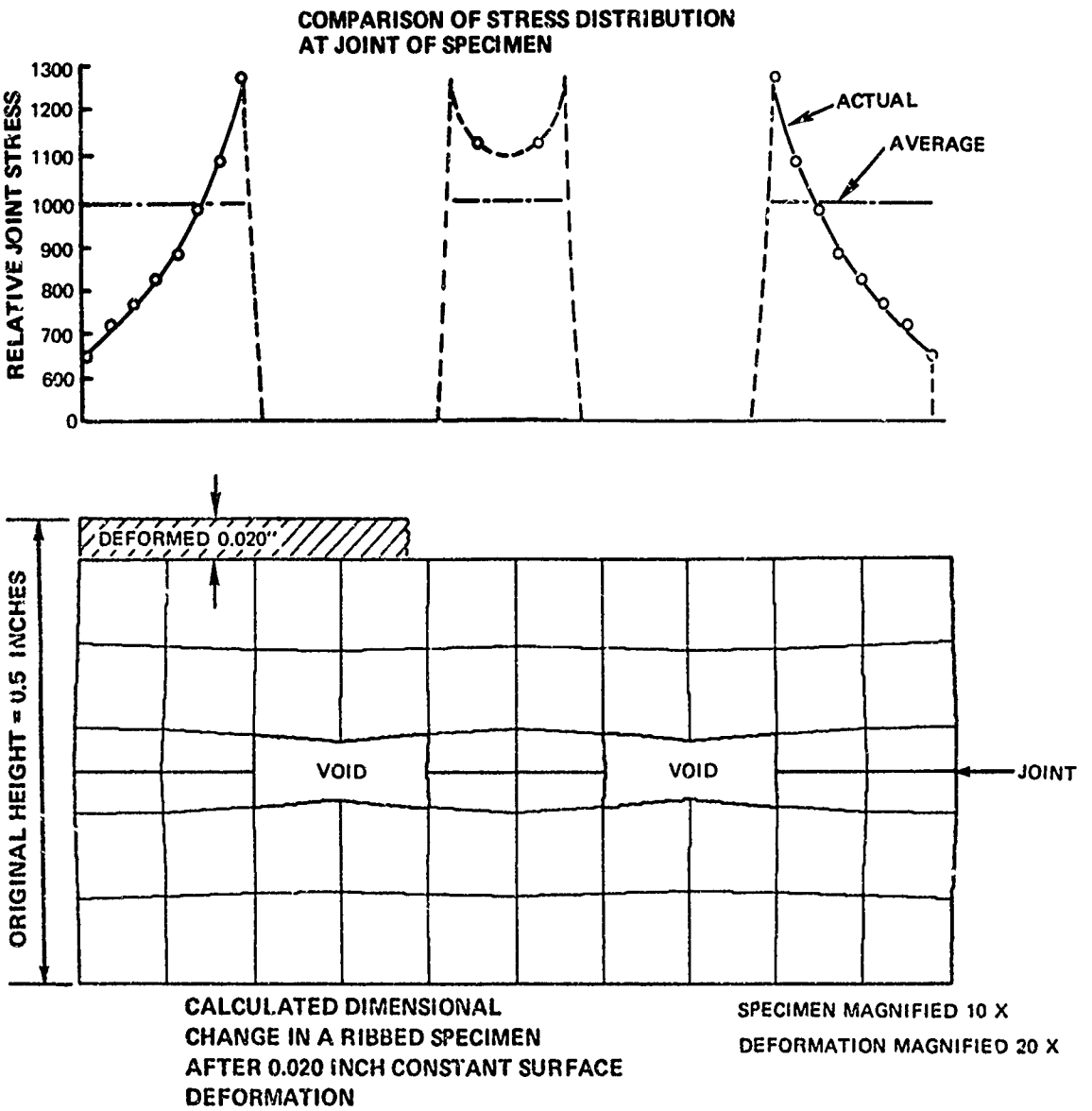

Figure 10 Finite Element Stress Analysis

B. TEST SPECIMEN FABRICATION

Test pieces were cast from material meeting the PWA 1422 specification, as shown in Table VII. In the first phase of the program equiaxed polycrystalline castings made by conventional shell mold and vacuum casting techniques were used. For the second two phases (determination of mechanical properties and fabrication of split blades) a directionally solidified form of PWA 1422 was used.

TABLE VII

COMPOSITION OF PWA 1422 SPECIMENS
HEAT CODE P-9181

	Specification ~ %	Actual ~ %
Carbon	0.08 – 0.14	0.12
Chromium	8.00 – 10.00	8.75
Cobalt	9.00 – 10.00	10.06
Tungsten	11.50 – 13.50	13.33
Columbium	0.75 – 1.25	1.19
Titanium	1.75 – 2.25	1.78
Aluminum	4.75 – 5.25	4.75
Hafnium	1.75 – 2.25	1.79
Boron	0.010 – 0.020	0.015
Silicon	< 0.20	< 0.10
Zirconium	< 0.20	0.11
Bismuth	< 0.5 ppm	< 0.5 ppm
Lead	< 0.5 ppm	< 0.5 ppm
Maganese	< 0.20	< 0.10
Copper	< 0.10	< 0.10
Nickel	Bal	Bal

C. DIFFUSION WELDING PROCEDURE

The sequence followed in making diffusion welded joints is indicated in Figure 11. After casting, the specimen's faying surface was grit blasted, flat ground for clean-up, and polished with 600 grit paper. After electroplating, the specimens were mated and the external dimensions and the internal rib-cavity space dimensions were recorded. Prior to being placed in the press, the external surfaces of the specimen were coated with a thin aluminum oxide/toluene slurry. The faying surfaces were washed with acetone and methanol and freon dried.

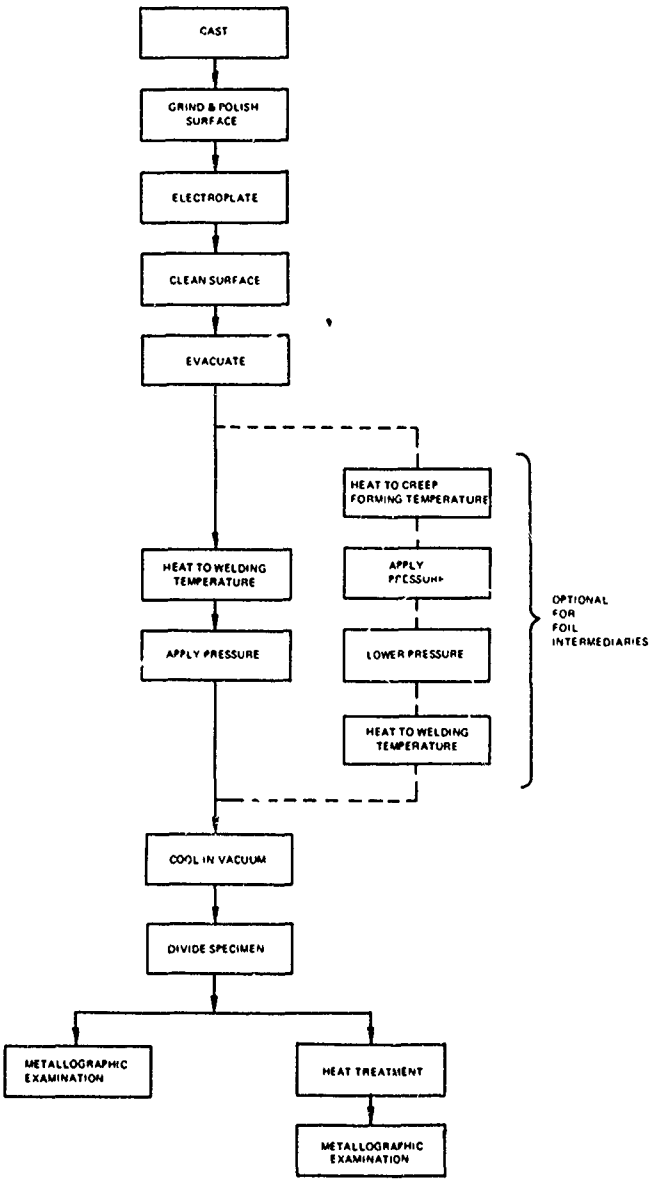

Figure 11 Diffusion Welding Process

Welding was accomplished in a hydraulic press at a vacuum level typically 10^{-5} torr or better. When appropriate, samples were stacked three-high. Typically, the specimens were directly induction heated to the diffusion welding temperature (2200°F) in less than ten minutes after the desired vacuum level was reached. The temperature at which the joint was made was chosen for compatibility with the solution heat treatment of PWA 1422, and was the practical maximum temperature to which the base material could be subjected while maintaining its properties. The reported temperature for each specimen was the average of a reading taken in the center of each channel using Inconel 702 clad chromel alumel (Type K) thermocouples contained in ceramic sleeves. Welding pressure (typically 500-1000 psi) was

applied through hydraulic rams when the specimen was stabilized at the welding temperature. Pressures reported in this report refer to the load divided by the faying surface (joint interface) area.

In the case of foils and thick interlayers the cycle was sometimes varied by heating the specimen to an intermediate creep-forming temperature (1800-2000°F) whereupon a high pressure (1000-4000 psi) was applied for a period of time. After lowering the pressure to that used for welding, the specimens were heated to the welding temperature and the normal sequence resumed.

After the welding phase was completed heating was terminated and pressure released; specimens were cooled fairly rapidly by radiation to the vacuum chamber. A segment of the specimen was cut off for examination and the remainder heat treated under argon, hydrogen, or vacuum, usually at 2200°F for varying times.

The initial phase of this program was restricted to an evaluation of diffusion welded joints through metallographic examination. Metallographic examination of the joint was made at planes perpendicular to the rib cavity length; photomicrographs presented here are typical of all three rib sections unless indicated. The criteria used in assessing joints included the homogeneity in structure with the parent metal, the amount of grain boundary migration in the joint location, and the presence of contaminants, voids, cracks, or other anomalies.

D. DIFFUSION WELDING WITH INTERLAYERS

PWA 1422 specimens were diffusion welded at a temperature of 2200°F and 500 psi for one hour, both without an interlayer and with an elemental nickel interlayer 0.1 and 0.3 mils thick.* After heat treatment (2200°F for three hours) both specimens revealed undesirable joint heterogeneity. As shown in Figure 12, the bare specimen joint exhibited deleterious fine precipitates inhibiting grain boundary migration across the interface. These formations can be attributed to a reaction between elements (predominantly titanium) in the base material and unavoidable adherent surface contaminants.

Joints made with the use of a nickel interl Figure 13) exhibited a heterogeneous structure containing large gamma prime precipitates. Electron microprobe analysis of joints made in similar nickel-base alloys with nickel interlayers has confirmed the excess concentration of titanium and aluminum in the joint.

Experience has also shown that poor mechanical properties will result from joints exhibiting the characteristics described above. The introduction of controlled amounts of cobalt into the nickel interlayers effectively alters the concentration gradients in the joint region and will give a nearly homogeneous microstructure. The effect of cobalt on the joint region microstructure is graphically evident in Figure 14.

* The interlayer thickness reported herein is the thickness of the electroplating applied to one side of the joint. Interlayers are applied to both faying surfaces except as noted.

2200°F/500 psi/1hr.
+
2200°F/3 hr.

A24H *

500X

Figure 12 Joint Formed Without Interlayer Contains Planar Interface with Intermetallic Phases (Arrows)

2200°F/500 psi/1 hr.
+
2200°F/3 hr.

A23H

500X

Figure 13 Joint Formed with a 0.3 Mil Nickel Interlayer Contains Large γ' Phases (Arrows) and Nickel Rich Regions

*The number (24) refers to the specimen number. The letter (H) indicates this specimen received ar additional 2200°F heat treatment after initial joining.

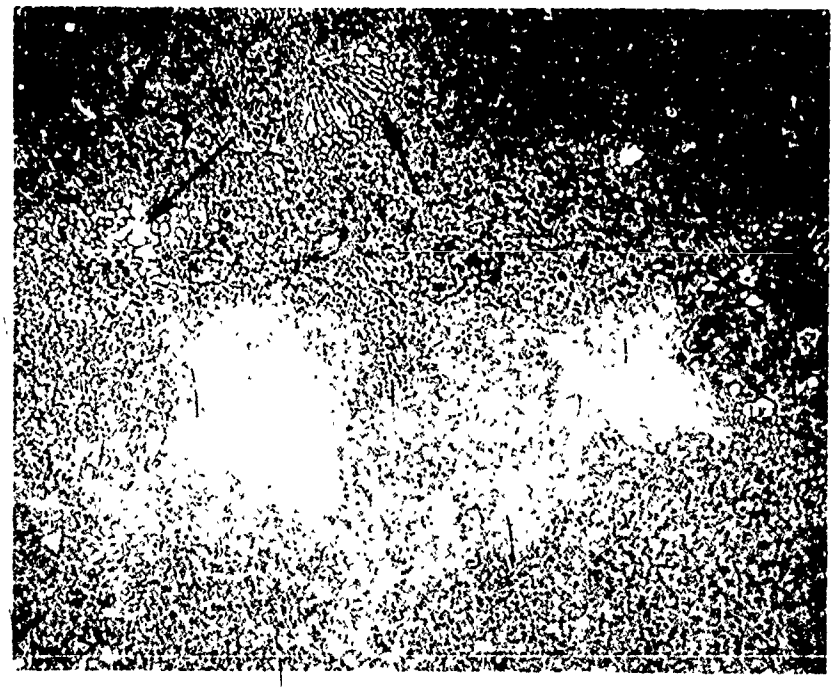

2160°F/500 PSI/2 Hr.
+
2200°F/2 Hr.

A139H 500X

Figure 14 Typical 0.2 Mil Nickel-20% Cobalt Joint Which is Homogeneous. Base metal eutectic gamma prime (arrows) is distinguished from the continuous array of precipitated gamma prime which gives the matrix a grainy appearance.

For expediency and economy the basic development work used conventionally cast PWA 1422 specimens, although this alloy is designed for and only used in service in the directionally solidified form. Ribbed 1 x 1 inch specimens with a directional structure parallel to the rib faces were diffusion welded resulting in the typical joint structure shown in Figure 15. On the basis of these results it was concluded that the results using polycrystalline material would be transferrable to the directional material.

E. NICKEL-COBALT DIFFUSION WELDING

Experimental diffusion welding with nickel-cobalt interlayers on PWA 1422 nickel base alloy showed that welds having uniformly good metallurgical quality were achieved with the following nominal parameters: Cobalt content of 20 percent for interlayers nominally 0.1 to 0.5 mils thick; welding pressure 500 psi or greater; temperature 2150-2200°F; welding time one hour or more under pressure; post-weld heat treatment 2200 ± 25°F for three hours. A listing of all joints is given in Appendix Table A-1.

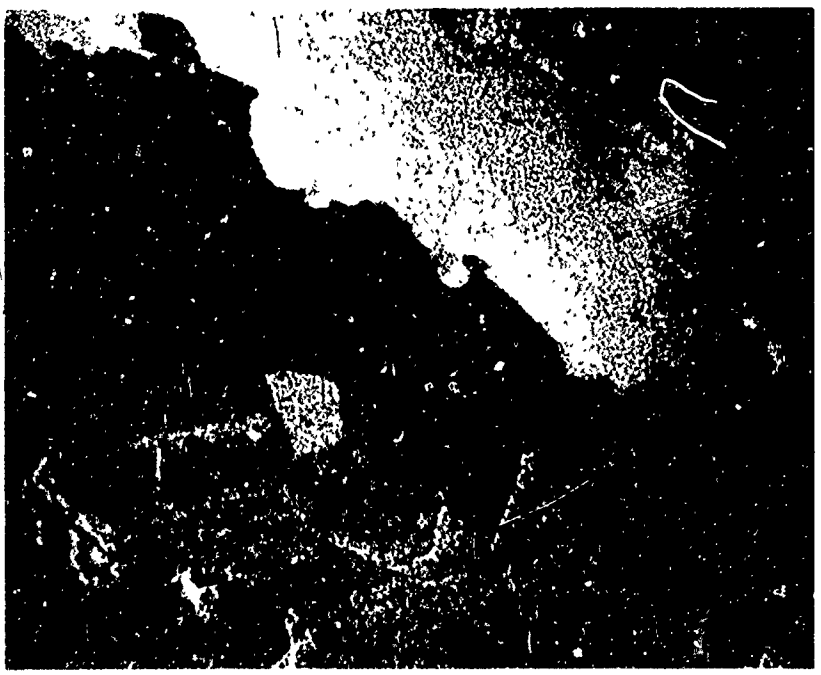

2190°F/500 PSI/2 Hr.
+
2200°F/3 Hr.

A109H 500X

Figure 15 Joint in Directionally Solidified PWA-1422 Using 0.2 Mil Nickel-25% Cobalt Interlayer

1. Effect of Time and Temperature

Time and temperature are known to be significant variables in diffusion phenomena. The diffusion welding temperature chosen was the practical maximum for avoidance of gross incipient melting in the base metal which can degrade properties. The time-temperature interrelation is important for its effect on the parent metal properties and practical manufacturing considerations.

Temperature during the diffusion welding cycle was varied for different specimens by 25°F above and 50°F below the nominal welding temperature of 2200°F, and while there was a significant effect on upset due to creep of the base metal, no significant effect was observed on joint microstructure after heat treatment.

Typically metallographic specimen joints were diffusion welded for one hour, and then heat treated for three hours. The heat treatment temperature, 2200 ± 25°F, is the normal solution temperature to which PWA 1422 castings are exposed. On the basis of prior investigation, total exposure to this temperature for up to four hours was believed acceptable.

As an example of the effect of time on the joint homogeneity, a 35 percent cobalt interlayer weld which was depleted at the end of the normal three hour heat treatment was subjected to an additional twenty-three hours at 2200°F, and yielded a homogeneous structure as shown in Figure 16. Such long heat treatment times may be acceptable from a practical standpoint without significant degradation of the parent metal properties, however, long diffusion times are preferably avoided.

A

500X

As Welded at
2200°F/500 psi/1 hr.

B

500X

Heat treated at
2200°F/3 hr.

C

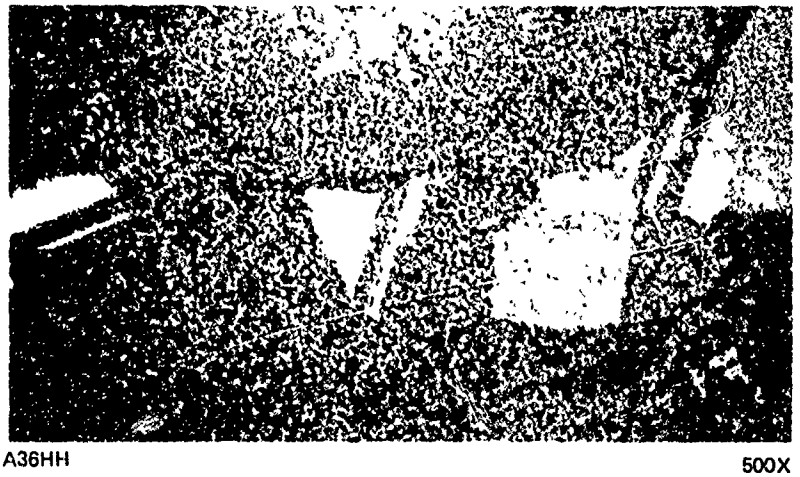

A36HH

500X

Heat treated at
2200°F/26 hr.

Figure 16. PWA 1422 Diffusion Welded With a 0.3 Mil Thick Nickel - 25% Cobalt Interlayer. Homogeneity is Only Achieved After Extended Heat Treatment Indicating Excessive Thickness. The Irregularity in Thickness of the Depleted Area in View B is Attributed to Base Metal Variations. A Line of Contaminants, (View A) at the Interlayer-Base Metal Interface Largely Disappears After Heat Treatment (Views B and C).

Additional study of nickel-25% cobalt interlayers 0.5 to 0.8 mil thick shows that homogeneity is not consistently achieved throughout the joint region after 2200°F post-weld heat treatment for 23 additional hours. Heat treatment of 16 hours produced complete homogeneity in nickel-20% cobalt joints. After similar processing, nickel-15% cobalt joints were homogeneous but still contained enlarged gamma prime particles. It is probable that homogeneity was achieved prior to the 16 hour period, but no systematic study of shorter times was made.

Based on these results, it is concluded that accurate initial composition and thickness are necessary to achieve homogeneity. When the proper conditions are not met, extended heat treatment cannot achieve homogeneity.

2. Effect of Pressure and Deformation

The joint pressure was varied from an average value of 280 psi to 2210 psi. At the lowest pressure levels, negligible upset, limited grain boundary migration, notching at the edges,and variations in joint quality were more pronounced. At the highest pressures, considerable intergranular cracking was observed in the specimen over the channel sections along with substantial deformation of the specimen in general. The most commonly used welding pressures were 500 to 1000 psi joint pressure which resulted in nominal upsets of 0.005 and 0.010 inches respectively.

Grain boundary migration is usually limited in diffusion welded joints in cast superalloys. The interface remained planar at the lower welding pressures (see Figure 17), a condition which is known to lead to poor properties. At pressures greater than 500 psi, desirable grain boundary migration occurred; however, there was no significant increase in degree of migration with further pressure increase. A similar lack of response was observed when the pressure was maintained during a welding cycle of four hours. The interfacial grain boundary movement achieved was considered acceptable.

In some specimens there was a lack of fit between the faying surfaces of up to 0.003 inches. Welding pressures of 500 psi and over produced consistent joints despite the local variation in upset. As a result it was concluded that the minimum welding pressure is 500 psi or greater, as required to produce contact throughout the specimen's faying surface.

It was noted previously that a plastic stress analysis of the ribbed specimen indicated that the actual joint pressure and deformation varied appreciably through the rib section. Only at the lowest pressure level did these variations become evident, primarily as the notching effect at the exterior edges (See Section III H-3; on page 60)

3. Effect of Thickness

Welded joints made with the thinnest interlayer (0.07 mils average thickness per side) were effective in preventing the formation of undesirable precipitates that occur when there is no interlayer.

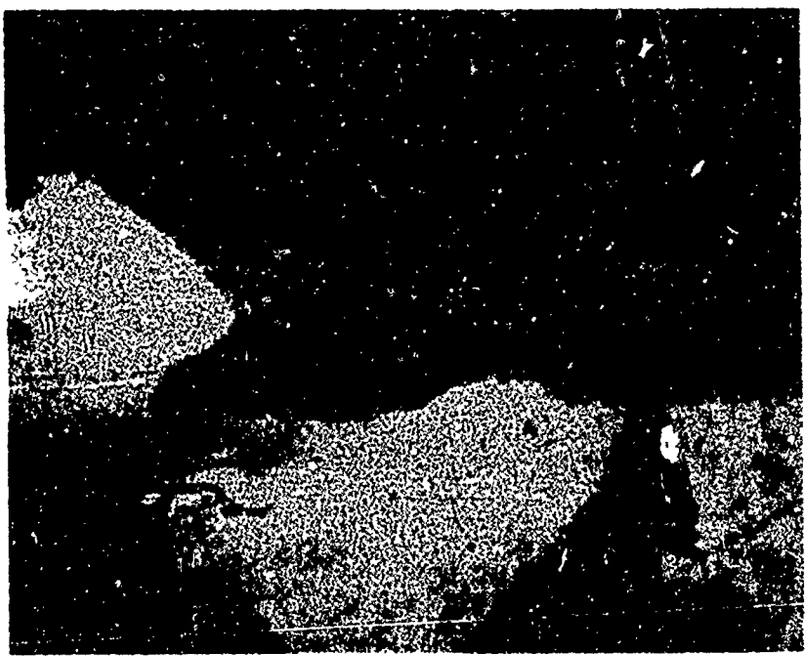

2200°F/280 psi/1 hr
+
2200°F/3 hr.

A21 500X

Figure 17 PWA 1422 Diffusion Welded with a 0.07 Mil Thick Nickel - 30% Cobalt Interlayer Contains a Planar Grain Boundary Interface that is Typical of Inadequate Joint Pressure.

Using the normal diffusion welding cycle it was found that for cobalt contents of 25 percent or greater, the maximum thickness interlayer which yielded consistently homogeneous joints was 0.2 mils. Joints using a thick 25 percent cobalt interlayer (0.55 mils) revealed a depleted region (see Figure 18). This depleted region was denoted by the lack of gamma prime and was presumed to be deficient in aluminum and titanium.

The maximum thickness for homogeneity was slightly greater for 15 percent cobalt, probably due to more favorable concentration gradients. Interlayers 0.3 mils thick produced consistent structures except for the occasional presence of enlarged gamma prime, characteristic of this composition. The interrelation between cobalt content and thickness is explored later in this section.

4. Cobalt Content and Composition Analysis

No distinction was observed for varying compositions with the thinner interlayers (0.07 mils), since all joints appeared equally good. Using nominally constant welding parameters (2200°F/1000 psi/1 hour) and heat treatment (2200°F/3 hour), significant structural differences were seen at thicknesses greater than 0.2 mils for 15, 25, and 35 percent cobalt.

Figure 19 shows the joint morphology when the concentration of cobalt was 15 percent. A region of enlarged gamma prime is prevalent along the joint region; other than this the microstructure is homogeneous. Five of sixteen specimens exhibited a structure similar to that shown; the others were completely homogeneous. This variability can be ascribed to fluctuations in the cobalt content and in the base metal.

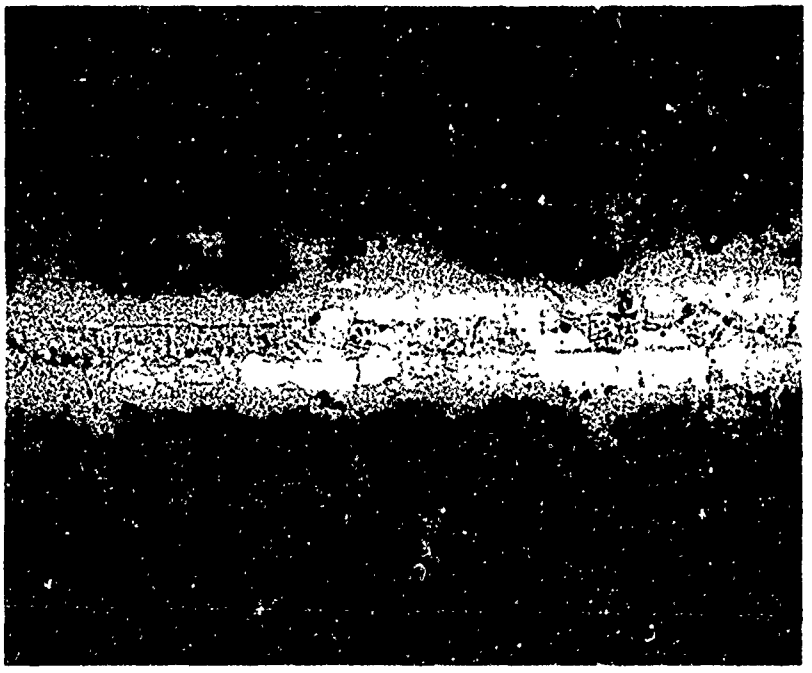

2200°F/1000 psi/1 hr.
+
2200°F/3 hr.

A67H 150X

Figure 18 PWA 1422 Diffusion Welded Using A 0.5 Mil Thick Nickel - 25% Cobalt Interlayer Contains A Joint Depleted In Gamma Prime Indicating The Interlayer Was Too Thick. A Line of Contaminants Adjacent To The Joint Interface Is Also Observed.

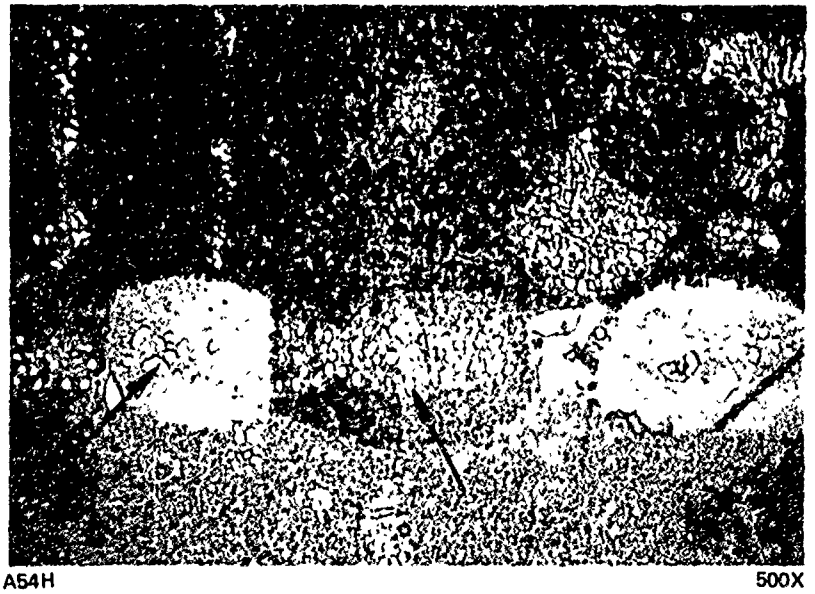

2200° F/1000 psi/1hr
+
2200° F/3 hr

A54H 500X

Figure 19 PWA 1422 Diffusion Welded Using a 0.3 mil Thick Nickel - 15% Cobalt Interlayer Produced a Homogeneous Joint with the Exception of the Presence of Large Gamma Prime (Arrows) Along the Joint

Higher concentration of cobalt tended to give a consistently homogeneous 0.2 mil interlayer joint, as indicated in Figure 20 for a 25 percent cobalt interlayer, and Figure 21, for a 35 percent cobalt interlayer. These results indicate that a sufficient amount of cobalt will prevent the formation of excess gamma prime in the joint. The role of cobalt in a diffusion weld interlayer is discussed further in Section III E-6, page 39. It was concluded that if the percentage cobalt in a nickel interlayer for PWA 1422 ranged between 20 and 35 percent, a consistent homogeneous structure would result. This correlates with similar findings for Udimet 700.

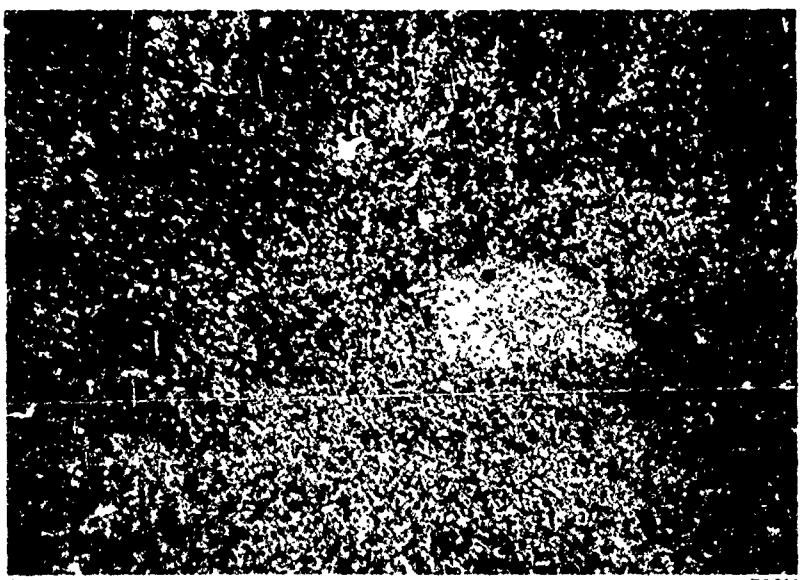

2200°F/750 psi/1 hr.
+
2200°F/3 hr.

Figure 20 PWA 1422 Diffusion Welded With A Nickel - 25% Cobtalt Interlayer 0.2 Mils Thick Produces a Homogeneous Joint

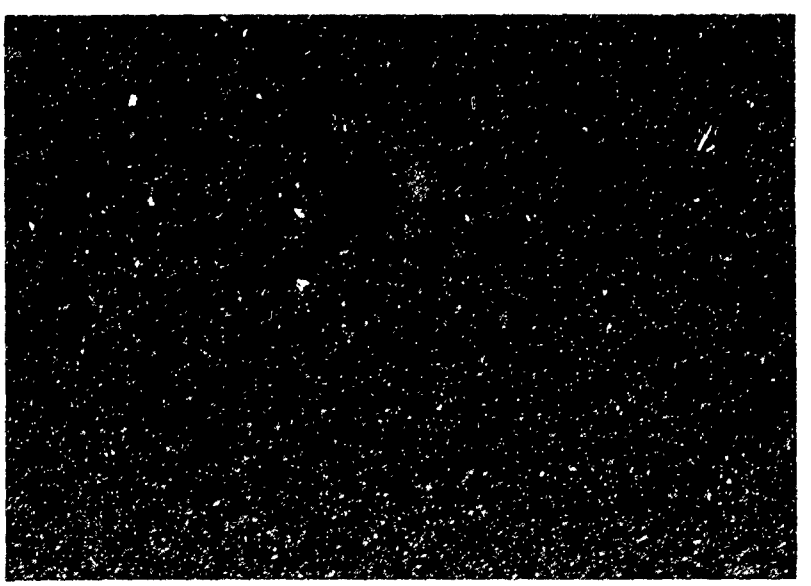

2200°F/750 psi/1 hr
+
2200°F/3 hr.

Figure 21 PWA 1422 Diffusion Welded With A Nickel - 35% Cobalt Interlayer 0.2 Mils Thick Yields A Consistent And Homogeneous Joint

Based on the metallographic observations, electron microprobe analyses were made of two welded and heat treated (2200°F/750 psi/1 hr + 2200°F/3 hr) nickel-25 percent cobalt interlayer joints. As shown in Figure 22, homogeneity was largely achieved in a 0.2 mil thick interlayer. Cobalt content was slightly higher, and tungsten content lower, in the joint center compared to the base metal. Metallographic examination showed that the joint was essentially microstructurally homogeneous with the base metal (Figure 23a).

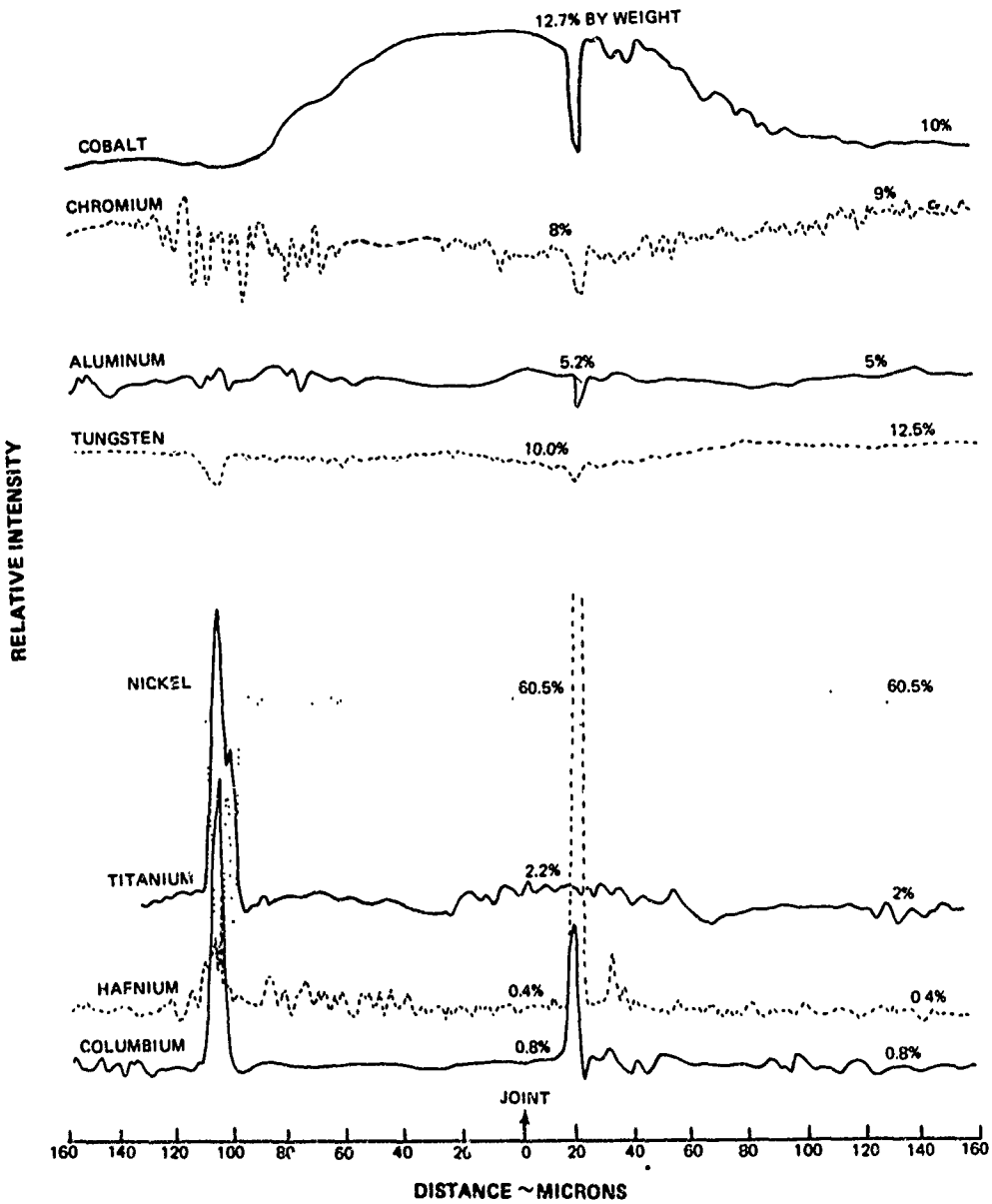

Figure 22 Electron Microprobe Analysis of 0.2 Mil Nickel-25% Cobalt Interlayer Diffusion Weld (2200°F/750 PSI/1 Hr. + 2200°F/3 Hr.). The Joint (See Figure 23b) is Homogeneous with Base Metal Except for Cobalt (Specimen A67H).

A47H 500X

(a)

Joint Using 0.2 Mil Ni-25% Co Interlayer

2220°F/750 PSI/1 Hr.
+
2200°F/3 Hr.

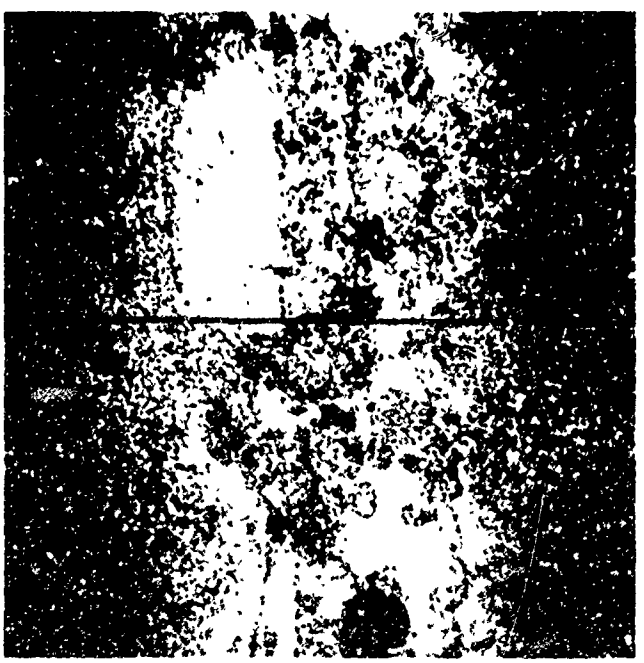

A67H 500X

(b)

Joint Using 0.5 Mil Ni-25% Co Interlayer

2200°F/1000 PSI/1 Hr.
+
2200°F/3 Hr.

Figure 23 Photomicrographs of Joints Examined by Electron Microprobe on a Traverse Indicated by the Solid Line

By comparison, a 0.5 mil interlayer (Figure 24) had a considerable excess of cobalt in the joint center. Aluminum, titanium, tungsten, and chromium contents were similar to the thinner interlayer, when the joint centers were compared. Despite the similarity in composition, metallography (Figure 23b) indicates the thicker interlayer joint is depleted of gamma prime. Therefore, it can be concluded that excess cobalt has inhibited the formation of gamma prime in the joint by altering the gamma prime solvus locally.

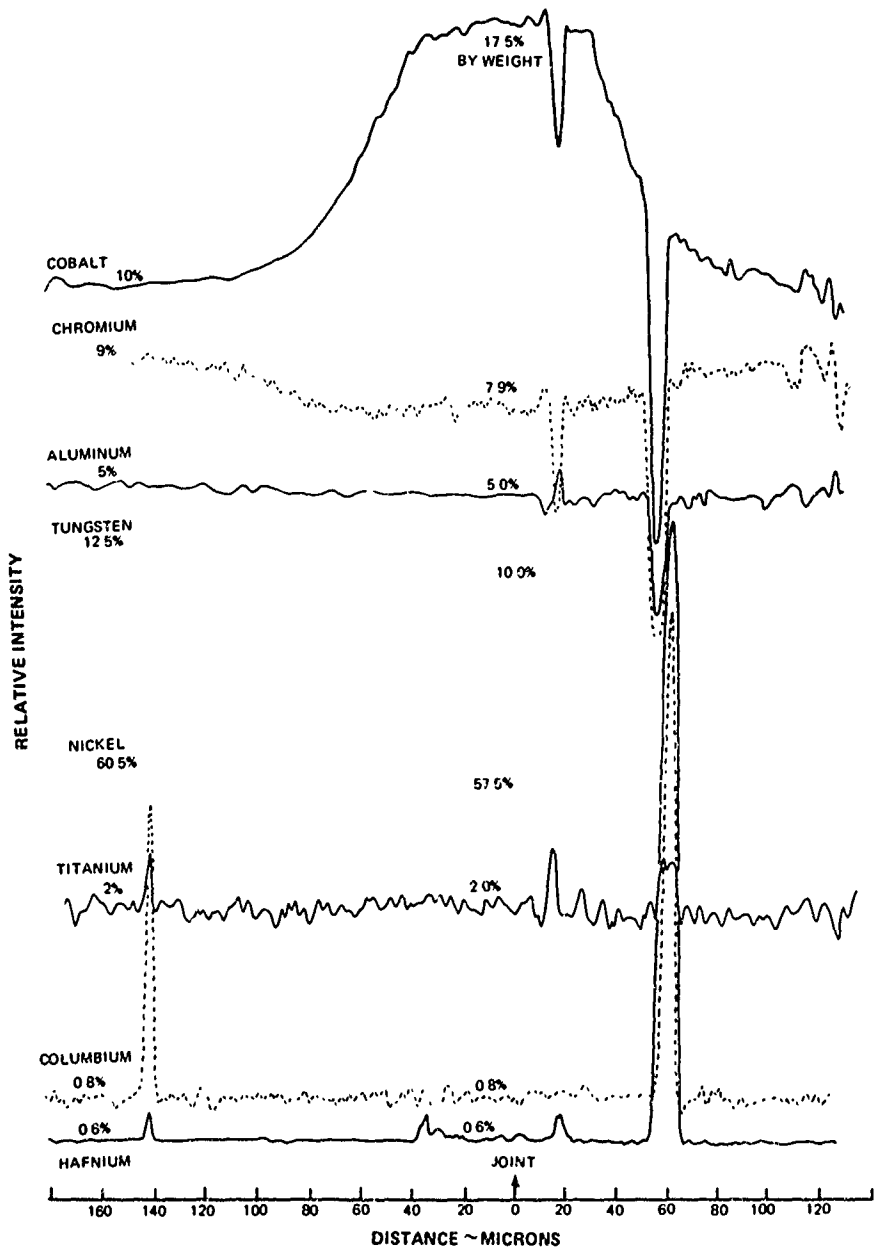

Figure 24 Electron Microprobe Analysis of 0.5 Mil Nickel-25% Cobalt Interlayer Diffusion Weld (2200°F/1000 PSI/1 Hr. + 2200°F/3 Hr.). The Joint (See Figure 23a) is Similar to 0.2 Mil Interlayer Except for Higher Cobalt Content.

It also follows that compositional control is more critical in thicker joints, since in contrast, prior work showed that the range of 15 to 35% cobalt yielded equally good joints with thin (0.07 mil) interlayers.

When compared to the base metal concentrations, it was concluded that nickel-25% cobalt interlayers were: (1) higher in cobalt, (2) slightly depleted in tungsten and chromium, and (3) essentially homogeneous in titanium and aluminum. Based on these results, a lower cobalt content interlayer appeared desirable when thicknesses approaching 0.5 mils were used. Since previously 15 percent cobalt interlayers tended to give intermittent enlarged gamma prime precipitates in the joint, interlayer joints with 20 percent cobalt were evaluated.

A number of diffusion welds confirmed that there was a qualitative improvement in microstructure when the cobalt content of the interlayer was lowered from 25 to 20 percent. Due to apparent local variations in base metal composition some sporadic large gamma prime was present when thinner (0.2 mil) nickel-20 percent cobalt interlayers were joined. However, as shown in Figure 25 and Figure 47c interlayers 0.5 mil thick yielded more microstructurally homogeneous joints than had been attained with 25 percent cobalt, even after only two hours at temperature.

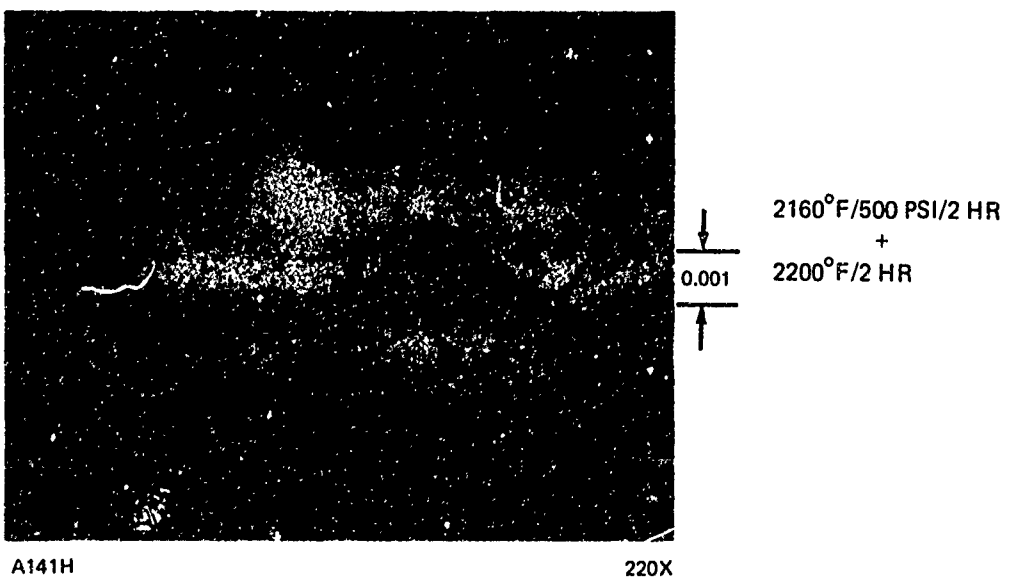

Figure 25 Joints Using 0.5 Mil Nickel - 20% Cobalt Interlayer Between As-Cast Surfaces. Dark phases (hafnium-rich oxides) are attributable to preparation of the as-cast surface.

A 0.5 mil nickel - 20 percent cobalt joint was examined by electron microprobe. Although the microstructural difference with the 25 percent cobalt joint was evident the microprobe analysis shown in Figure 26 did not indicate a significant change in homogeneity, especially in cobalt content. An additional check by microprobe in another 0.5 mil nickel - 20 percent

cobalt joint indicated a lower cobalt content, 14.7 percent, in the joint center. Both analyses showed that tungsten and chromium were somewhat lower than previously in the nickel 25 percent cobalt joint. In view of the small change in cobalt content and the limited probe data, local variations in the base metal probably account for the anomalies.

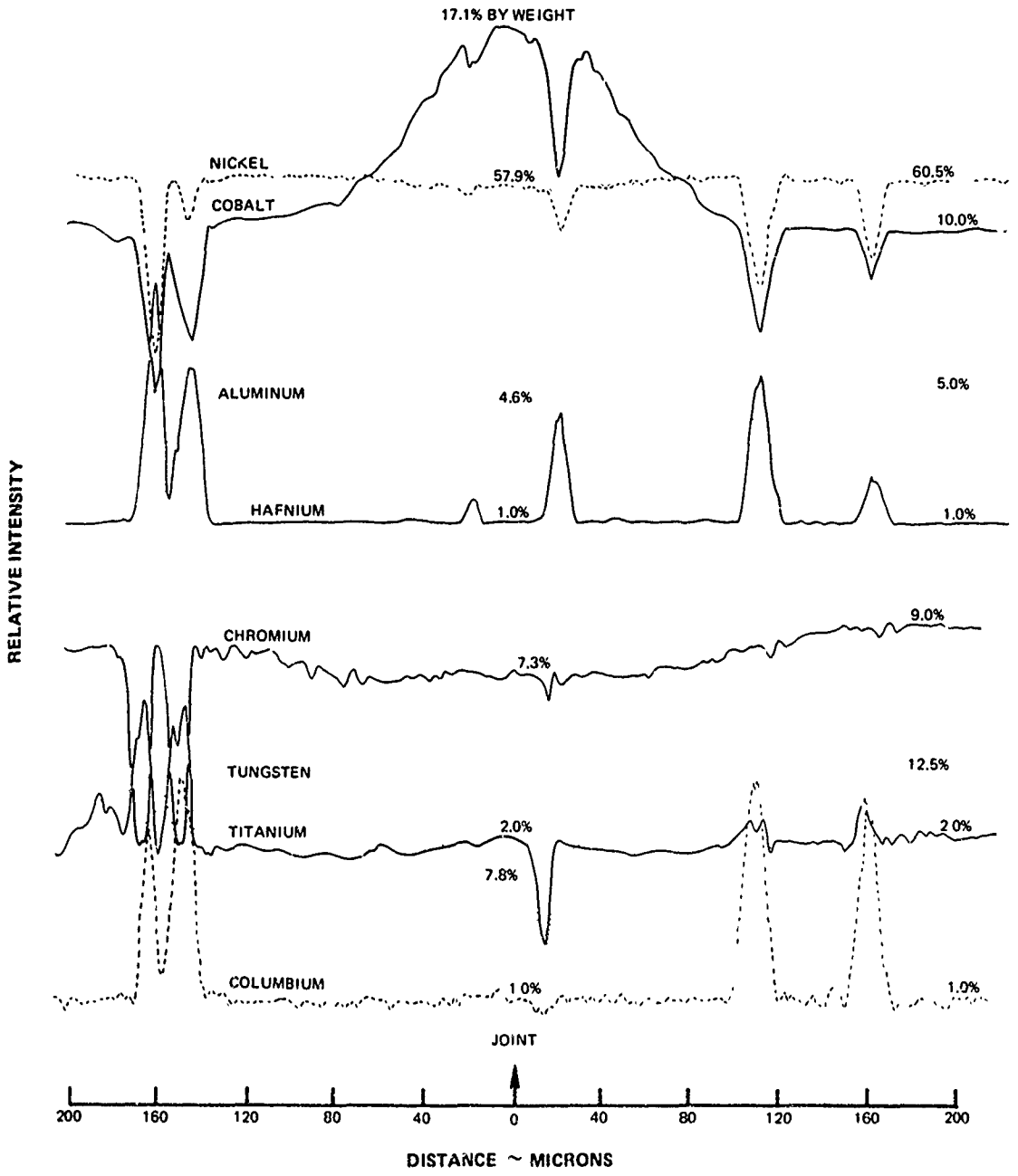

Figure 26 Electron microprobe analysis of 0.5 Mil nickel-20% cobalt interlayer diffusion weld between as-cast PWA 1422 surfaces (2160°F/500 psi/2 hr + 2200°F/2 hr). (See Figure 25).

Microprobe analysis also indicated that the dark phases at the interlayer-base metal interface were hafnium rich oxides. As discussed later these were attributed to the method of preparation of the as-cast surface.

Based on the metallographic and microprobe analyses it was concluded that, provided adequate cobalt content is present to prevent the formation of enlarged gamma prime phase in the joint, microstructural homogeneity appears limited by the outward diffusion of cobalt, rather than the inward diffusion of aluminum and titanium.

5. Contamination

In about 25 percent of the joints using machined PWA 1422 specimens, the presence of a line of particles or precipitates was observed after welding in the region where the electroplated interlayer and base metal interface had been, and was characterized as contamination. Due to its location it was attributed to the pre-plating preparation. This contamination, which is shown in Figures 16 and 18 often could not be seen after heat treatment.

A number of specimens were electroplated and diffusion welded to study the cause of the sporadic contamination. Electron microprobe analysis could not identify the fine particles due to their small size. The presence of the contamination generally did not inhibit grain migration, but it was felt to be a potential site for failure initiation. The formation of gamma prime can obscure these particles; therefore the judgement of relative intensity from one joint to another was a very subjective matter.

Prior work on UDIMET 700 using nickel-cobalt electroplates deposited from a sulfamate bath had minimized a similar effect through close control of the pre-plating procedure. The location of the particles leads to the logical observation that they are probably associated with the pre-plating procedure in this case. Several steps were taken to evaluate the causes of the contamination.

- The pre-plating procedure was varied in a controlled manner:

  a. A heavy etch was compared to no-etch.
  b. A de-smutting step was introduced.
  c. Hydrogen pitting was purposely accentuated.

  None of these factors significantly affected the degree of contamination in joints made with electroplates from a heavily used bath.

- Controlled base material having varying hafnium content, and no hafnium (MAR-M200) were diffusion welded with the same electroplate. The degree of contamination was not affected by the hafnium content.

- A review of all prior diffusion welds was made and the contamination characterized as best as possible on a relative basis. This assessment showed that the diffusion welding procedure was not a factor since contaminated and uncontaminated joints were produced in specimens which were welded simultaneously. It was found that electroplates made from baths as they progressively grew older tended to exhibit more contamination.

To evaluate the intrinsic qualities of the electroplate, new baths were prepared. Also, interlayers were applied by other suppliers using different types of baths and their own techniques. Joints were made and metallographically evaluated for contamination in the as-welded condition. Using the same pre-plating procedure, it was found that (1) conventional pure nickel sulfate electroplates (which produced gamma prime rich joints); (2) nickel-cobalt sulfamate baths of nominally nickel-25 and -30% cobalt, and; (3) new baths compounded of nickel-cobalt sulfate for 20, 25, and 30% cobalt, all produced joints which had minimal or no contamination.

Comparative welding results for new and old baths are shown in Figures 27a and 27c, the contamination variance is marked. In Figure 27b a joint is shown which was made using an old-bath interlayer on one faying surface and a new-bath interlayer on the other. The as-welded joint has contamination of both sides, indicating that the contamination causing agents have diffused within the joint.

Therefore, it was concluded that degradation with time of the electroplating bath was the cause of the contamination However, the reason for the location of contaminants at the interlayer – base metal interface is not clear. A cursory analysis of an old bath compared to a new one was made spectrochemically. These results which were presented in the section on electroplating development did not indicate any metallic contamination of old baths.

Although the initial evaluation had shown the preplating procedure was not a factor insofar as contamination, an interaction with aged plating baths appeared possible. Therefore, a methanol rinse after degreasing, and anodic-alkali cleaning in place of the usual anodic-cathodic cleaning, were evaluated using platings from both old and new baths. The modified procedures did not alter the microstructural appearance of the joint since all joints appeared equally homogeneous. The capricious nature of the contamination was demonstrated by the absence of contamination even in interlayers using the standard procedure and old baths.

A review of the preparatory electroplating and welding techniques shows that nickel-cobalt interlayer contamination is:

- Independent of interlayer thickness, composition, or welding parameters.
- Unrelated to the preplating procedure.
- Probably related to bath quality or plating parameters.
- Eliminated by compounding a new bath

A114-S36 500X

(a)

Contamination in an As-Welded Joint with 0.2 Mil Ni-25% Co Interlayer Using a 6-Month Old Bath

2225°F/1000 PSI/1 Hr.

A150 500X

(b)

Contamination in an As-Welded Joint with 0.2 Mil Ni-25% Co Interlayer. Top Basemetal using Old Bath [(a) Above]; Bottom Basemetal Using New Bath [(c) Below].

2160°F/1000 PSI/1 Hr.

A145-S53 500X

(c)

Absence of Contamination in As-Welded Joint with 0.2 Mil Ni-30% Co Interlayer Using New Bath

2200°F/1000 PSI/1 Hr.

Figure 27 Contamination From Various Electroplating Baths

Contamination of a different morphology was observed in joints between as-cast surfaces, as shown in Figures 25 and 47c. These larger dark phases were identified by electron microprobe through fluorescence as hafnium-rich oxides. It is clear these are associated with the method of surface preparation, since they are not manifested on ground surfaces. Purposeful silica contamination in a diffusion weld yielded a similar appearing phase after welding at 2200°F, whereas a joint omitting the sandblast in favor of a fine alumina or water blast appeared to have minimized the contamination. Consequently it has been concluded that silica particles entrapped in the surface, reduced by hafnium during the welding, are the cause of the contamination. Subsequent joints between as-cast surfaces used the better methods of preparation.

6. Interrelation of Cobalt Content and Thickness

The practical goal of joining real superalloy parts precluded extensive evaluation of the fundamental role of cobalt in the microstructure of PWA-1422 diffusion welds. However, it is worthwhile to present tentative conclusions as to the interrelation of cobalt content, thickness, and joint microstructure. In view of the complexity of the nickel alloy system to which PWA 1422 belongs and the limited data, these relations should only be considered as reasonable supposition.

In the following discussion, the stated relations are based only on diffusion welds which have had a total high temperature exposure of 4 hours at 2200°F. For simplicity, diffusion phenomena are related solely to cobalt content although in reality they are dependent in complex fashion on the concentrations of the other base metal elements.

Cobalt in a nickel interlayer affects the ultimate appearance of the microstructure:

- The gamma prime solvus decreases as cobalt content increases.

  The effect of cobalt on the gamma prime solvus has been described for both alloys[1] and diffusion welds in Udiment 700[2]. This cobalt effect is demonstrated in PWA 1422 by comparing Figures 22 and 23a with Figures 24 and 23b. With the same initial nickel - 25% cobalt interlayer, the diffusion of aluminum, titanium and other elements into the joint center was nearly the same. However, the joint with the higher cobalt remaining (Figures 24 and 23b) had less apparent gamma prime, indicating the aluminum and titanium remained in solution.

- High initial cobalt content decreases diffusion of aluminum and titanium (gamma prime formers) into the joint region.

---

(1) Bollenrath, F., and Rohde, W. "Precipitation Hardening Behavior and Mechanical Properties of Heat Resisting Alloys Containing Up to 35% Cobalt" Cobalt, 34, p 18-36 (1967).

(2) Duvall, D.S., Owczarski, W. A., and King, W. H. and Paulonis, D. F., "Methods for Diffusion Welding the Superalloy U-700", Welding Journal, V51 - No. 2, February 1972.

It is well known that elemental diffusion rates differ for various matrices. Prior microprobe analysis of Udimet 700 has shown that the concentration of aluminum and titanium in a 100% nickel interlayer diffusion weld, (analogous Figure 13) is above that of the base metal[2]. In this program microprobe analyses (Figures 22, 24, and 26) show that the presence of cobalt prevents the "uphill" diffusion of aluminum and titanium in PWA 1422.

Four figures are presented in this section. The first indicates the relationship between cobalt in the interlayer with that in the final diffused joint; that is based in part on the microprobe data summarized in Table IX. The second and third figures present relations which are fundamental to an understanding of the propensity for gamma prime to form in the joint microstructure. The fourth figure is based on the metallographic observations made during this program, and enables the empirical prediction of microstructure based on interlayer cobalt content and thickness.

Figure 28 presents the final cobalt content in the joint as a function of initial interlayer content and thickness. The shaded area indicates the region within which homogeneous appearing joints are achieved. It is evident that the initial cobalt content must be sharply confined at the higher thicknesses if a desired final joint composition is necessary.

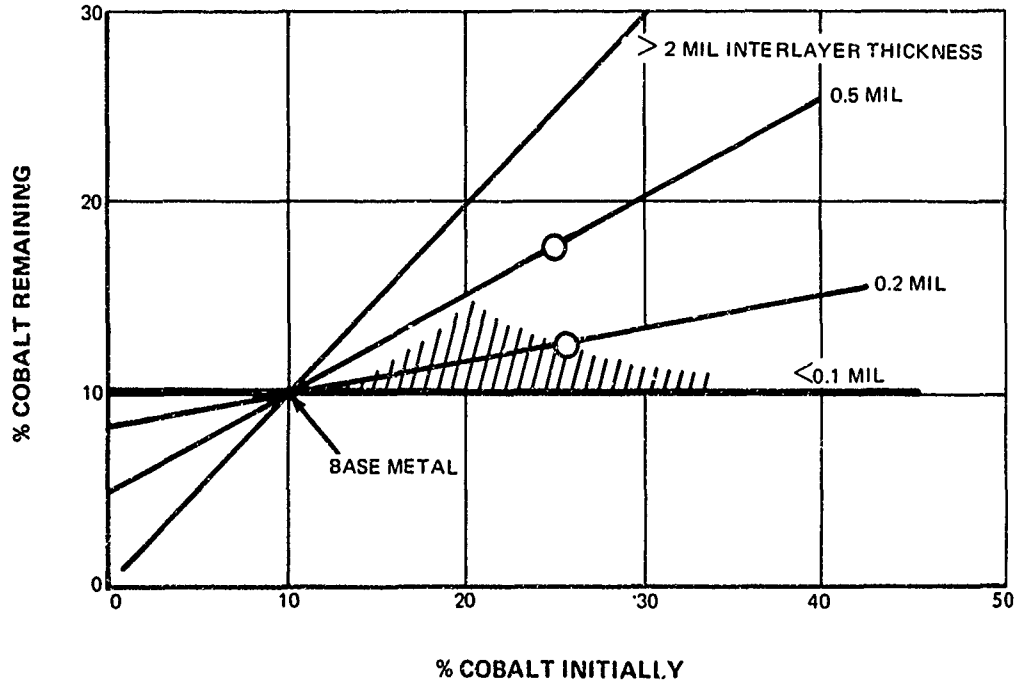

Figure 28 Final Joint Center Cobalt Content as a Function of Initial Interlayer Cobalt Content for Varying Thickness of Interlayer, After Diffusion Weld is Exposed to 2200°F for 4 Hours. Shaded area Represents Metallographically Homogeneous Joints

(2) Duvall, D. S., Owczarski, W. A., and King, W. H. and Paulonis, D. F., "Methods for Diffusion Welding the Superalloy U-700", Welding Journal, V51 - No. 2, February 1972.

In Figure 29, the final cobalt content and interlayer thickness are shown as they interrelate with the aluminum-titanium which diffuses into the joint. Naturally, the diffusion of the latter two elements is a function of the interlayer thickness. The shaded region in Figure 29 represents homogeneous microstructure; the positive slope is reflective of the depression of the γ' solvus by cobalt. As the cobalt content remaining in the joint increases, proportionately greater amounts of aluminum-titanium must be present to precipitate γ'.

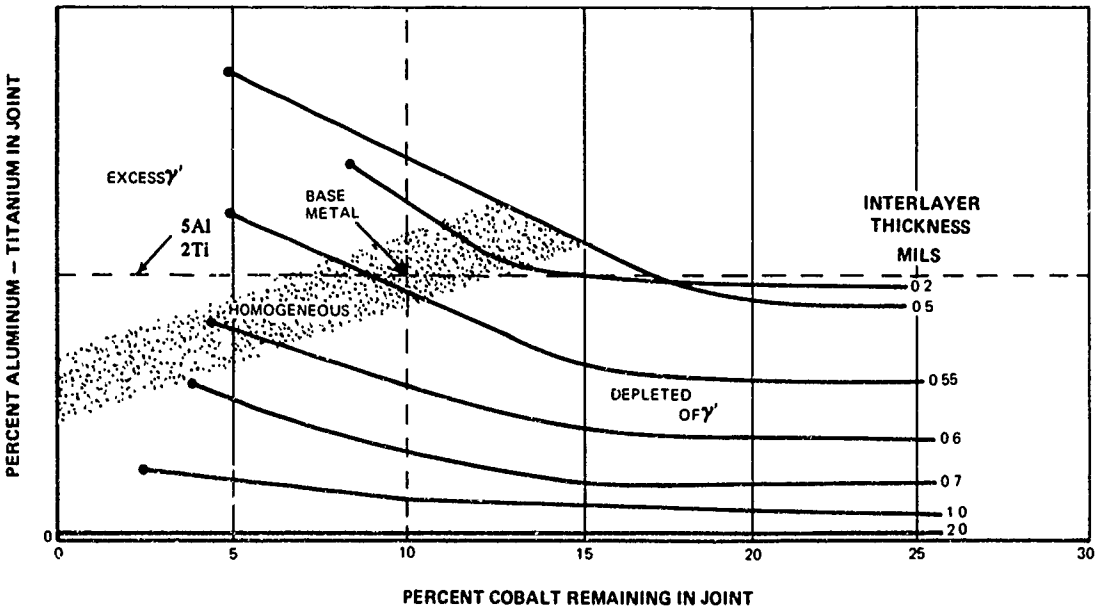

Figure 29 Relationship Between Microstructure and Diffusion Weld Joint Composition and Thickness After 2200°F/4 Hour Exposure. The Percent Cobalt Remaining is Determined From the Initial Interlayer Composition Using Figure 28. For a Given Thickness and Remaining Cobalt Content the Curves Indicate the Amount of Aluminum-Titanium in the Joint Center. Points at the Left End of Constant Thickness Lines Indicate the Percent Cobalt Remaining When a 100% Nickel Interlayer is used Initially.

Points to the right of the shaded region are depleted because of excess cobalt compared to the amount of aluminum-titanium (which can diffuse in). Points to the lef of the shaded region have excess γ'. Those points above the nominal base metal content of 5 percent Al, 2 percent Ti, represent conditions where "uphill diffusion" takes place against the apparent concentration gradient. (Uphill diffusion is evidently due to the effect of the distribution of the other elements (W, Cr, Cb, etc.) which are present in the base metal and absent in the joint.)

For any given interlayer thickness the aluminum-titanium content is related to the final cobalt content. This range is shown by lines intersecting the shaded region. The slight negative slope of these thickness curves is indicative of greater diffusion of aluminum-titanium into the joint as cobalt content lessens.

The termination of the lines at the left side of the figure indicates the minimum final cobalt (and Al-Ti) content which will result when a pure nickel interlayer is used.

In homogeneous joints between 0 and 0.5 mils, the concentration of aluminum-titanium increases with thickness. Very thin joints become essentially stabilized and equilibriated with the base metal regardless of transients they endured. It is important to remember in the following discussion that the relationships presented in Figure 29 are those which are existent (as a transient) after four hours at 2200°F. Under these conditions a joint near 0.5 mils with a final cobalt content in the range of 8-15 percent will have more titanium-aluminum than a thinner joint. Diffusion of elements against their apparent gradient in complex alloys is consistent with thermodynamic and diffusion theories.

Consequently, the surface which is the locus of aluminum-titanium/cobalt compositions will rise above base metal levels and then fall as thickness increases. Figure 30, which is a three-dimensional plot of Figure 29, shows this graphically. As thickness increases between 0 and 0.6 mils, the tolerable range of final cobalt, to achieve homogeneity is about the same. However, referring again to Figure 28, the initial cobalt content which will achieve that final range becomes quite narrow as thickness increases.

Figure 31 represents in graphic form the metallographic results of nickel-cobalt diffusion welds. The effect of initial interlayer thickness and cobalt content are related to the microstructure. For reference, isobars of remaining cobalt are shown - - these correlate with the relations shown in the preceeding figures.

The following general relations regarding diffusion dynamics are indicated:

- With thin (<0.05 mils) interlayers, homogeneous joints are achieved over a wide range of initial cobalt contents. Even at extreme cobalt levels the joint is sufficiently thin in relation to the diffusion time that any initial or transient gradients are overcome.

- As the interlayer thickness increases the range of cobalt content which gives homogeneous microstructure narrows because:

  a. At high cobalt levels outward diffusion of cobalt and inward diffusion of aluminum-titanium are insufficient resulting in a depleted joint.

  b. At low cobalt levels, the more rapid inward diffusion of aluminum and titanium compared to cobalt causes a consistent excess formation of gamma prime.

- As thickness increases the point is reached where cobalt is not necessary to prevent inward diffusion; in fact it must be decreased to promote gamma prime formation. This region, the narrow tail section on the right of Figure 31, is characterized by a joint which is deficient in all elements and not satisfactory despite its gamma prime homogeneity. Therefore, the absolute limit for thickness can be defined as that point at which the remaining cobalt content is lower than the cobalt content in the base metal.

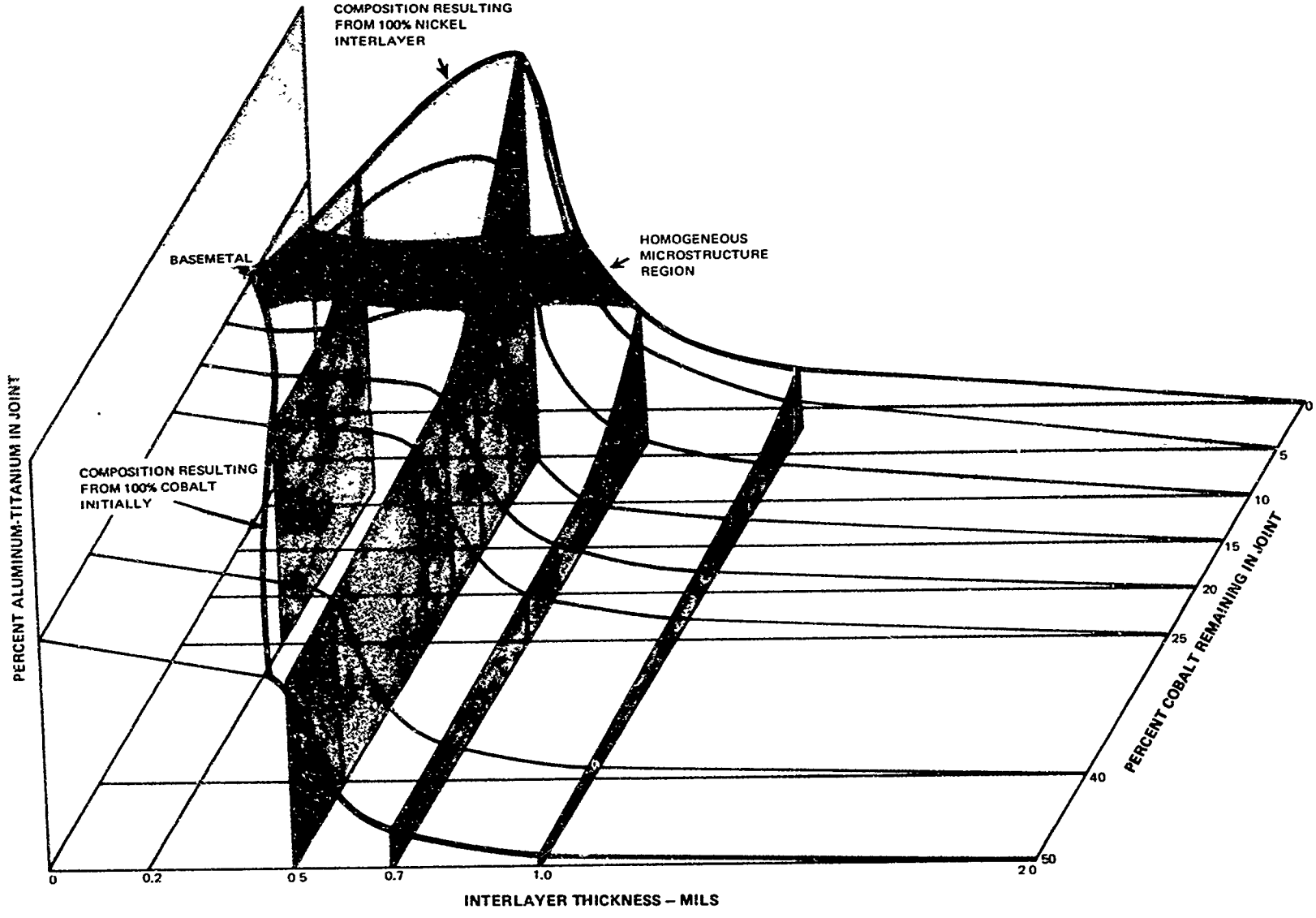

Figure 30 A Three-Dimensional Plot of the Relations Shown in Figure 25, Showing as a Surface the Compositions Which Occur in Diffusion Welds at Varying Interlayer Thicknesses.

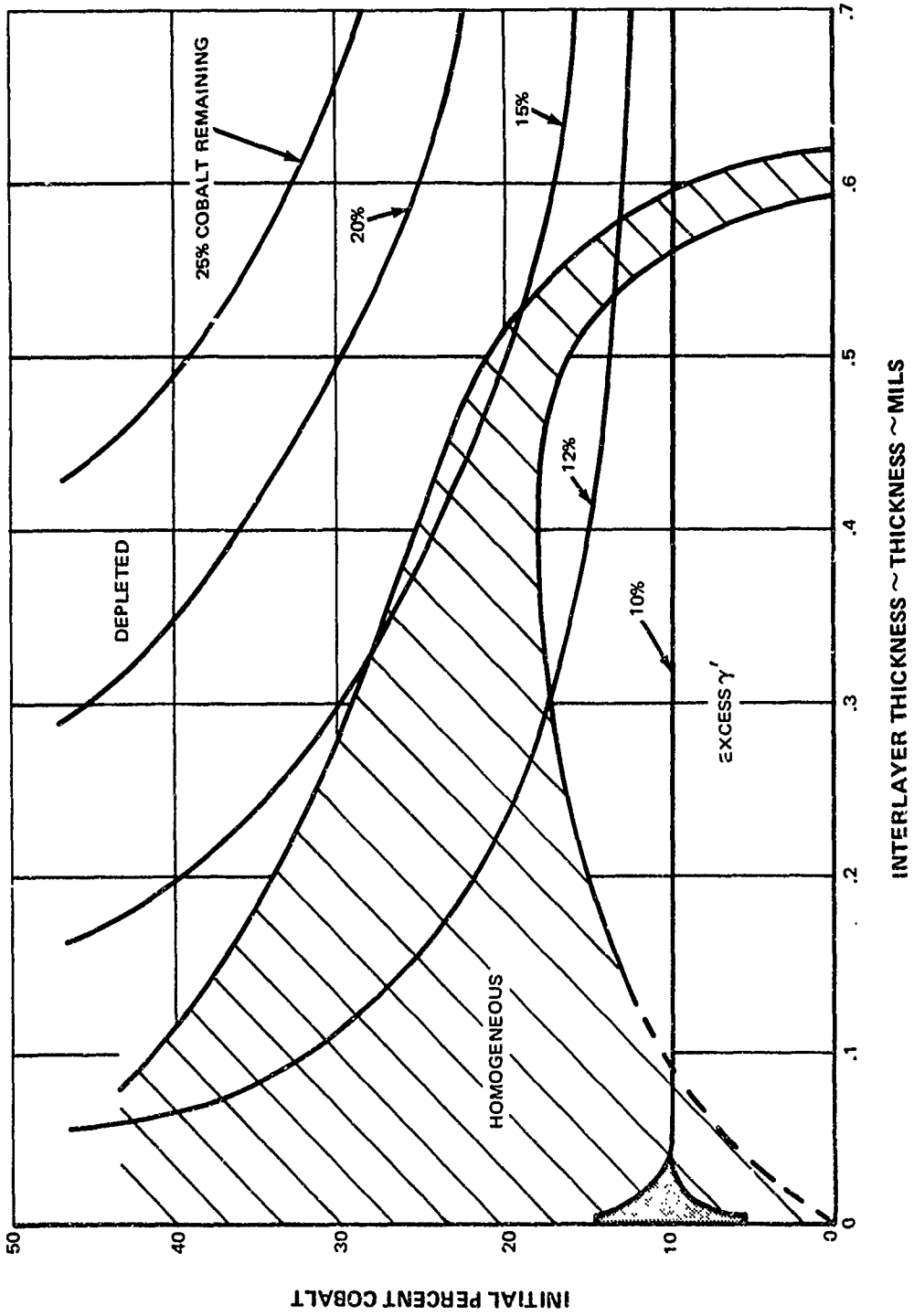

Figure 31 Empirical Relation Between Initial Interlayer Thickness and Composition and Microstructure in a Diffusion Weld After 2200°F/4 Hr. Exposure. Composition Becomes more Critical as Thickness Increases. This Figure Also Relates to Figures 28, 29, and 30.

Practically speaking, the limit on thickness is determined when the usable cobalt range narrows to the extent that reliable consistent joints are not produced due to the effect of minor base metal or parameter variations.

Based on the foregoing discussion, together with the results presented in the prior sections, the following general conclusions can be reached:

- Composition is not critical in very thin interlayers
- The range of satisfactory cobalt content decreases as thickness increases
- The practical maximum interlayer thickness for PWA 1422 diffusion welds is 0.5 mils and the optimum cobalt content is 20 percent when welding conditions are 2200°F/4 hours.

F. DISPERSION ELECTROPLATED DIFFUSION WELDS

To make possible thicker interlayers while achieving homogeneous joints, the principle of including heavier, slow-diffusing elements into a nickel-cobalt interlayer was evaluated. Tungsten and chromium particles were introduced in controlled amounts through the technique of dispersion electroplating previously described. Table A-2 in the Appendix lists dispersion plate diffusion welds.

A 0.1 mil dispersion electroplated interlayer joint (42Ni-28Co-9W-21Cr) was essentially homogeneous after diffusion welding and heat treatment (2200°F/1000 psi/1 HR + 2200°F/3 HR). However, several joints made using a slightly different composition (49NI-32Co-9W-10Cr) interlayer 0.5 mils thick cracked during heat treatment although they appeared sound as-welded. As shown in Figure 32 the joints contained fine particles throughout; these particles were unlike the contamination concentrated at the interlayer-base metal interface in the case of the nickel-cobalt joints. A third composition dispersion plate interlayer (61Ni-27Co-8Cr-4W) diffusion welded under constant pressure for a five hour period, and not subsequently heat treated, was sound as shown in Figure 33. All the aforementioned joints were depleted of gamma prime due to the high cobalt content.

The second composition joint described in the previous paragraph and shown in Figure 32 was examined by electron microprobe. The results shown in Figure 34 indicate that tungsten and chromium have been homogeneously solutioned in the interlayer and are present in somewhat greater concentration than in the base metal. The results also indicate that the fine joint particles are hafnium rich; fluorescence under the probe indicates that they are probably oxides.

A direct comparison is possible between this dispersion electroplated joint and the 0.5 mil nickel-25 percent cobalt joint previously described. It can be seen that dispersion electroplating is an effective way of getting tungsten and chromium homogeneously into the joint since they were slightly low when the nickel-cobalt system was used. It can also be concluded that the higher residual cobalt content (resulting from high percent cobalt in the interlayer) has prevented the formation of gamma prime in both cases.

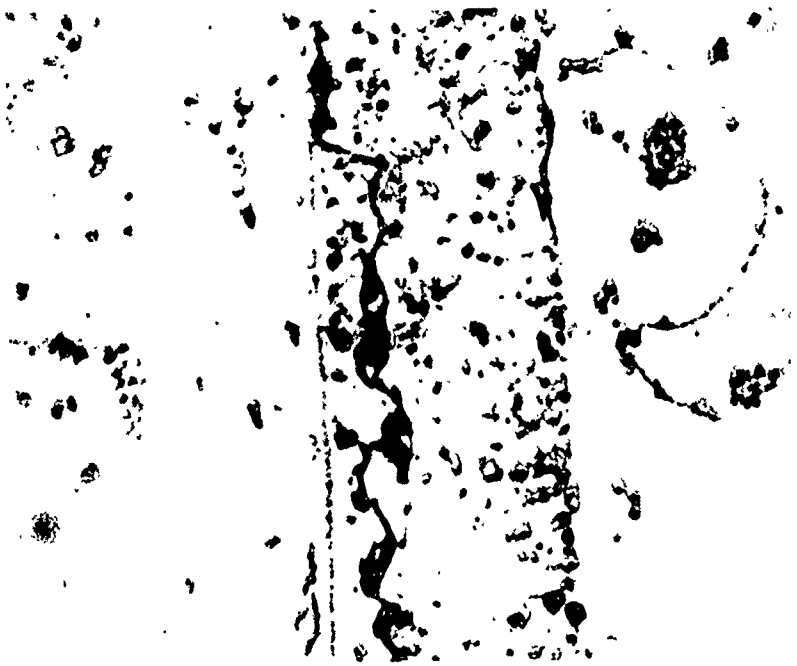

2200°F/500 PSI/1 Hr.
+
2200°F/3 Hrs.

A34H 1000X

Figure 32 Joint Using Dispersion Plate No. 40 (49Ni-32Co-9W-10Cr) Which Cracked After Heat Treatment; Interlayer was 0.5 Mils Thick

1950°F/2000 PSI/1 Hr.
+
2200°F/1000 PSI/4 Hrs.

A58-S46 500X

Figure 33 Joint Using 0.5 Mil Dispersion Plate (61 Ni-27Co-8Cr-4W) is Not Homogeneous Due to High Cobalt

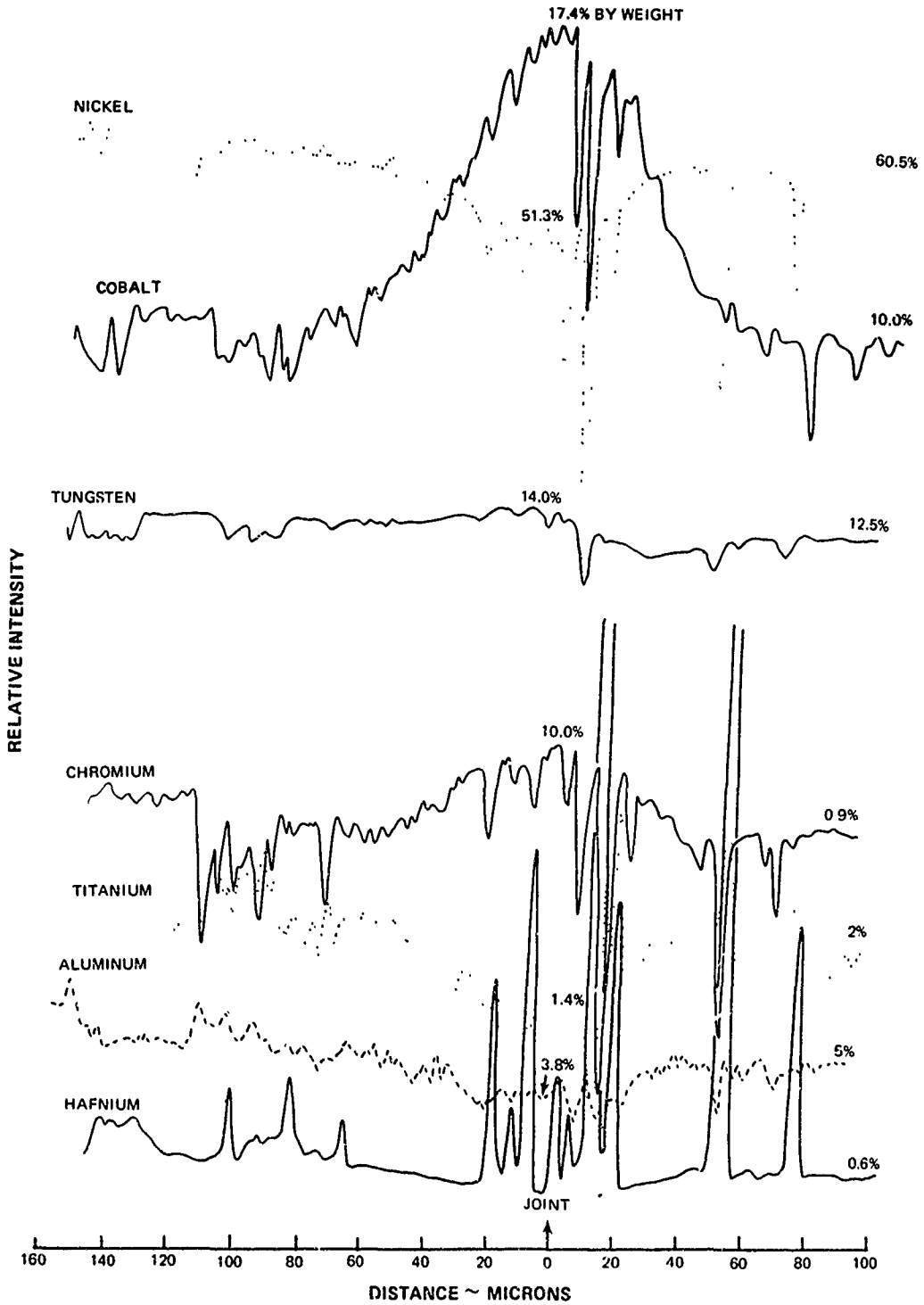

Figure 34 Electron Microprobe Analysis of a 0.5 Mil Dispersion Electroplated Interlayer (49Ni-32Co-9W-10Cr) Diffusion Welded (2200°F/500 PSI/1 Hr. + 2200°F/ 3 Hr.). The Joint Was Cracked (see Figure 32); Fine Particles Were Identified as Hafnium Rich Oxides. Tungsten and Chromium Have Been Solutioned; Cobalt Content is High.

Although they are relatively heavy elements, both hafnium and tungsten diffuse significantly at the temperature and times used. It can be speculated that hafnium has migrated into the joint region and reduced oxygen-containing compounds which were there.

As mentioned previously, when dispersion electroplated joints were formed by a one hour welding cycle they were sound. However, subsequent heat treating caused the weld to crack. This was attributed to the formation of oxide compounds during the diffusion cycle, as well as cooling stresses. Cracking was also observed within thick electroplates which were heated in air after detachment from the substrate. Welding specimens in one thermal cycle only, e.g. 2200°F/4 hr, produced joints which were generally sound although some were still intermittently cracked.

Based on the foregoing results, an additional bath (solution No. 52) was made with the aim of producing a lower-alloyed electroplate. The plating results were:

	Ni	Co	Cr	W
Target %	68	10	10	12
Actual	64	13	8	15

Diffusion welds made using the lower alloy content dispersion electroplate from solution No. 52 tended to be more homogeneous than prior joints. With the exception of the fine oxides, 0.1 and 0.3 mil joints were homogeneous. As shown in Figure 35, a 0.5 mil interlayer joint was almost completely homogeneous at the end of the 2200°F/500 psi/5 hr. welding cycle, and superior to prior welds with higher cobalt content dispersion interlayers.

Some dispersion electroplates were heat treated under vacuum both without joining, and prior to the joining cycle, to ascertain the effect of such a cycle (2100°F/1 hr) on the formation of particles. There was no discernible improvement. MAR-M200 (hafnium-free PWA 1422) was electroplated with an interlayer from solution No. 52 and diffusion welded. The joint region was found to contain fine particles, slightly different in appearance, which are presumably oxides of titanium or aluminum as shown in Figure 36. Consequently the formation of particles within the dispersion electroplated interlayer is not peculiar to hafnium-containing base metals.

As described previously in the section on dispersion electroplating development, an analysis was made for oxygen and sulfur in the as-plated interlayer after observation of fine oxide particles in the joint. The analysis showed high amounts of oxygen and sulfur in the dispersion electroplate which were not removed prior to welding, indicating an inherent problem in the process.

The deleterious effect of the inclusion of oxygen is indicated in the prevalent failure of specimens during heat treatment. Therefore, even though dispersion electroplating seems to have merit insofar as its intended purpose of increasing interlayer thickness or reducing diffusion times, it is inherently unusable as cu··ntly developed.

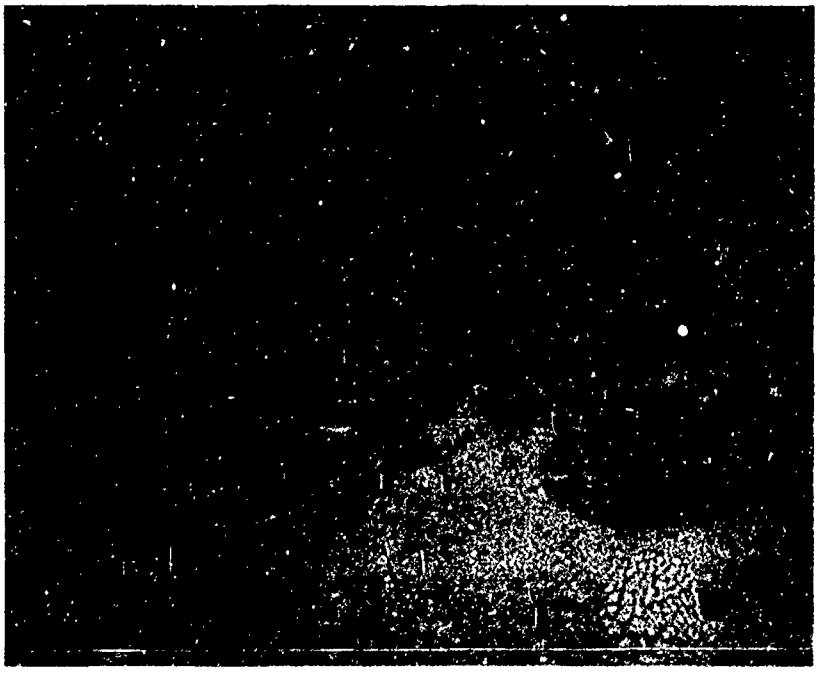

2130°F/500 PSI/5 HRS.

Figure 35 Lowering of the Cobalt Content Makes a Joint Using 0.5 Mil Dispersion Plate (64 Ni-13Co-8Cr-15W) Homogeneous Except for Typical Fine Oxides

2170°F/4000 PSI/30 Min.
+
2165°F/1500 PSI/90 Min.

A143 1000X

Figure 36 MARM 200 (Hafnium-Free PWA 1422) Joint With 0.3 Mil (64Ni-13Co-8Cr-15W) Dispersion Interlayer Showing Fine Particles Also Occur in the Absence of Hafnium

G. INTERMEDIARY FOILS

The intent of using a thin ductile foil as an intermediary between the faying surfaces of a ribbed specimen was to ascertain the capacity of such a system to accommodate the lack of fit and surface irregularities in the joint surfaces. A depleted alloy Foil A (67Ni-10Co-9Cr-12W-1Cb) was used to observe the mechanical phenomena, but it was not anticipated that this foil would yield a completely homogeneous joint. Table A-III in the Appendix lists foil intermediary diffusion welds.

Parameters typical of joints without intermediaries (2200°F/500 psi/1 hr) were used for welding and sound but heterogeneous joints were formed (see Figure 37). Similar results were obtained whether an electroplate was applied or omitted from the foil surface; in all cases the specimen's base metal surfaces were electroplated. The inhomogeneous structure remained after heat treatments of up to 26 hours at 2200°F (see Figure 37). A widening of the region deficient in gamma prime indicated a decrease in concentration of aluminum and titanium in the adjacent base metal.

These observations were borne out in the microprobe analysis of the foil joint shown in Figure 37b. This analysis shown in Figure 38 indicated that the joint was homogeneous with the base metal with the exception of aluminum and titanium. Regions of locally high cobalt are observed on either side of the joint due to the 0.2 mil ni-25% cobalt interlayer applied. It appeared joint homogeneity is not feasible with a foil of this thickness without the introduction of additional titanium and aluminum.

Observations were made of the degree to which the foil was deformed during the diffusion welding cycle. Since normal parameters produced no preferential upset in the foil, an additional creep-forming step was introduced. Pressure of 1000-4000 psi was applied in constant or progressively increasing steps while the specimen was at 1800-2000°F for approximately one hour, before starting the normal diffusion cycle. No substantial plastic deformation, upsetting, or extrusion of the foil was observed, although severe cracking due to the specimen configuration occurred in the channel sections at the higher pressures.

As a result of apparent low rates of deformation in initial Foil A joints, tests were run to compare the creep behavior of the foil alloy to the base metal. Bars ¾ inch diameter by 1 inch long were compressively stressed at 1000 psi for four hours at 2200°F. The results, presented in Table VIII, show there is considerable variation in the creep behavior of both the superalloy and foil material. Scatter in creep data from tensile and compressive tests of cast alloys is not unusual. In addition, the test temperature here approximates the incipient melting point, and therefore otherwise minor test or material variables can become significant.

Analysis of the data shows that Alloy A creeps three times faster than equiaxed PWA 1422 (significant within 95% level of statistical confidence) Consequently, the choice of foil alloy was correct from the standpoint of deformability. Observed limitations in defect accommodation by foils can be attributed to mechanics of the joint, e.g., the aspect ratio--the ratio of the width to thickness of the intermediary within the joint.

A

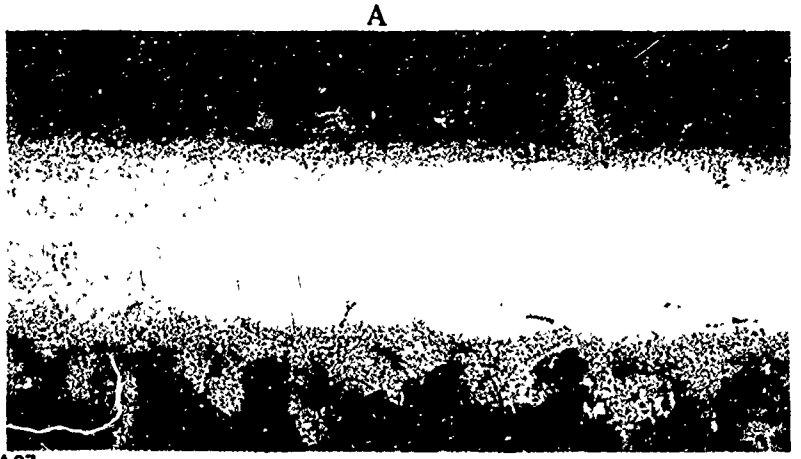

A27 150X

As welded at
2200°F/500 psi/1 hr.

B

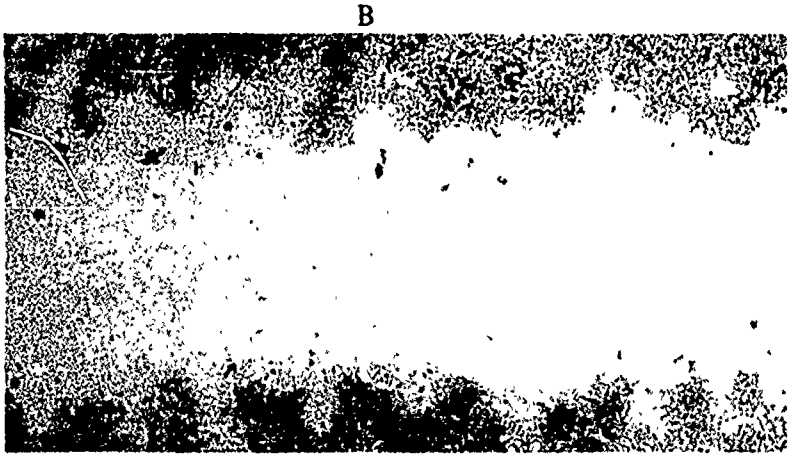

A27 150X

Heat treated at
2200°F/3 hr.

C

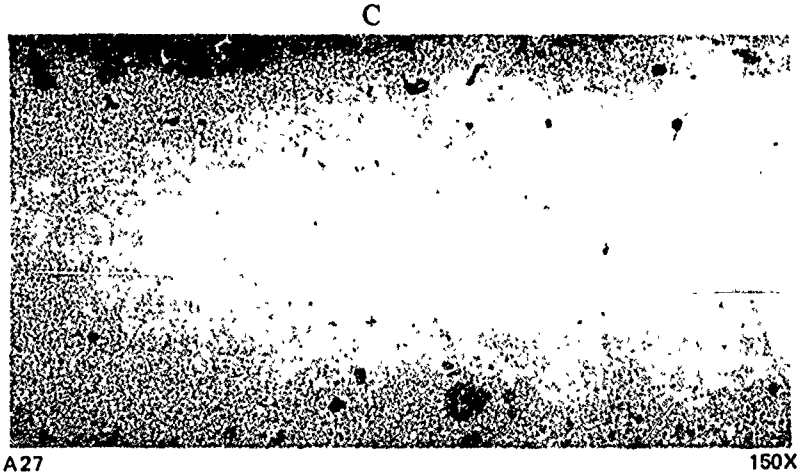

A27 150X

Heat treated at
2200°F/26 hr.

Figur. 37 PWA 1422 Diffusion Welded With A Rolled Modified Alloy Intermediary Foil 3.5 Mils Thick; 0.1 Mil Nickel - 30% Cobalt Interlayer On All Surfaces. The Depleted Region Expands With Increasing Heat Treatment Time Due To The Diffusion Of Aluminum And Titanium In The Joint.

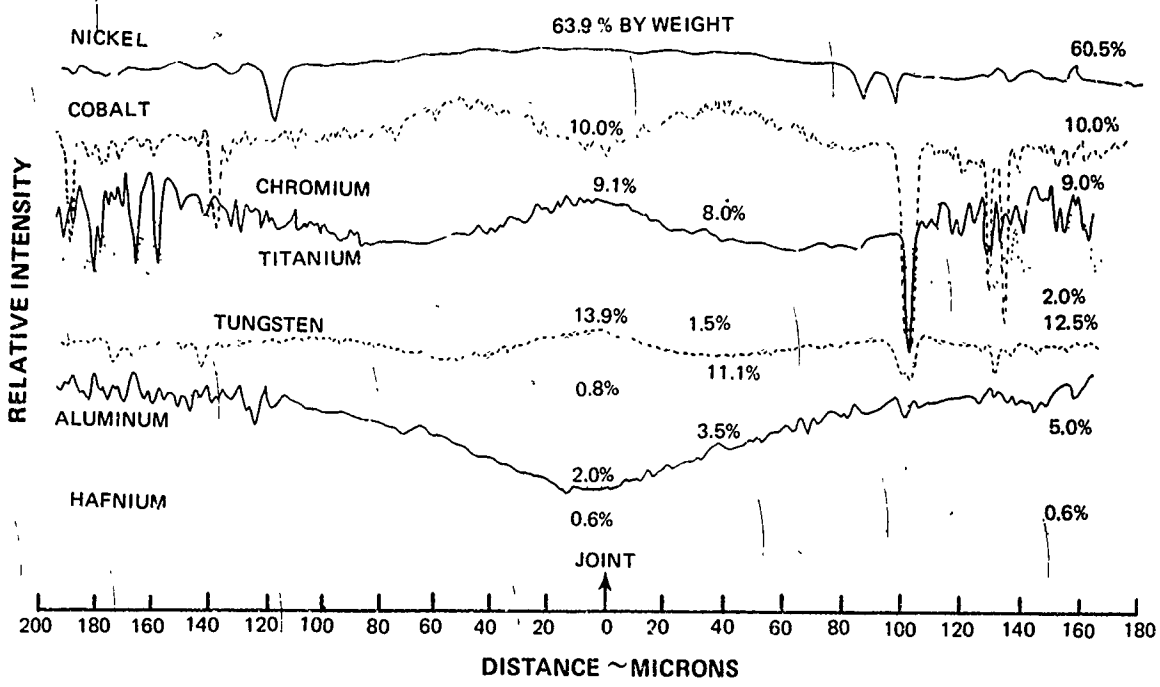

Figure 38 Electron Microprobe Analysis of 3 Mil Foil A Intermediary (68Ni-10Co-9Cr-12W-1Cb) Diffusion Weld (2200°F/500 PSI/1 Hr. + 2200°F/3 Hr.), Also Shown in Figure 3d. Joint Center is Low in Aluminum and Titanium; the 0.2 Mil Nickel-25% Cobalt Interlayer Left Residually High Cobalt on Either Side of the Joint

TABLE VIII
COMPARISON OF CREEP BEHAVIOR

Compressive Creep Behavior Under 1000 psi at 2200°F for 1 Hour, Using ¼ Inch Diameter by 1 Inch Long Bars

Material	Specimen	% Creep
PWA 1422 (equiaxed)	38	.03
	39	.44
	40	.04
	41	.93
	42	.00
	43	.09
	Average	.26
	2σ	.73
Foil Alloy A	44	.13
	45	1.22
	46	1.26
	47	.55
	49	.67
	Average	.77
	2σ	.94

Based on the metallographic and microprobe results, Foil B (60Ni-10Co-8Cr-12W-2.5Ti-5Al-0.85Cb) was cast and rolled. As anticipated, joints made using 6 mil Foil B exhibited a considerably more homogeneous structure than Foil A as shown in Figure 39, even though Foil B is shown only as-welded. After a weld cycle of 2150°F/200 psi/5 min + 2200°F/500 psi/2 hr., the joint region is rich in gamma prime, reflective of the original foil composition (see Table VI). The angular appearance of the gamma prime is attributable to recrystallization during welding following the considerable strain imparted during foil rolling. Figure 47d, an additional Foil B joint, is shown wherein homogeneity is virtually achieved after two hours using a 0.5 mil interlayer. In contrast to Foil A, the presence of aluminum and titanium necessitated the application of an 0.2 mil Ni-25 percent cobalt interlayer to Foil B to avoid the formation of undesirable interfacial precipitates.

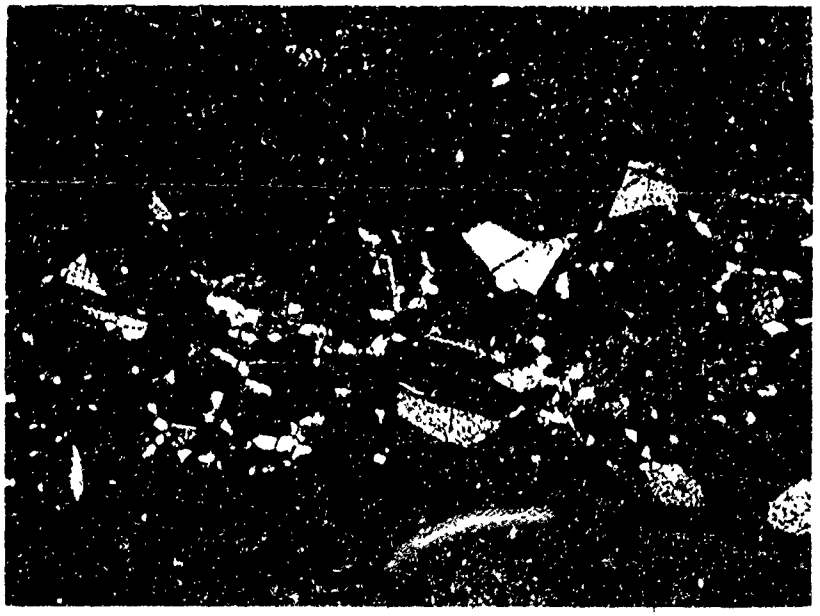

2190°F/500 PSI/2 Hrs

A155 250X

Figure 39 As-Welded Joint Made With 6 Mil Foil B and 0.2 Mil Nickel-25% Cobalt. White Phase is Believed to be Massive Gamma Prime (γ')

Another joint (Figure 47d) using an 8 mil Foil B intermediary between 0.5 mil nickel-20 cobalt as-cast surfaces was examined by electron microprobe in the as-welded condition (2200°F/2 hr). The results (Figure 4C) confirm metallographic observations and indicate the joint is considerably more homogeneous than a comparable joint made with Foil A despite the increased thickness and shorter bonding time. The local areas of high cobalt concentration on either side of the joint are attributable to the nickel-cobalt interlayers. The white phases which appeared in the joint center are high in nickel, titanium, and aluminum, and therefore are evidently gamma prime. Although the joint region is slightly richer than the base metal in gamma prime the usual additional two hour heat treatment at 2200°F improved homogeneity somewhat. The composition and thickness of Foil B appeared acceptable for the purposes of the program.

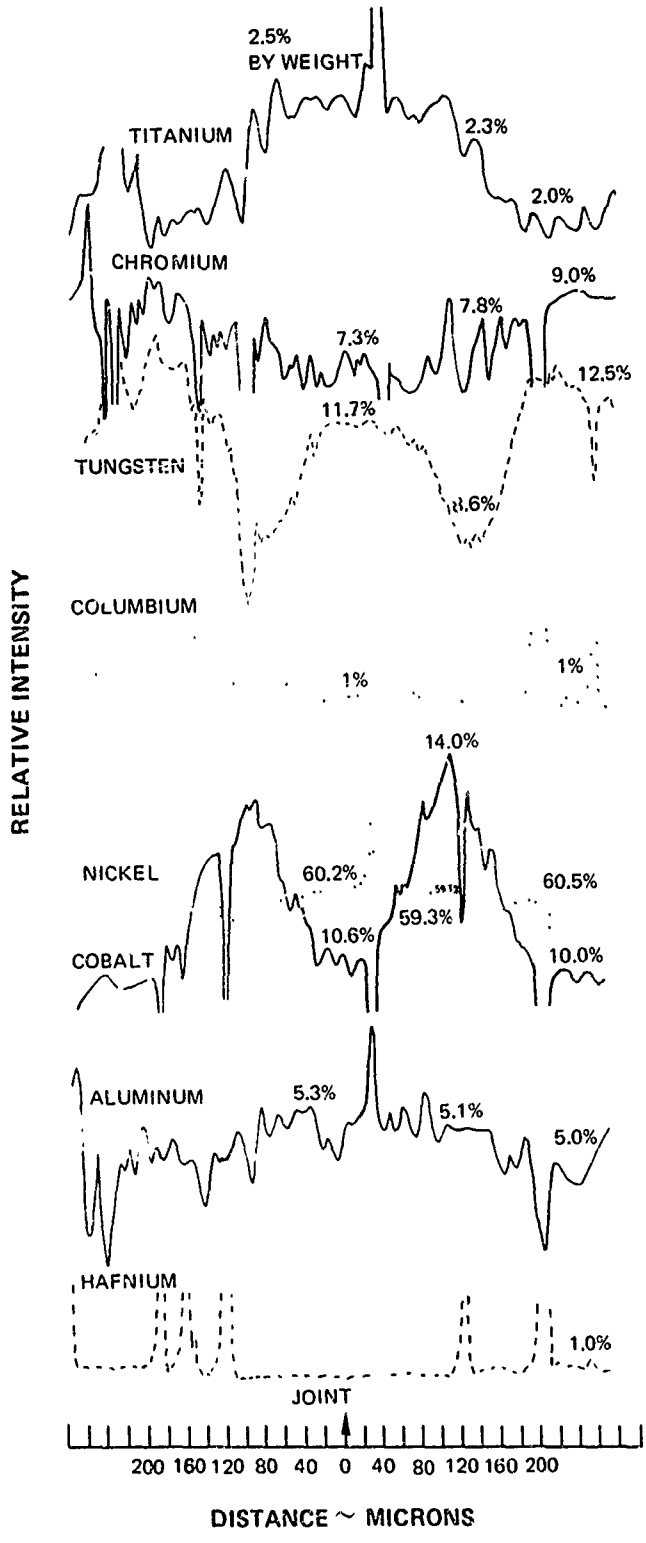

Figure 40 Electron microprobe analysis of an 8 mil Foil B intermediary and 0.5 mil nickel-20% cobalt interlayer diffusion weld between PWA 1422 as-cast surfaces (2170°F/750 psi/2 Hr). Although slightly rich in aluminum and titanium the joint is fairly homogeneous after a two hour cycle.

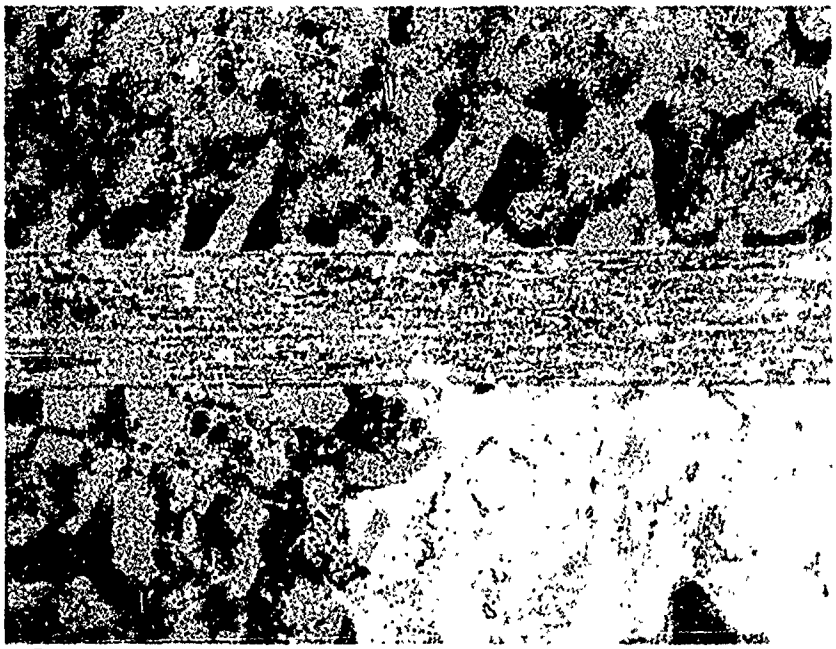

A25 150X

2200°F/500 psi/1 hr.
+
2200°F/3 hr.

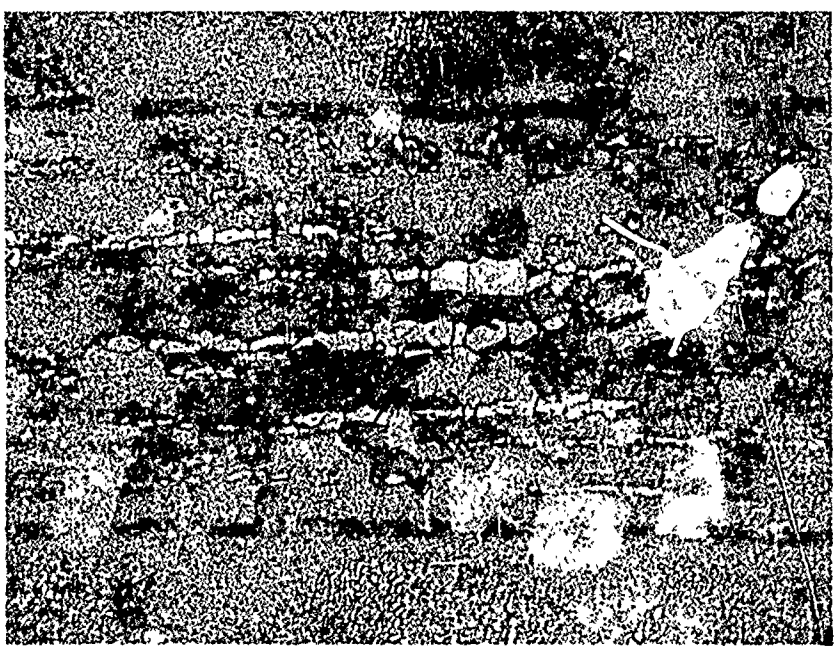

A25 500X

2200°F/500 psi/1 hr.
+
2200°F/3 hr.

Figure 41 PWA 1422 Diffusion Welded with a Rolled PWA 1422 Intermediary Foil 4 Mils Thick; 0.1 Mil Nickel - 30% Cobalt Interlayer. A Sound Joint is Produced With Retention of the Directional Structure of the Foil.

Although the program scope precluded extensive investigation, a few joints were made using cold rolled 4 mil PWA 1422 foil intermediary. Metallographic analysis revealed the microstructure shown in Figure 41. The joint has retained the orientation of eutectic gamma prime which existed in the rolled foil and which appears to reflect excess gamma prime in the original foil casting.

H. MECHANICAL RESULTS OF 1 X 1 SPECIMEN WELDING UPSET IN WELDED SPECIMENS

While in some types of welding, as well as analysis of diffusion welding, upset or deformation is an input parameter, in this program it was considered to be an output – the effect of the combination of pressure, temperature, and time inputs. It is evident that the meaning of upset, as well as its relation to pressure, is dependent on specimen shape and the manner in which upset is measured. The most meaningful measure, when it is possible, is to measure the local deformation in the weld region.

Ribbed 1 x 1 inch PWA 1422 specimens with nickel-cobalt interlayer joints in varying composition and thickness have been diffusion welded over the following range of parameters:

Temperature:	2140 to 2240°F
Pressure:	280 to 2200 psi
Time:	1 to 4 hrs.
Thickness:	0.07 to 0.7 mils

Figure 42 illustrates the effect of pressure on upset for the 1 x 1 inch ribbed specimen when temperature is nominally 2195°F. (Upset is the average of four readings of the change in dimension of the internal channels - see Figure 9). The width of the 2σ band for the least squares line shown in Figure 42 is 6.2 mils, and is reflective of the substantial variations in upset.

Figure 43 illustrated the effect of temperature on upset, when the pressure is maintained constant at 1000 psi on the joint. As with the effect of temperature, the trend seems consistent with related experience. The width of the 2σ band is 6.8 mils for the least squares line shown.

The variability in upset can be in part ascribed to experimental error, but probably more to the variable compressive creep properties of the base metal. The results of the comparative evaluation of creep strength of Foil A and PWA 1422 base metal which were previously discussed, indicated that there was considerable variability in the PWA 1422 creep behavior under carefully controlled conditions. It is apparent that adequate die design or external mechanical constraint is needed to closely control dimensions of structures made from PWA 1422.

1. Cracking in the Base Metal

Cracking has been frequently observed in the specimen away from the joint, primarily over the channel section. Generally, this has occurred at higher upsets (> 0.010 inches) produced by excessive pressure or temperature. An example of this type of cracking is illustrated in Figure 44.

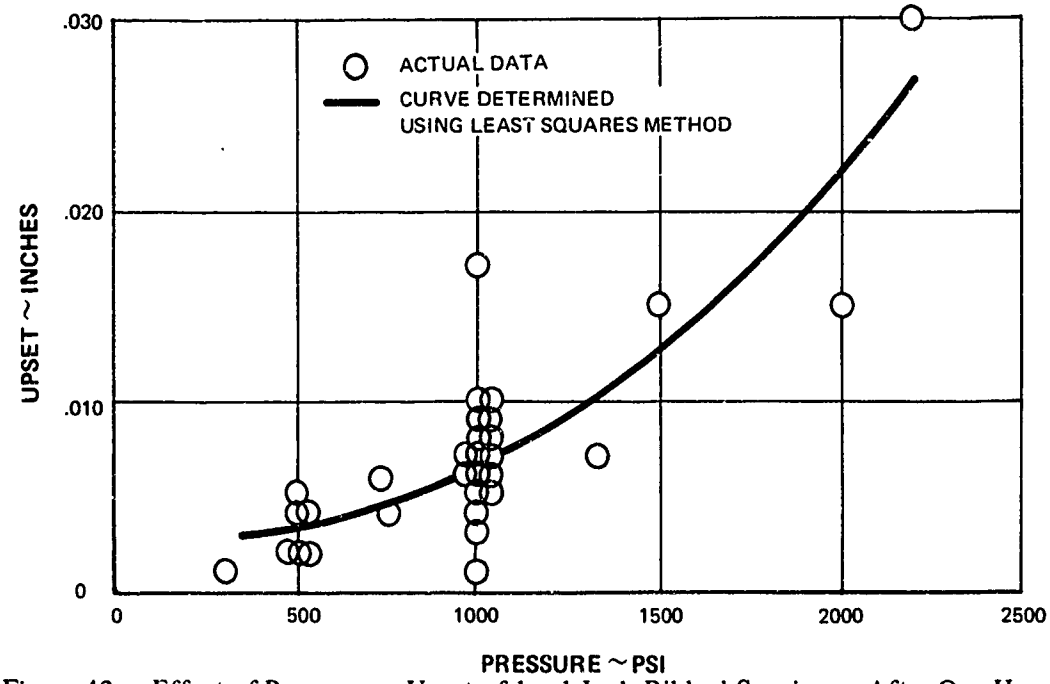

Figure 42 Effect of Pressure on Upset of 1 x 1 Inch Ribbed Specimens After One Hour at 2190-2200°F With Nickel-Cobalt Interlayers

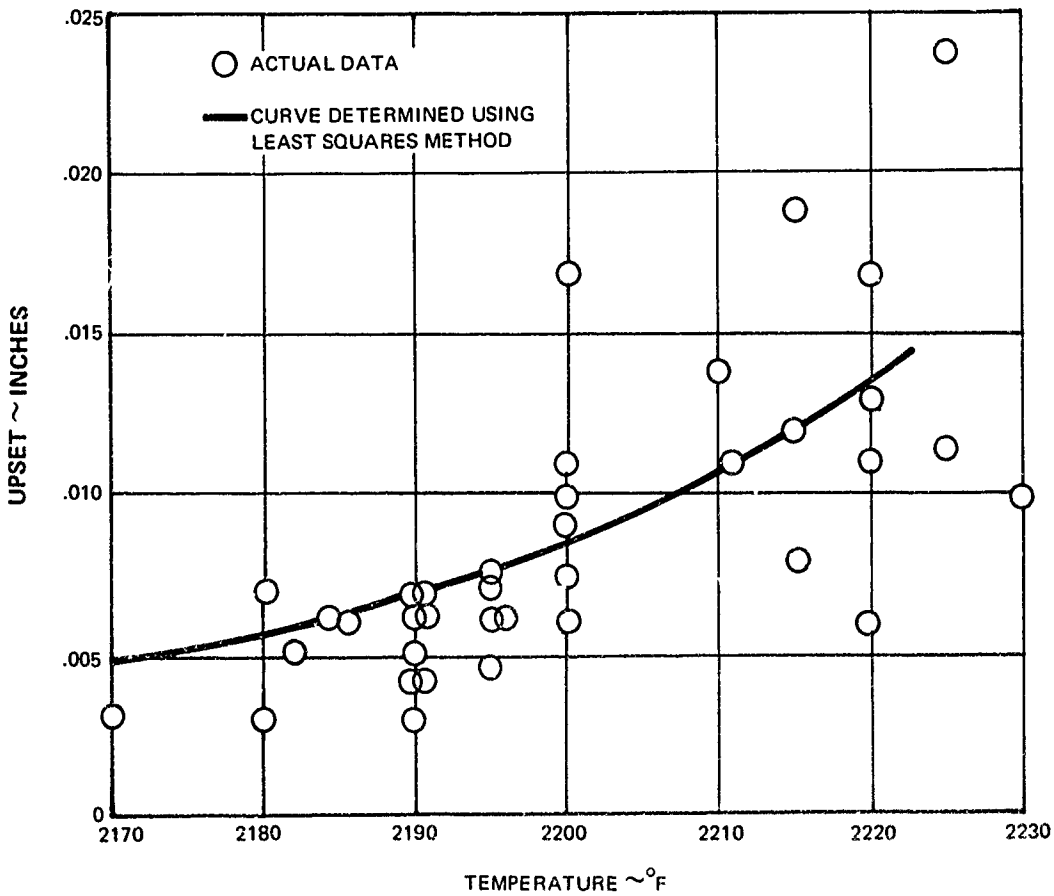

Figure 43 Effect of Temperature on Upset of 1 x 1 Inch Ribbed Specimens After One Hour at 1000 PSI Average Joint Pressure With Nickel-Cobalt Interlayers

2170°F/750 PSI/2 Hrs

A158 10X

Figure 44 Intergranular Channel-Section Cracking in Base Metal Due to Excess Pressure on Foil Joint

Cracks can be avoided by lowering the temperature or welding pressure. A successful joint between poorly fitting specimens can only be achieved by pressure sufficient to bring the surfaces together; excess deformation must be limited to avoid cracks.

To assess the difficulty in welding thin wall structures using the necessary parameters for a good metallurgical joint, standard 1 x 1 ribbed specimens were altered so that the web thickness was reduced from 0.200 to 0.050 inches. Using flat PWA 1422 dies six successful joints were made without base-metal cracking, using a pressure of 1,000 psi and a temperature biased downward slightly to the 2175°F range. Normal looking joints were also produced between 1 x 1 inch specimens which had been electric discharge machined on the faying surface. (Due to the state of process development and the tooling complexity, electric discharge machining (EDM) was not used for preparing the split halves in this program. It would, however, be applicable in any production situation.)

2. Cracking in the Weld

Several welds made using nickel-cobalt interlayers of varying thicknesses were found to be cracked after the completion of the one hour welding cycle, although prior joints of similar thickness and composition had been sound.

The following comments can be made of the cracked welds:

- Some were associated with purposely altered plating procedures or very thick (0.8 mils) interlayers.
- Generally specimens had low upset, and consequently a reduced contact area in the joint as well as deep notches at the edges.
- Single specimens between ceramic spacers were more likely to crack than specimens stacked three-high.
- All were cooled by radiation to the chamber when power was turned off at the end of the cycle.

It was presumed that cracking was primarily a function of the thermal stresses to which the specimen is subjected on cool-down. The specimen design probably accentuated the effect, especially when coupled with the decreased joint area of low upset joints and the inhomogeneity (and low strength) of as-welded joints.

Cracking was effectively eliminated by decreasing the cooling rate through controlled power reduction at the end of the cycle. An altered rate which prevents cracks is shown in Figure 45 compared to the natural radiation cooling rate.

Other steps that were also taken to reduce the likelihood of any as-welded cracks include increasing the welding cycle time to promote more homogeneity, increasing the joint pressure to achieve total joint contact, and holding long-cycle welded joints at a high temperature (nominally 2000°F) to promote the strengthening formation of gamma prime prior to the final cool-down.

3. Edge Effects

Due to the as-cast nature of the ribs, precise alignment of the specimens was rarely achieved. Therefore, the joint configuration at the edge approximated that of a tee rather than a straight butt. Notching, or a vee-shaped gap, is often reported at the external edges of diffusion welds. This can be attributed to a combination of rounded edges, inadequate upset and lowered stresses in this region. In this program there was no propensity toward edge notching in specimens with mean welding conditions and discernible upset. The distribution of the electroplating thickness on the faying rib surface was viewed as a constructive element towards this result.

Flashing or extrusion at the edge of the joint was observed quite commonly (see Figure 46). This is attributed to the variation in the electroplate thickness (edge build-up) coupled with the ductility of the interlayer. To the extent that this effect aids in avoiding the notching effect sometimes observed in low upset diffusion weld joints, it can be considered favorable. In the production of actual parts various steps could be taken to eliminate flashing if desired.

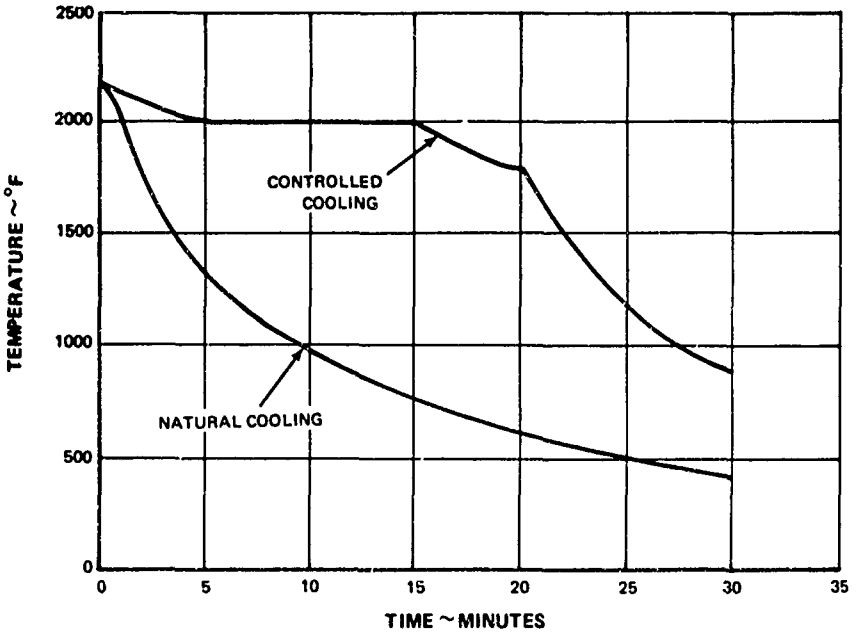

Figure 45 Cooling Rates of 1 X 1 Inch Ribbed Specimens in Diffusion Welding Press

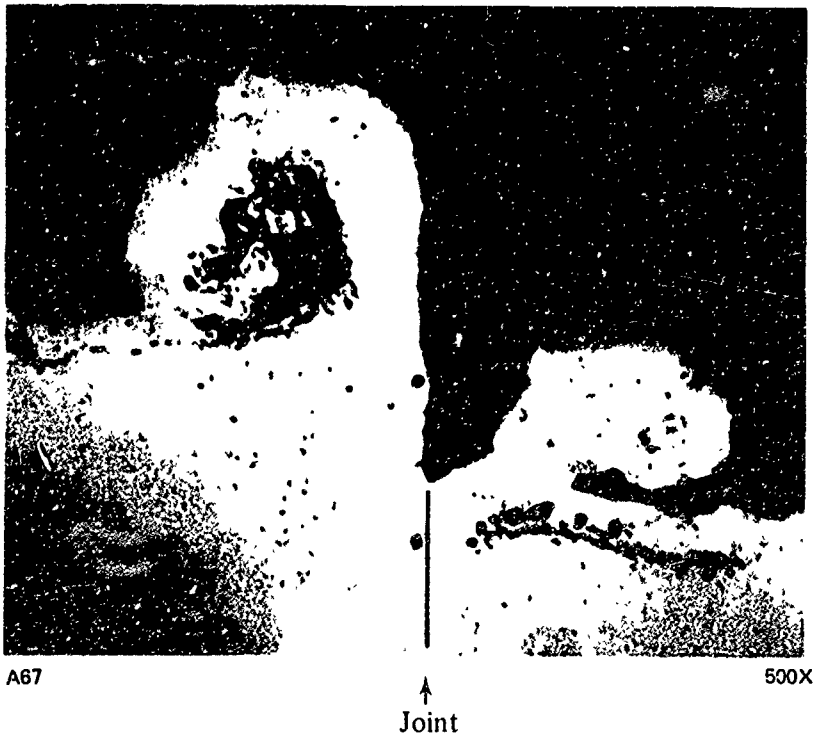

Figure 46 PWA 1422 Diffusion Welded with a 0.5 Mil Nickel - 25% Cobalt Interlayer Shows a Flashing at the Joint Edge that is Believed to be Related to Electroplate Buildup at the Edges and Extrusion During Welding

I. COMPARATIVE EVALUATION OF JOINING SYSTEMS

1. Defect Accommodation

One of the objectives of this development program is to extend the useful range of heretofore thin interlayers for diffusion welding cast superalloys to split blade fabrication. A suitable specimen to compare the ability of the various systems to accommodate lack of fit was difficult to contrive.

A cursory evaluation of the capability of a ductile foil to fill in small purposely machined-in defects was made. Tapered grooves (0.001 to 0.010 inches deep by 0.075 inches wide) were machined through the ribs perpendicular to the channel length in one faying surface of the joint. These filled to a depth of 0.005-0.007 inches by lateral local flow of the foil in the initial trials. However, this type of defect was difficult to accurately prepare and was considered unrealistic with respect to the anticipated lack of fit between split blade halves.

When joints were made between as-cast surfaces it appeared that a measure could be made of the ability of the system to accommodate lack of fit. As-cast surfaces are nominally planar, and have a surface roughness of nominally 60 rms. When mated as pairs, the faying surfaces may have a gap of 10 mils or more prior to application of the welding pressure.

When welding as-cast surfaces it appeared advisable to yield, rather than creep, the specimens together. The functional aspects of the interlayers could be obviated if the faying surfaces were not in contact before diffusion altered interlayer composition significantly. Consequently, high pressure was applied for a short duration, usually five minutes, and then reduced to a lower level, as reported in the Tables in the Appendix.

Joints were made between as-cast , vapor-honed surfaces using different interlayer systems and identical welding parameters. Metallographic examination and ultrasonic inspection yielded the following results:

- No interlayer, as shown in Figure 47a, produced a joint which had considerable porosity.
- A 0.2 mil nickel-25% cobalt interlayer, shown in Figure 47b, produced greater contact in the joint, but still contained slight porosity.
- A 0.5 mil nickel-20% cobalt interlayer (Figure 47c), 0.5 mil dispersion electroplate, and 8 mil Foil B with 0.1 mil Ni-20% cobalt interlayer against a 0.5 mil interlayer base metal (Figure 47d) all produced sound joints, as indicated by the ultrasonic C-scans accompanying the figures.
- Between the faying surfaces of the as-cast specimens it was observed that an 8 mil foil compressed within the joint nominally varied in thickness between 4 and 6 mils, seeming to accommodate a 2 mil lack of fit.

(a)
No Interlayer Showing Unsoundness (2100°F/ 2000 PSI/5 Min. + 2120°F/750 PSI/4 Hrs.)

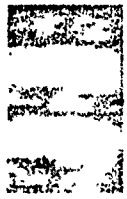

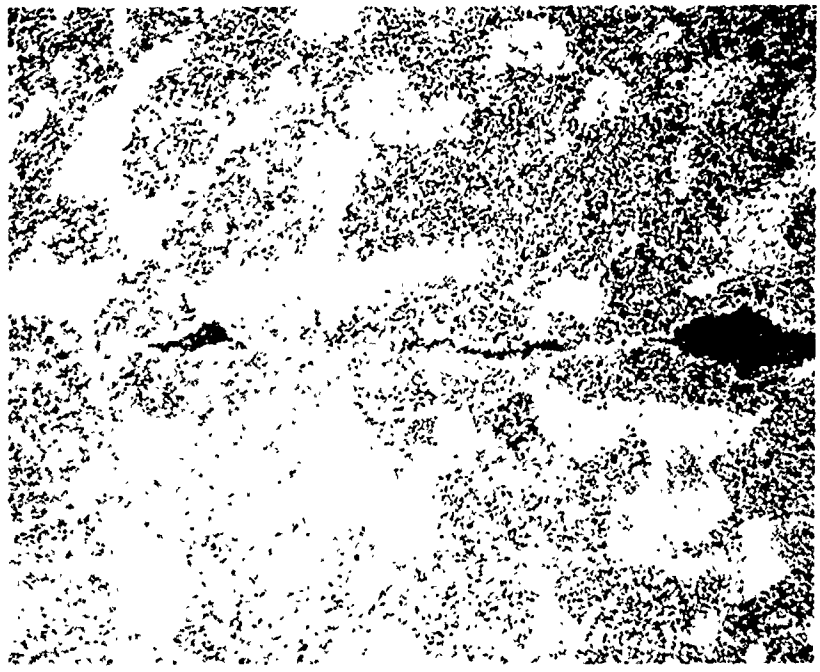

A156 250X

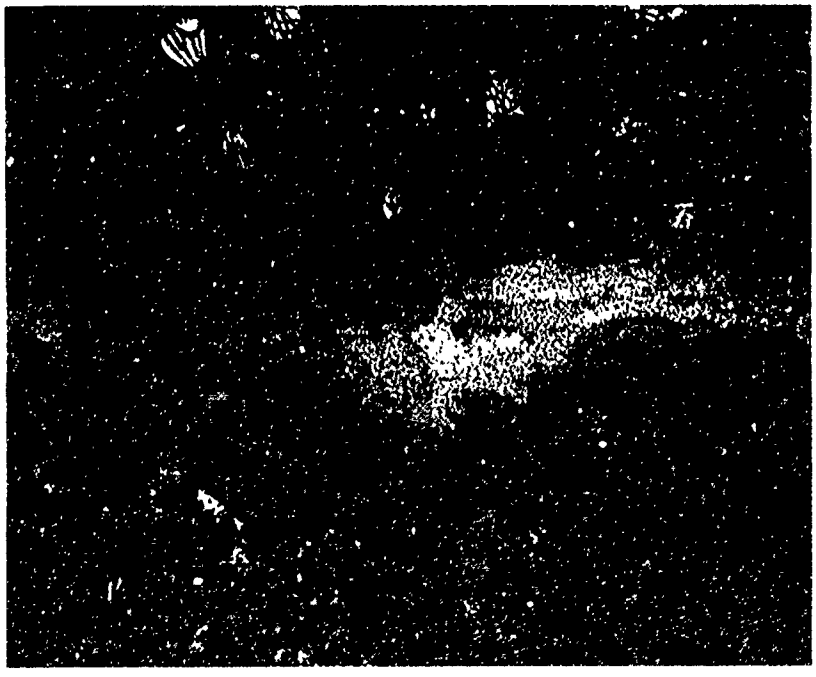

(b)
0.2 Mil Ni-25Co Interlayer Shows an Improvement Over No Interlayer. Slight Porosity Shown in C-Scan Can Be Found Occassionally.
(2060°F/2000 PSI/5 Min. + 2120°F/500 PSI/2 Hrs.)

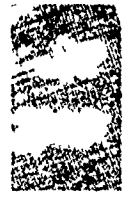

A142 250X

Figure 47 As-Cast Faying Surface Joints Showing Defect Accommodation of Interlayer Systems and Correlation with Ultrasonic C-Scan Prints (Small Inset)

(c)
0.5 Mil Ni-20%Co Interlayer is Sound and Homogeneous Even After 2 Hours. Improperly Sandblasted As-Cast Faying Surface Joints Have the Dark Phase Shown. (2110°F/2000°F/5 Min. + 2160°F/500 PSI/2 Hrs.)

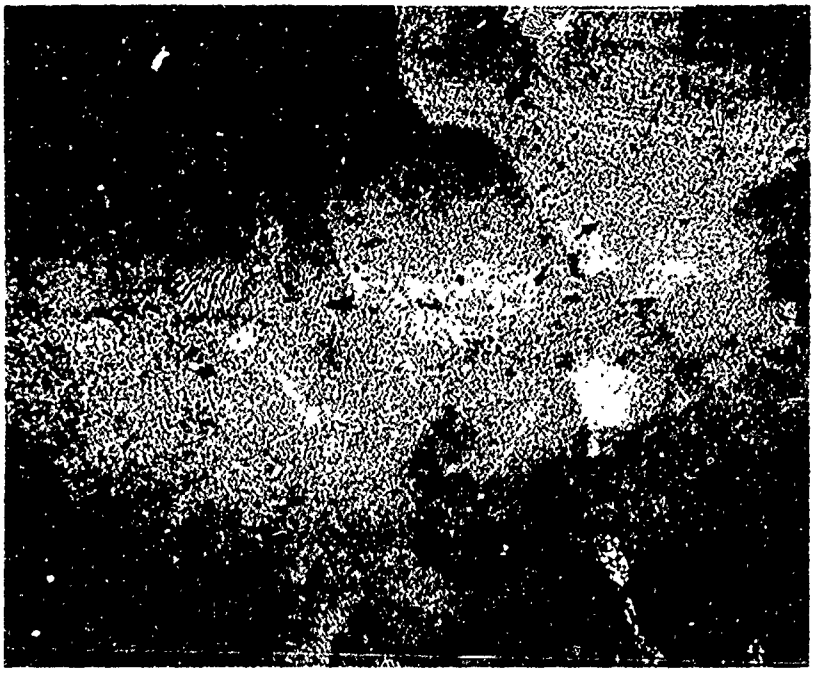

A141 250X

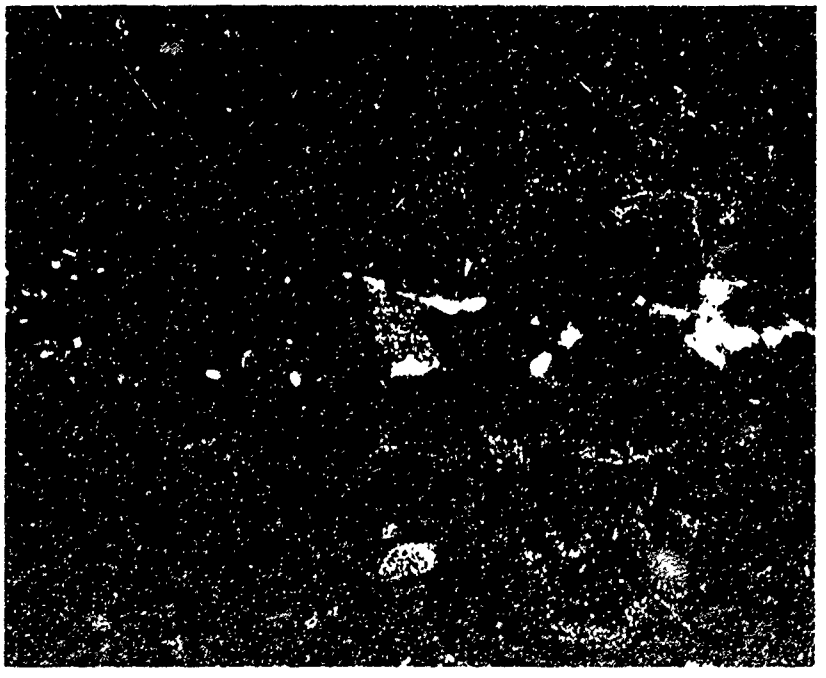

(d)
8 Mil Foil B Joint is Sound After 2 Hours; Ni-20%Co Interlayer
0.1 Mil on Foil and 0.5 Mil on Base metal.(2185°F/2000 PSI/ 5 Min. + 2170°F/750 PSI/2 Hr.)

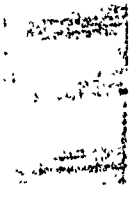

A158 250X

Figure 47 (Cont'd) As-Cast Faying Surface Joints showing Defect Accommodation of Interlayer Systems and Correlation with Ultrasonic C-Scan Prints (Small Inset)

Specimens containing a controlled defect for use as a standard were not used; therefore, the sensitivity level of the ultrasonic inspection was not determined, although a high level was used.

2. Room Temperature Fracture Surfaces

Typical better joints for the various systems considered were fractured by room temperature impact parallel to the joint of a segment of 1 x 1 inch ribbed specimen. Failure was forced in the joint region, and the surface examined for failure mode.

As shown in Figure 48, the fracture surfaces vary significantly. In contrast with the typical base metal fracture, the joint made with no interlayer failed in a planar manner. Dispersion electroplated interlayer joints also fail with comparatively low strength in a planar manner. At higher magnification, Figure 48c shows a plateau type of fracture surface, correlating with dispersion joints which had cracks metallographically. Joints made in conventionally cast and directionally solidified material using a nickel-cobalt interlayer failed in a manner similar to the base metal, as did the Foil B joint.

Based on these observations, the latter group could be expected to have relatively good properties compared to the former group. While the fracture observations correlate with the metallographic observations, no fine distinctions can be made within the group yielding rough fracture surfaces. Furthermore, behavior at elevated temperature may not necessarily be consistent with that observed at room temperature.

3. Metallurgical Features

A summary of the microprobe analysis in the joint centers compared to base metal is given in Table IX. It can be seen that the foil joint results are a function of the initial composition of the foil intermediary, with the relatively minor inward diffusion owing to the thickness and fixed-time high temperature exposure. The nickel-cobalt joints attain relatively good homogeneity with the base metal although the cobalt content is consistently somewhat higher and the tungsten slightly low. Generally, the metallographic observations of gamma prime concentrations correlated with the microprobe analysis results for aluminum, titanium, and cobalt content.

A24

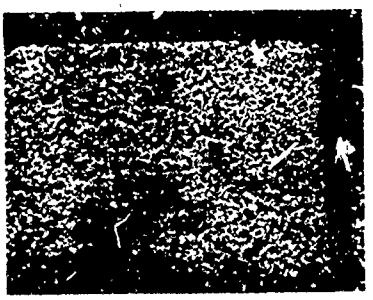

(a) No Interlayer 10X

A148

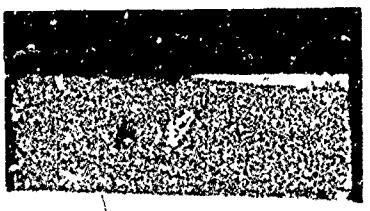

(b) 0.1 Mil Ni-Co-Cr-W Dispersion 10X
Plate No. 52

A147

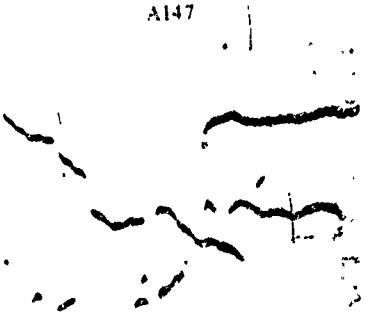

(c) Dispersion Plate No. 52

A114H

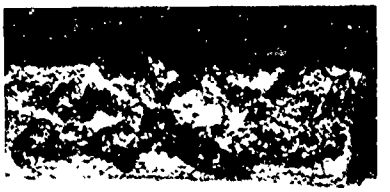

(e) 0.2 Mil Ni-25% Co 10X

A130H

(f) 0.2 Mil Ni-25% Co Directionally 10X
Solidified Basemetal

A133H

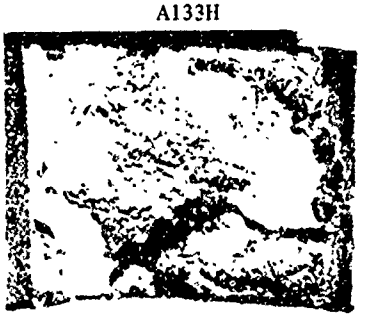

(g) 0.2 Mil Ni-25% Co. 5 Mil Foil B 10X

(d) Basemetal 10X

Figure 48 Room Temperature-Bend Fracture Surfaces of Diffusion Welded Joints. Nickel-Cobalt and Foil Joints Fail Similarly to Basemetal, Dispersion Plate and No-Interlayer Joints Fail in a Planar Manner and Probably Have Inferior Properties. Identifying numbers over each picture refer to the specimen number in Table A-III and relates to the identifying numbers on the photomicrographs.

TABLE IX

SUMMARY OF ELECTRON MICROPROBE ANALYSIS OF CENTER OF DIFFUSION WELDED JOINTS

Interlayer	Ni	Cr	W	Co	Al	Ti	Hf*	Metallographic Comment
0.2 Mil Ni-25Co (2200°/4 Hr)	61	8	10	13	5	2	0.4	Joint appears homogeneous with base metal
0.5 Mil Ni-25Co (2200°/4 Hr)	58	8	10	18	5	2	0.6	Joint is depleted of γ', probably due to high cobalt content
0.5 Mil Ni-20Co (2200°/4 Hr)	58	7	8	16	4.6	2	1.0	Joint appears homogeneous
0.5 mil Dispersion Plate No. 40 (49Ni-32Co-10Cr-9W) (2200°/4 Hr)	51	9	14	17	4	1.5	--	Joint is cracked, contains hafnium oxide particles, and is depleted of γ', probably due to high cobalt content
3.5 mil Foil A, 0.1 Mil Ni-25Co (2200°/4 Hr)	64	9	14	10	2	0.8	0.6	Joint is depleted of γ' probably due to deficiency of aluminum and titanium
8 mil Foil B, 0.5 mil Ni-20Co (2200°/2 Hr)	60	7	12	10	5	2.5	1.0	Joint center is slightly excess in γ' due to initial composition
Base Metal	60	9	13	10	5	2	0.4-0.6	

*Hafnium content is that in the matrix only; when metal combined as carbides is included, the specification level of 2% will be indicated.

J. CONCLUSIONS

Considering the preceding information relating to metallographic examination, microprobe analysis, fracture surface evaluation, and defect accommodation, the following summary can be made:

- Nickel-cobalt interlayers are effective in joining PWA 1422; 25-35% cobalt may be used on 0.1-0.2 mil interlayers, 20% cobalt for interlayers from 0.3 to 0.5 mils thick.

- Nickel-cobalt interlayer joints will be somewhat deficient in tungsten and chromium but generally microstructurally homogeneous with the base metal.

IV
PHASE IB -- SHEAR SPECIMENS

A 1 x 3 inch conventionally cast PWA 1422 specimen (Figure 49) having the same internal surface configuration as the 1 x 1 inch ribbed metallographic specimens was chosen to evaluate shear strength. This specimen was bonded from four separate pieces to avoid the cost and difficulty of machining the square bottom slots and to utilize the capability of diffusion welding to make multiple welds simultaneously. After welding, parts were heat treated, non-destructively tested, drilled, and loaded in tension at 1800°F. A welded specimen ready for testing is shown in Figure 50. After shear testing, upset was measured in the vicinity of the gage section in the same manner as upset was measured in the 1 x 1 ribbed specimens.

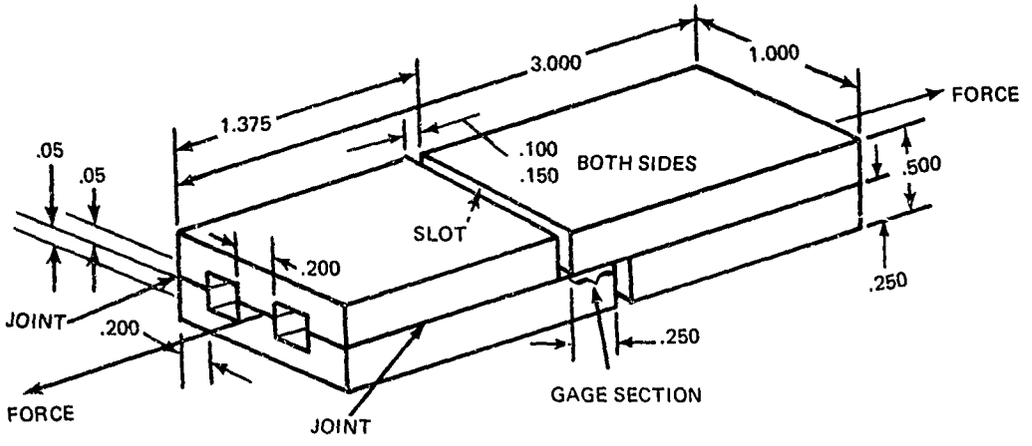

Figure 49 Ribbed Specimen For Evaluating 1800°F Shear Strength Has Internal Dimensions Similar To The 1 x 1 Specimen in Figure 9

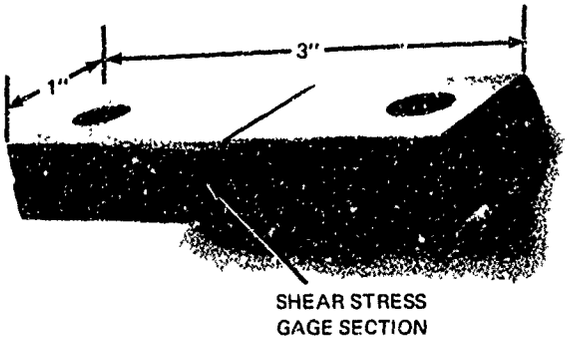

Figure 50 Diffusion Welded Ribbed Shear Specimen

On the basis of the metallographic development work, the following methods were selected for screening through shear testing:

- 0.2 mil nickel-20 percent cobalt
- 0.5 mil nickel-20 percent cobalt
- 0.5 mil nickel-20 percent cobalt with Foil B

In addition, limited testing was conducted on joints made with no interlayer, dispersion plate, and varied cobalt content.

A. WELDING SHEAR SPECIMENS

The results of the processing of shear specimens are summarized in Table X. The first shear specimens (Numbers 115-120) were welded in stacked groups of three using parameters that were extrapolated from the 1 x 1 inch specimens (shear specimen loading was three times greater based on joint area). The second lot (Numbers 118-120) of similarly welded shear specimens showed notching at the specimen edge after welding; these welds were manually hammered apart and the contact area was found to be incomplete as shown in Figure 51. This was attributed to rounding of the edges due to polishing, slight differences in thickness between the several parts, and a low upset. The nominal parameters based on these first shear specimens (2200°F/1000 psi/1 hr.) produced less upset than would be anticipated in 1 x 1 inch specimens at the same unit pressure.

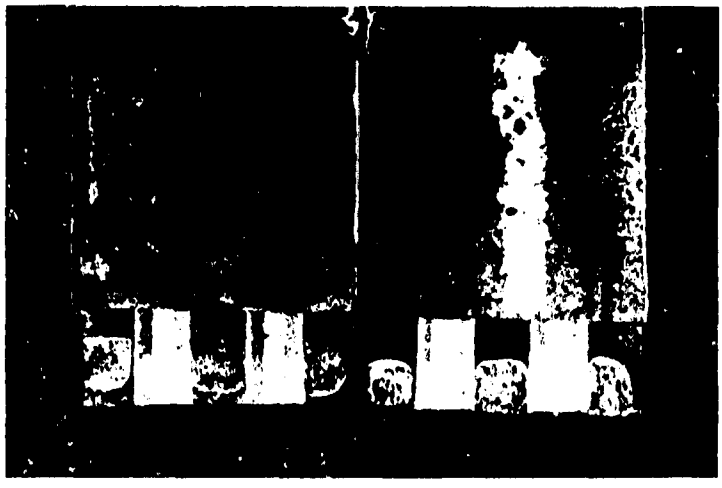

Figure 51 Fractured Shear Specimen Indicating Incomplete Contact Due to Mis-Machining and Low Upset.

B. WELDING AT HIGHER PRESSURES

When specimens (Numbers 169-170) were welded at a higher pressure a high upset was achieved but the stacked specimens welded to one another despite the use of the usual alumina-toluene stop-off. An ethyl-silicate binder was incorporated to allow a thicker coating. Subsequent specimens (Numbers 170A-185) welded at the same conditions were not subject to welding to each other but they failed to reproduce the high upset previously attained. Even with progressively increased applied pressure (through specimen Number 185) the erratic response to applied load seen in the 1 x 1 inch specimens was encountered. Although complete contact was evident with the more carefully machined specimens, most specimens had very low upset (from 1 to 3 mils).

TABLE X

SHEAR SPECIMEN WELDING RESULTS
(1 By 3 Inch Ribbed Specimens)

Specimen	Interlayer Thickness (Mils)	Interlayer Composition (%)	Intermediary	Welding Cycle Temp (°F)	Welding Cycle Press (PSI)	Time (Hr)	Upset (Mils)	Ultrasonic Inspection	Nominal Shear Strength (KSI)	Remarks
FOUR-PIECE SPECIMENS WELDED IN GROUPS BETWEEN PWA 1422 DIES										
115	0 2	Ni 35 Co		2210			3	PARTIAL CONTACT	18	IMPERFECT FIT
116	0 2	Ni 25 Co		2180	750* 500	0 5 1 5	2	PARTIAL CONTACT	13	IMPERFECT FIT
117	NONE			2195			1	POOR	JF	FAILED IN HEAT TREATMENT
118	NONE			2200			2	NT	NT	SPECIMENS INTENTIONALLY BROKEN APART AFTER WELDING FAILED IN BASE METAL WHERE WELDED, NEED FOR BETTER FIT ASCERTAINED
119	0 4	Ni 25 Co		2190	1000* 500	1 1	2	NT	NT	
120	0 1	Ni 25 Co		2190			2	NT	NT	
FOUR-PIECE SPECIMENS WELDED SINGLE OR IN STACKED GROUPS BETWEEN MOLYBDENUM DIES										
1178	0 2	Ni		2200	1500*	1	3	NT	NT	INTENTIONALLY DESTROYED TO ASCERTAIN JOINT CONTACT
169	0 1	Ni 20 Co		2190				NT	NT	SPECIMENS WELDED TO EACH OTHER, DUE TO INADEQUATE STOP-OFF BROKEN IN SEPARATING
170	NONE			2190	1800*	2	14	NT	NT	
170A (RR170)	NONE			2210			3	FAIR	JF	FAILED IN HEAT TREATMENT
172	0 2	Ni 25		2175	1500*	2	3	PARTIAL CONTACT	7	ETHYL SILICATE ALUMINA SLURRY USED
173	NONE			2195			2	GOOD	18	OK
174	0 5	Ni 20 Co	6 MIL FOIL B	2175			3	POOR	JF	FAILED IN MACHINING
175	0 5	Ni 20 Co		2210	1800*	2	10	FAIR	19	OK
176	0 2	Ni 25 Co		2180			1	NT	JF	FAILED DURING HEAT TREATMENT.

* PRESSURE WAS 1 5 – 2 TIMES NOMINAL DURING FIRST 15 MINUTES

** PRESSURE RELEASED AT END OF CYCLE BEFORE COOLING

NT - NOT TESTED

RR = RE RUN OF PREVIOUS SPECIMEN AFTER RE MACHINING

JF = JOINT FAILED PRIOR TO SHEAR TEST

BRACKETS INDICATE SPECIMENS WELDED IN ONE RUN AS A STACKED GROUP

TABLE X (Cont'd)

Specimen	Interlayer Thickness (Mils)	Interlayer Composition (%)	Intermediary	Welding Cycle Temp (°F)	Welding Cycle Press (PSI)	Time (Hr)	Upset (Mils)	Ultrasonic Inspection	Nominal Shear Strength (KSI)	Remarks
FOUR PIECE SPECIMENS WELDED SINGLE OR IN STACKED GROUPS BETWEEN MOLYBDENUM DIES (Cont'd)										
177	0 2	Ni 25 Co		2155			1	NT	JF	FAILED IN HEAT TREATMENT
178	0 5	Ni 20 Co	6 MIL FOIL B	2190	2000*	2	6	POOR	JF	FAILED DURING MACHING
179	0 5	Ni 20 Co		2175			2	POOR	5	LOW UPSET DESPITE HIGH PRESSURE
180	NONE		6 MIL FOIL B	2160			2	POOR	JF	FAILED IN MACHINING
181	0 5	DISPERSION		2200	2000*	2	1	NT	JF	FAILED DURING HEAT TREATMENT
182	0 5	DISPERSION		2180			1	NT	JF	FAILED DURING HEAT TREATMENT
183	0 5	Ni 20 Co	6 MIL FOIL B	2195			2	POOR	JF	FAILED IN MACHINING
184	0 5	Ni 20 Co		2190	3000	2	6	GOOD	20	OK
185	0 5	Ni 20 Co		2185			3	GOOD	9	PARTIAL CRACKING DURING HEAT TREATMENT
FOUR PIECE SPECIMENS RUN SINGLY BETWEEN MOLYBDENUM DIES (AS IN FIGURE 53)										
187	0 2	Ni 20 Co		2205	3500	2	28	NT	NT	GAGE SECTION FRACTURED AFTER WELDING
188 (RR 175	0 2	Ni 20 Co		2195	3200	2	8	GOOD	7	PARTIAL CRACKING DURING HEAT TREATMENT
189	0 5	Ni 20 Co		2200	460	2	4	NT	NT	GAGE SECTION FRACTURED NOTE UNREPRODUCIBLE UPSET BASED ON PRIOR TWO
190	0 5	Ni 20 Co	6 MIL FOIL B	2200	3600**	2	11	GOOD	21	OK
191	0 5	Ni 20 Co		2195	5200**	2	20	NT	NT	GAGE SECTION FRACTURED
192	0 5	Ni 20 Co		2190	5200**	1	3	NT	NT	GAGE SECTION FRACTURED
FOUR-PIECE SPECIMENS RUN BETWEEN PWA 1422 DIES (AS IN FIGURE 55)										
193 (RR 178)	0 5	Ni 20 Co		2180	5000	1	1	FAIR	3	LOW UPSET DESPITE PRESSURE, EVIDENCE OF CRACKING DURING HEAT TREATMENT
194 (RR 170)	0 5	Ni 20 Co		2195	6000	2	2	GOOD	0 5	SAME AS NO 193
TWO PIECE SPECIMENS RUN BETWEEN MOLYBDENUM DIES (AS IN FIGURE 56)										
195	0 2	Ni 20 Co		2200	6000	2	29	GOOD	24	NOTE UPSET VARIABILITY COMPARED TO PRIOR SPECIMENS
196	0 5	Ni 20 Co	6 MIL FOIL B	2185	3000	4	10	GOOD	20	SAME AS NO 196
197	0 5	Ni 20 Co		2185			14	GOOD	NT	SPECIMEN MIS-MACHINED

* PRESSURE WAS 1 5 2 TIMES NOMINAL DURING FIRST 15 MINUTES

** PRESSURE RELEASED AT END OF CYCLE BEFORE COOLING

NT NOT TESTED

RR RE RUN OF PREVIOUS SPECIMEN AFTER RE-MACHINING

JF JOINT FAILED PRIOR TO SHEAR TEST

BRACKETS INDICATE SPECIMENS WELDED IN ONE RUN AS A STACKED GROUP

C. JOINT THERMAL STRESS

During heat treatment [2200°F (2 hr) AC + 1975°F (4 hr) AC + 1600°F (32 hr) AC] some of the lower upset specimens fractured in the lapped joint area only, even though selective metallography showed sound, albeit low upset, joints. Undue thermal stresses may have arisen in the joint due to the specimen design since many low upset 1 x 1 inch specimens were similarly processed without failure. After heat treatment, x-ray and zyglo inspection were found to be ineffective in discriminating between the welded specimens. Ultrasonic inspection using 25 MHz transducer and the pulse echo method located controlled defects an revealed several joints which were very poor. Typical ultrasonic C-Scan traces are shown in Figure 52. Despite the typical ragged appearance of the traces due to edge effects, the varied joint quality in the gage section is evident. In specimen Number 183 (Figure 52) purposeful defects, formed by leaving spaces between three 4.5 mil foil segments, were detected. The correlation between the cursory ultrasonic inspection, shear strength, and subsequent examination of the joint contact area is shown in Table XI. It is evident that while ultrasonic inspection can indicate the presence of cracks and contact area it cannot predict joint strength.

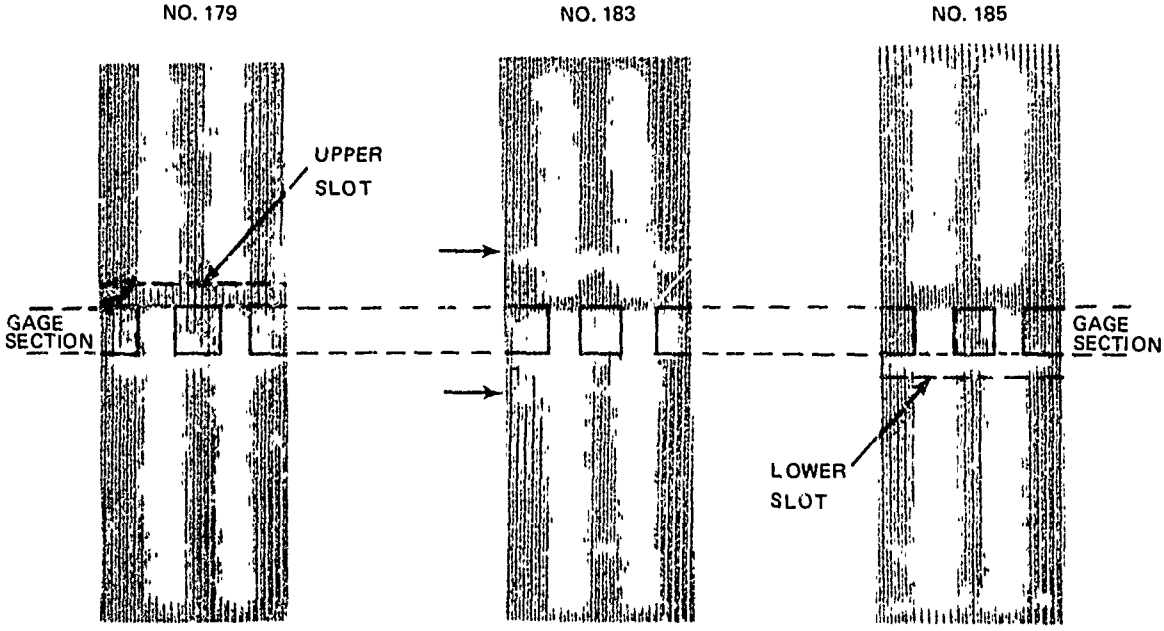

Figure 51 Typical Ultrasonic C-Scans of 1 x 3 Ribbed Shear Specimens. Slot Region Varies in Appearance Depending on Orientation to Transducer.

The poor results of the first series of shear specimens were attributed in large part to a lack of adequate joint deformation, as well as thermal stresses during heat treatment. To achieve greater upset and eliminate the use of ethyl silicate (not identified as a problem) single specimens (Numbers 187-192) were welded between molybdenum dies at considerably higher pressures. The setup is shown schematically in Figure 53. Although considerable upset was achieved at the higher pressures, the major portion of the specimens failed in the lapped joint gage section upon removal from the rig. A rough, full contact, fracture surface indicated that a good joint had existed (Figure 54). This type of failure occurred whether the pressure was maintained or released during cooldown.

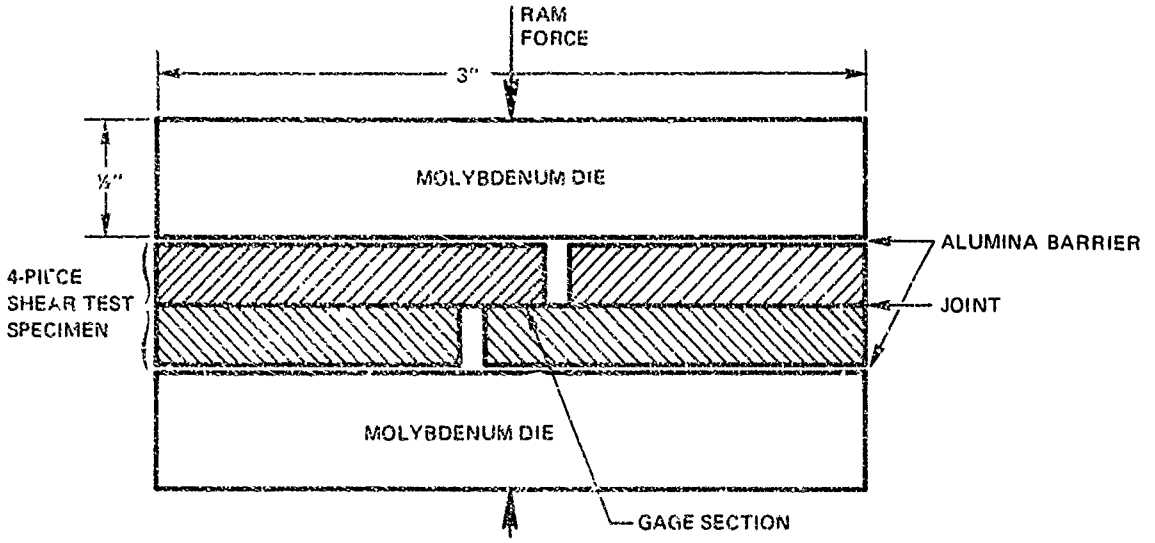

Figure 53 1 x 3 Shear Specimens and Die Configuration Which Often Yielded Gage Section Fractures After Welding.

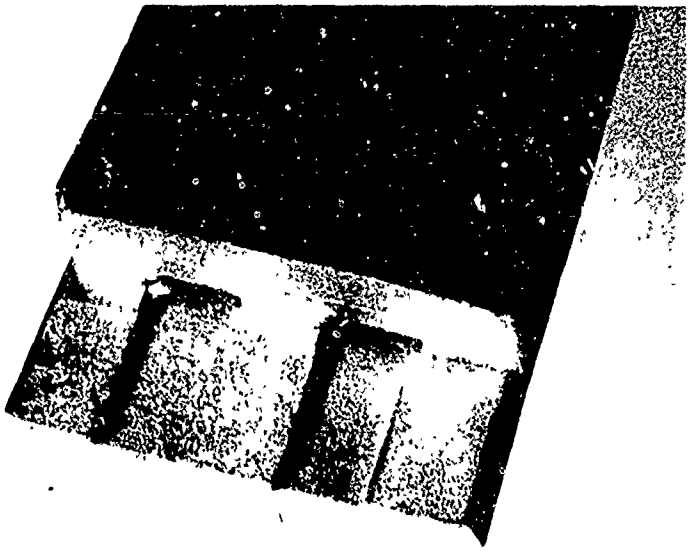

A-191 1.6X

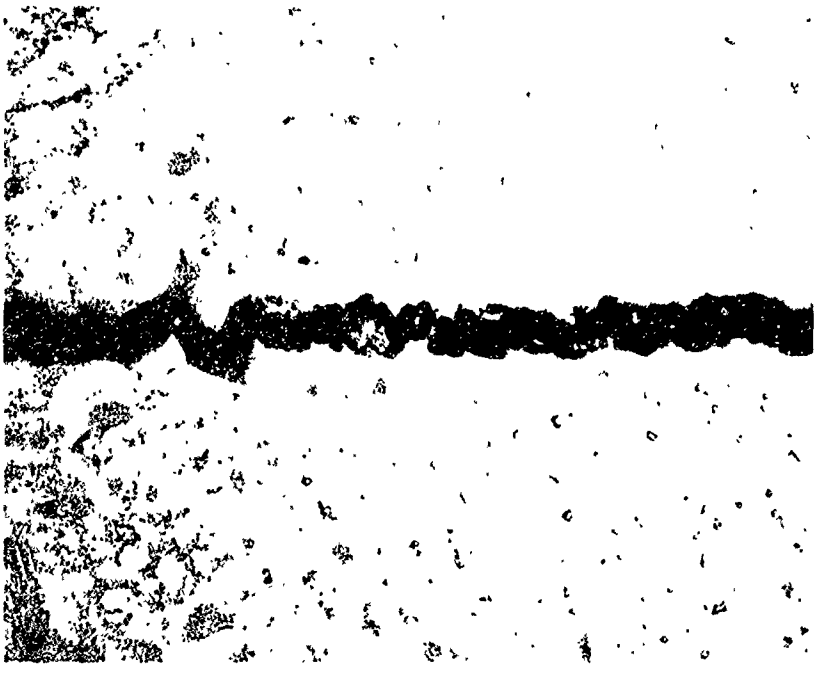

A-191 100X

Figure 54 Shear Specimen #191 Which Fractured on Cooldown From Welding, Probably Due To Thermal Stress, Despite High (20 mil) Upset And Apparent Good Joint.

D. EFFECT OF MOLYBDENUM DIES

A review of all the specimens welded in stacks of three showed that poor results were more common in those adjacent to the molybdenum die than those in the center. Significantly, although the first six specimens of the entire series had poor fit and low upset, the joint quality appeared good. These were welded using PWA 1422 rather than molybdenum dies. To further evaluate these effects specimens (Numbers 192-194) were fabricated using PWA 1422 on either side of the specimen as shown in Figure 55.

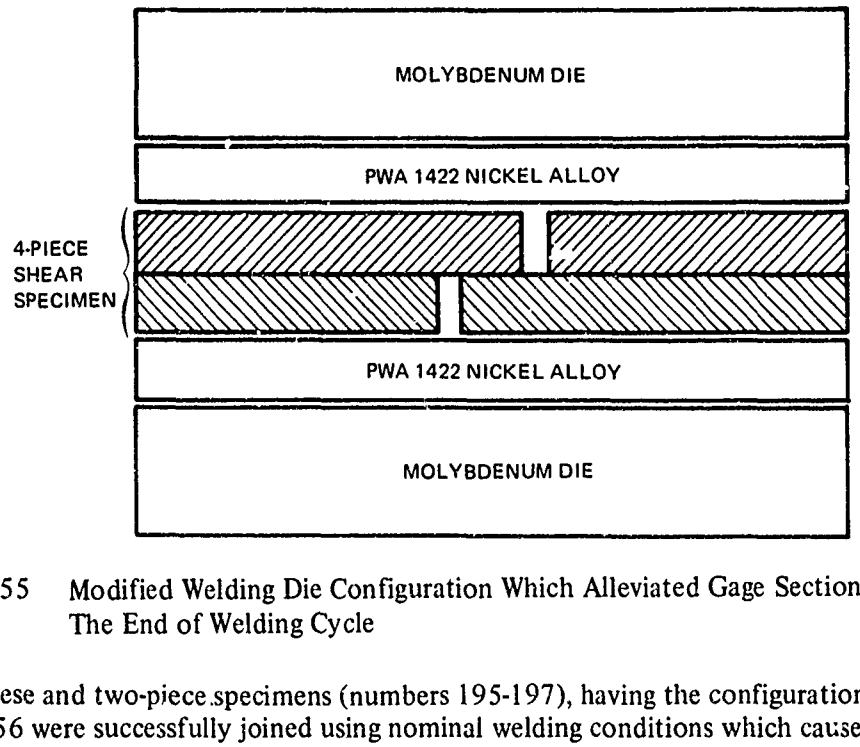

Figure 55 Modified Welding Die Configuration Which Alleviated Gage Section Failure At The End of Welding Cycle

Both these and two-piece specimens (numbers 195-197), having the configuration shown in Figure 56 were successfully joined using nominal welding conditions which caused gage section failure previously.

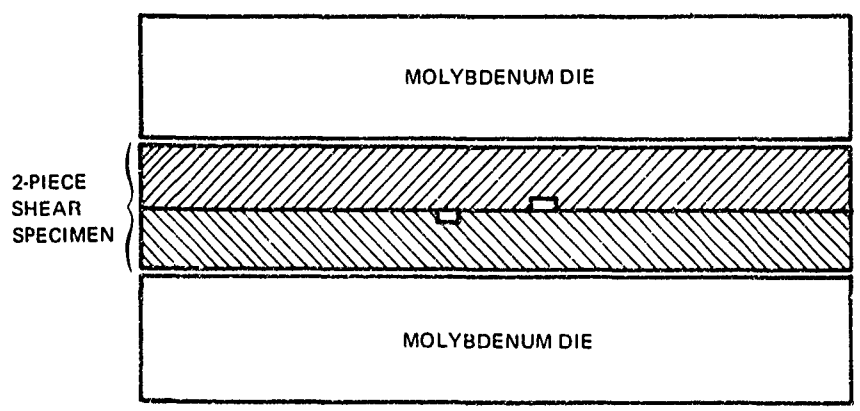

Figure 56 Modified Shear Specimen Configuration Which Avoids Localized Gage Section Stress; Full Slots Are Machined After Welding.

The results of testing indicated that the four-piece specimens between PWA 1422 dies did not have good strength, probably due to their marginal low upset. The two piece specimens had high strength, consistent with those of the base metal.

Based on the foregoing, there appeared to be an interaction between the molybdenum dies and the shear specimen during the cooldown. Calculations show that differences in thermal expansion can theoretically induce shear stresses of up to several hundred thousands of pounds per square inch in the gage section. However, failure of specimens on which the die contact pressure was fully relieved indicates the problem is not simply explained. It can also be speculated that although many specimens were intact after welding, some may have endured significant strain and damage at the interface resulting in subsequent failure at a low test value.

E. SHEAR TESTING

The results of testing at 1800°F of the specimens which were intact after heat treatment are summarized in Table XI. Two one-piece cast specimens (A and B) having the same configuration in the gage section as a welded ribbed shear specimen were tested. When the shear stress in the joint region reached approximately 20,000 psi, these specimens failed in the slot region instead of the gage section. This mode of failure indicates the specimen design is inadequate to produce shear failure and therefore test results do not reflect the true shear strength. As a reference, the shear stress failure level of these specimens can be compared to 27,500 psi, which is 0.5 times the typical minimum 1800°F tensile strength for this material.

After shear testing the fracture surface was examined and measured by a planimeter for the approximate joint contact area. There was indication that several of the specimens had been welded but parted prior to, or during, the heat treatment. Of those which had essentially full joint contact (Numbers 115, 173, 175, 184, 190, 195 and 196) the shear stress levels were comparable to the baseline value. However, it is evident that no systematic correlation can be made between the joining system and the strength of the joint in view of the difficulties and uncertainties attendant to producing these parts.

TABLE XI

SHEAR TESTING RESULTS FOR 1 X 3 INCH RIBBED FLATS
(TESTED AT 1800°F

Specimen	Interlayer Thickness-Mils	Composition	NDT[1]	Contact Area-%[4]	Shear Strength[2]-PSI	Comment
A		Cast one-piece	Good	–	23,000	Failed in tension
B		Cast one-piece	Good	–	18,000	Failed in tension
115	0.2	Ni-35Co	Good	90	18,000	Mis-machined
116	0.2	Ni-25Co	Fair	70	13,400	Mis-machined
172	0.2	Ni-20Co	Poor	35	7,000	Note (3)
173	None		Good	90	18,000	Good weld
175	0.5	Ni-20Co	Good	95	19,000	Good weld
179	0.5	Ni-20Co	Poor	25	4,800	Note (3)
184	0.5	Ni-20Co	Good	100	20,000	Good weld
185	0.5	Ni-20Co	Good	40	8,500	Note (3)
188	0.2	Ni-20Co	Good	30	6,500	Note (3)
190	0.5	Ni-20Co + 6 Mil Foil B	Good	100	20,500	Good weld
193	0.5	Ni-20Co	Fair	66	3,250	Note (3)
194	0.5	Ni-20Co	Poor	100	350	Note (3)
195	0.2	Ni-20Co	Good	90	24,000	Good weld
196	0.5	Ni-20Co + 6 Mil Foil B	Good	100	20,000	Good weld

Notes:

1 Ultrasonic inspection rating relative to one another
2 Strength corrected for percent contact area
3 Joint appears locally to have been cracked and oxidized during heat treatment
4 Contact area, measured by planimeter after shear testing, is that percent of the faying joint surface which appeared to be fractured during the test.

TABLE XII

WELDING RESULTS FOR PWA 1422
RECTANGULAR BLOCKS USING Ni-20Co INTERLAYERS
(Welded at 2200 ± 15°F Except As Indicated)

Run	Interlayer Mils	Weld Time Hrs.	Intermediary[2] 6.5 Mil Foil B	Joint Pressure Ksi	Upset-Inches Overall	Upset-Inches Channel	Change in Joint Area - %	Percent Upset in Joint[1]
B1-L	0.5	2	No	4.5	.012	.003	1	25
B2	0.5	2	No	4.[illegible]	.062	.032	10	52
B3	0.5	2	No	4.1	.037	.022	5	60
B4	0.5	4	Yes	4.8	.033	.022	6	67
B5	0.5	4	Yes	6.5	.062	.042	8	68
B6-L	0.5	4	No	4.8	.035	.023	5	66
B7	0.2	4	No	4.2	.047	.030	7	64
B8-L	0.5	4	Yes	3.5	.043	.027	4	63
B9-LL	0.5	2*	No	7	.001	.005	0.3	–
B10-L	0.5	3**	No	4.4	.003	.015	0.2	–
B11	0.2	4	No	7.6	.047	.021	4.5	45
B12	0.2	4	Yes	8.0	.046	.023	5.0	50
B13	0.5	4	No	8.0	.048	.022	4.7	46
B14	0.5	4	No	8.0	.063	.024	6.3	38
B15-L	0.2	4	No	8.0	.040	.020	4.2	50

* At 2000°F
** Power supply failed.
1. Ratio of channel upset to overall upset
2. Foil B had 0.1 Mil Ni-20Co interlayer on both sides.

NOTE: Blocks were 3 inches high and had 1½ x 1½ inch joint area except for those designated (-L) which were 1½ x 2 at the joint and those designated (-LL) which were 1½ x 3 at the joint.

It was again evident that the joint design and specimen configuration were significant in determining the upset under an applied load. The blocks were directly induction heated, and therefore slightly hotter at the joint (center) than near the dies. Consequently, the deformation was desirably localized near the joint, as indicated by comparing the channel upset to the overall upset.*

*The channel upset is greater than the upset in the joint calculated from the change in area. No consequential cracking was observed in the channel.

When examined, the first three blocks had joints as sound and homogeneous as the best of the 1 x 1 inch ribbed specimens. However, due to the low upset, B1 had slight joint edge separation which progressed through the piece during heat treatment. Several specimens from runs B2 and B3 failed during machining. Oxidation on the joint fracture surface indicated that failure had initiated during, or prior to, the final thermal cycle of the heat treatment (1600°F/ 32 hrs AC). Investigation revealed that these blocks had inadvertantly been subjected to forced air cooling during heat treatment.

Recognizing that failure of the joint occurred during heat treatment, tests were conducted on shear specimen stubs, block segments, and other fragments of 1 x 1 inch ribbed specimens. When water quenched from either 2200°F or 1975°F cracks occurred in the joint. There were no cracks in the specimens that were furnace cooled from these temperatures. Air cooled specimens showed intermittent cracking. Cracking is not encountered in normal heat treatment of the PWA 1422 castings used in engine parts. The cooling rate in the range 2200 - 1000°F in the vacuum diffusion welding press is considered approximately equal to air cooling.

Because the structure of the joint appeared normal during all phases of the heat treatment, it was not obvious what caused failure. It was apparent that for this configuration the stresses of the thermal cycling (heat treatment) were greater than the joint's ability to resist them. To lessen these stresses, the heat treatment was modified to utilize a furnace cool from the higher temperatures instead of air cooling. Also, the subsequent blocks were welded for four hours to improve the joint quality prior to heat treatment.

Blocks (B4-5-6) which were heat treated using the modified process were cut into rough shapes after heat treatment. Block B4 was examined metallographically at each step, and remained sound. Several specimens from other blocks failed during machining; however, inspection showed these parts had local base metal pullout at the fracture surface and an unoxidized metallic appearance across the generally planar face. Fracture occurred within the 0.5 mil interlayer and, in the specimens made with foil, the fracture crossed from one side of the joint to the other.

These results showed that despite the favorable metallographic appearance of blocks welded with a 0.5 mil interlayer, these blocks did not have satisfactory enough properties for testing. This was ascribed to several possible causes:

- Hafnium failed to act as a ductility-increaser in the as-cast joint region.
- The joint region had a composition similar to MARM-200 which, unlike PWA 1422, experiences sharply reduced ductility after solutioning at 2200°F.
- Mechanical interaction occurred at the joint between the incongruent anisotropic structure of each block.
- Insufficient joint homogeneity.

Additional diffusion welds were made using a 0.2 mil interlayer both with and without a foil and a 0.5 mil interlayer subjected to extended (20 hour) heat treatment at 2200°F. Since tensile testing of these blocks (B7-11-12-13-14-15) generally showed satisfactory properties, the major problem was indicated to be resolved through improved joint homogeneity.

B. TESTING OF MECHANICAL PROPERTIES

After welding, the blocks were sectioned into three pieces for metallographic examination, heat treated, fluorescent penetrant inspected (ultrasonic inspection was ineffective due to the thickness and grain structure), and machined into tensile, stress rupture, and thermal fatigue specimens (shown in Figures 58, 59, and 60). All procedures not described in detail were according to conventional industry standards. Location of the specimens within each block was recorded but no correlation was observed with properties. In the test results presented in this section the specimens are identified only by the block from which they came, e.g., B7, B12, B15.

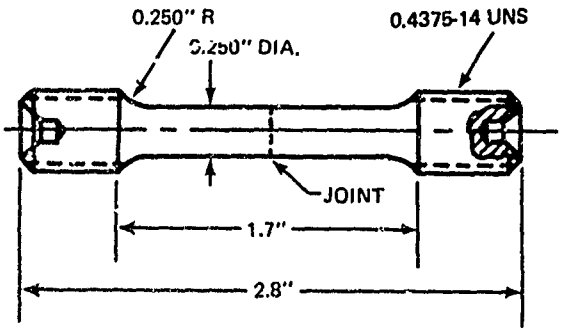

Figure 58 MDL 2351 Tensile Specimen

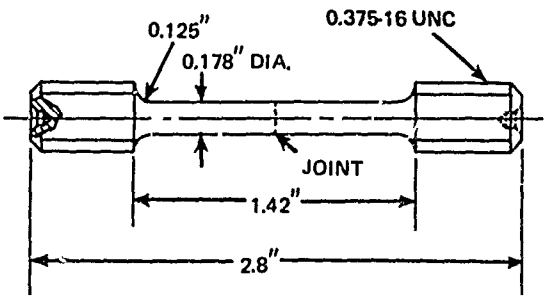

Figure 59 MDL 4528 Stress Rupture Specimen

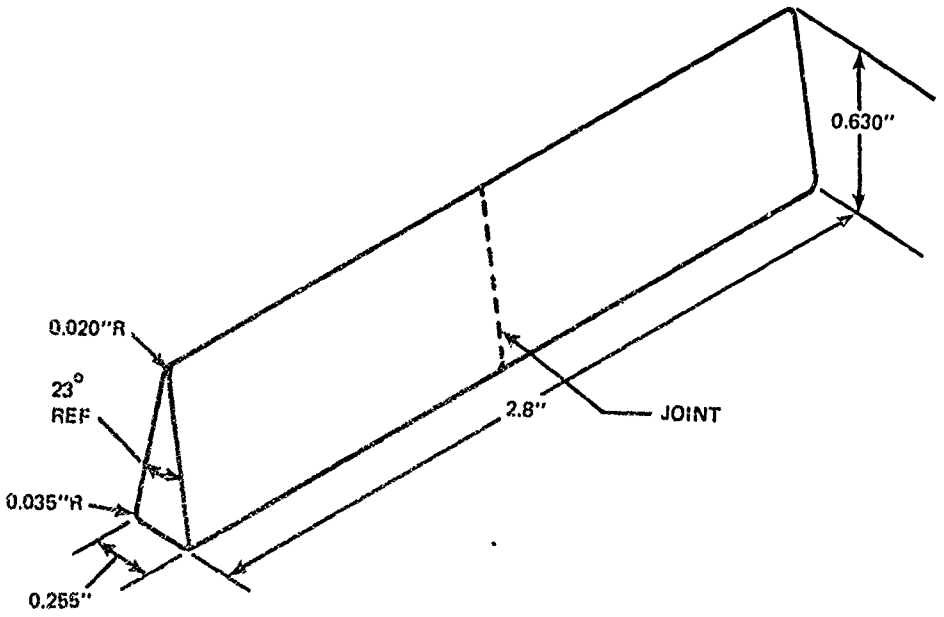

Figure 60 Thermal Fatigue Specimen Machined From Retangular Block

1. Tensile Tests

After machining, specimens were examined by fluorescent penetrant and tested using conventional techniques. The 1400°F and 1800°F tensile properties are summarized in Table XIII. (Table XIV shows the specific tensile results for each block.) The results show that 0.2, 0.5 (2200°F/20 hr), and 0.2 mil + Foil have essentially the same strength at 1400°F (nominally 90% of base metal) and 1800°F (nominally 80% of base metal). At 1400°F the fracture in some specimens is typified by a rough surface crossing into and through the base metal, and appears as would base metal under similar conditions. At 1800°F the fracture surface was planar within the joint; because PWA 1422 fails intergranularly at 1800°F, and due to the fine grain size in the joint, preferential planar failure was not unexpected. Compared to the measured base metal strength (Table XV) and the specification minimums for PWA 1422 the joint tensile properties were quite acceptable. Limited data in Table XV shows base metal properties are not adversely effected by weld cycling.

TABLE XIII

COMPARISON OF TENSILE STRENGTHS OF PWA 1422 DIFFUSION WELDS
(These Are Averages of Results Presented in Tables XIV and XV)

Interlayer	1400°F UTS Ksi	1400°F UTS %*	1800°F UTS Ksi	1800°F UTS %*
0.5 mil	88	64	22	29
0.5 mil (20 Hr. H.T.)	142	99	65	86
0.2 mil	130	91	67	88
0.2 mil + Foil B Intermediary	132	94	59	78
Base metal (weld cycled, Table XV)	143		76	
Base metal-transverse minimum spec	117		58	

*Percent of base metal (weld cycled, Table XV)

TABLE XIV

TENSILE TEST RESULTS FOR SPECIMENS MACHINED
FROM DIFFUSION WELDED RECTANGULAR PWA 1422 BLOCKS
After Aging Heat Treatment [1975°(4 Hr) + 1600°(32 Hr)]

Specimen ***	1400°F Tensile Strength - Ksi	1800°F Tensile Strength - Ksi	Comment
B2 – 0.5 Mil	86		Planar fracture in joint; negligible elongation
B3 – 0.5 Mil	90		
B3 – 0.5 Mil		23.7	Planar fracture in joint; negligible elongation
B3 – 0.5 Mil		18.6	
B4 – 0.5 Mil + Foil B		12	Fluorescent penetrant indication; failed in interlayer either side of foil
B4 – 0.5 Mil + Foil B		25.7	
B4 – 0.5 Mil + Foil B	113		Base metal type failure
B6 – 0.5 Mil	36 **	**	Fluorescent penetrant indication before testing; planar fracture
B6 – 0.5 Mil		8	
B7 – 0.2 Mil	119		5-7% elongation; base metal type failure
B7 – 0.2 Mil		64	
B11 – 0.2 Mil	130		1400° tensile elongation was 7-11%; 1800°F tensile elongation was 1-3%; generally fractures were planar.
B11 – 0.2 Mil		67	
B12 – 0.2 + Foil B	132		
B12 – 0.2 + Foil B		59	
B13 – 0.5 Mil*	142		
B13 – 0.5 Mil*		71	
B14 – 0.2		63	
B14 – 0.2		75	
B15 – 0.5 Mil *		70	
B15 – 0.5 Mil*		59	
B15 – 0.5 Mil*		59	

* Blocks given additional 20 hours heat treatment at 2200°F before aging.
** These results are not included in averaging 0.5 mil tensile properties in Table XIII due to NDT defects in joint.
*** Blocks diffusion welded as reported in Table XII, but which are omitted here, cracked during heat treatment or machining.

TABLE XV

TRANSVERSE TENSILE STRENGTH OF PWA 1422 BASE METAL

Condition	Temperature - °F	0.2% YS - Ksi	UTS - Ksi	% Elongation
Weld Cycle*	1400	107	143	10
Typical**	1400	109	144	5
Weld Cycle	1800	55	76	13
Typical	1800	64	83	14

* 2200°F/4 hr + 1975°F/4 hr + 1600°F/32 hr; average of two tests each condition.
** 2200°F/2 hr + 1975°F/4 hr + 1600°F/32 hr; average for several heat codes.

2. Stress Rupture

The 1800°F stress rupture tests made a sharper distinction between the joining systems. Foil joints had substantially inferior properties compared to the 0.5 and 0.2 mil interlayers as indicated in Figure 61 and Table XVI. The fracture surface in the joint region of all specimens was planar; foil joints failed at the foil-base metal interface (interlayer region). The 0.2 mil and 0.5 mil interlayer (20 hr. at 2200°F) joint properties were greater than 70 percent of the minimum for MARM-200, the only available properties.

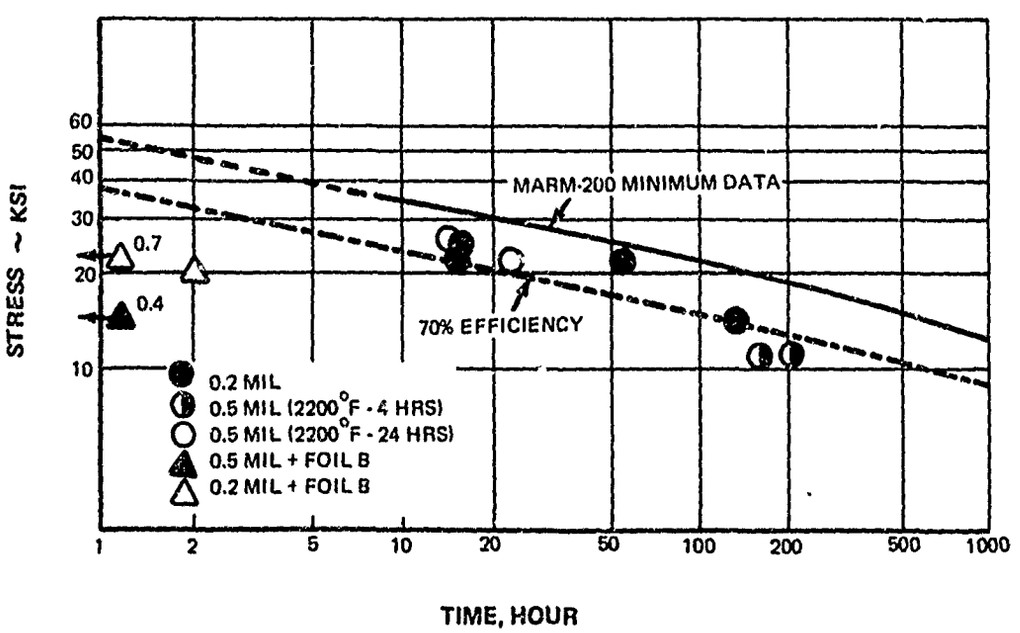

Figure 61 1800°F Stress Rupture Strength of Ni-20Co Interlayer Diffusion Welds of PWA 1422

TABLE XVI

SUMMARY OF 1800°F STRESS RUPTURE TESTS*

Specimen	Interlayer mils	Stress Ksi	Time to Fail Hours	Joint Efficiency** %	Comments
B7	0.2	14.5	131	>75	Test discontinued
B7****	0.2	25	0	--	Failed on loading
B7	0.2	22	15	70	Fracture
B11	0.2	22	53	90	Fracture
B11	0.2	25	15	80	Fracture
B1	0.5	11	204	60	Fracture
B3	0.5	11	159	>60	Test discontinued
B3****	0.5	14.5	20	--	Fracture
B13	0.5 (2200°F/24 hrs)	22	23	79	Fracture
B13	0.5 (2200°F/24 hrs)	25	15	81	Fracture
B4	0.5 + Foil B	14.5	0.4	~1	Fracture
B12	0.2 + Foil B	20	2	~1	Fracture
B12	0.2 + Foil B	22	0.7	~3	Fracture
MARM-200	Minimum***	19	200		
		30	20		

* All specimens welded 2200° F/4 hrs. except as indicated, and fully heat-treated (1975° F/4 Hr. + 1600 ° F/32 hr.)

** Joint efficiency is determined by dividing the test stress by the stress which would cause failure in an equal time for a specimen meeting the specification minimum as shown in Figure 61.

*** In absence of data for transverse PWA 1422.

**** Previous test discontinued and same specimen step-loaded to higher stress level; joint efficiency is not applicable to such specimens.

3. Thermal Fatigue Tests

Nine specimens from various diffusion welded blocks, machined to the configuration shown in Figure 60 were tested for thermal fatigue resistance. This test consisted of alternate immersion for two minute periods in air-fluidized sand beds held at 1800°F and 70°F until failure or 1000 cycles occurred. Specimens were examined periodically using fluorescent penetrant; failure was defined as a crack which was 1/32nd of an inch long. The thermal gradients and specimen configuration produced a nominal total strain of 0.4% on the joint at the nose of the specimen.

The results shown in Table XVII are consistent with prior heat treatment experience in showing that the 0.5 mil interlayer joint is inferior to the 0.2 mil interlayer and base metal. A limited metallographic examination of some failed 0.5 mil interlayer specimens indicated that cracking occurred within the original interlayer region with some tendency to propagate into the base metal. There was evidence of slight plating contamination at the original interlayer-base metal interface.

It is difficult to characterize the results without more extensive data for both the joints and the base metal. However, since some failures were observed in the base metal and only one of the 0.2 mil interlayer joints failed in less than 1000 cycles, the thermal fatigue resistance appears good, although perhaps somewhat less than the base metal.

TABLE XVII

Results of Fluidized Bed Thermal Cycling
PWA 1422 Diffusion Welds Between 1800°F and 70°F

Block	Interlayer-Mils	Cycles to Failure	Comment
B7	0.2	Runout	--
B11	0.2	868	Joint Failure
B7	0.2	928	Base Metal Failure 1/8" From Joint
B11	0.2	Runout	--
B13	0.5	628	Joint Failure; Slight Contamination
B13	0.5	295	Base Metal Failure ¼" From Joint
B14	0.5	Runout	--
B14	0.5	228	Joint Failure; Slight Contamination
B15	0.5	573	Joint Failure

C. CONCLUSIONS

Mechanical testing showed that the best joint was the 0.2 mil nickel-20 cobalt interlayer. Properties of the 0.5 mil interlayer with a long time homogenization were almost as good, but this joining system exhibited a greater propensity to crack during heat treatment and thermal cycling. Naturally, this limitation directly relates to the thermal strain anticipated in a part. Joints made with 0.2 mil interlayer + Foil B had inferior stress rupture properties compared to 0.2 mil interlayer joints. This was attributed to the properties of the foil which were expected to be inferior. It is logical to assume that if a base metal composition intermediary had been used, test results similar to the plain interlayer would have been achieved.

VI
PHASE III – JOINING OF SPLIT BLADES

This program was primarily oriented to metallurgical development of superalloy joining systems. Consequently only a limited amount of effort was expended on demonstrating the application of the joining system to an actual airfoil. The approach and results should be considered in the absence of the greater effort including design studies of parts and tooling which would accompany a manufacturing investigation.

Cast split blade halves made by the precision shell mold method were utilized for this program. Although precision castings have relatively good fidelity, some warpage and dimensional deviation in thin sections was unavoidable. Previous work had demonstrated that machining the faying surface only was not desirable for two reasons: (1) internal passage and overall dimensional control was lost, and (2) even the best machining accuracy could leave up to 0.015 inch lack of fit on a highly contoured surface. It was not considered realistic to machine the blade halves all-over by conventional methods.

Considering the foregoing, together with the restraint of the program scope to the development of joining methods per se, machining was avoided altogether. An existent wax pattern die was used to produce blade halves split down a central parting line with no faying surface machining allowance. Interlayers were applied to the as-cast faying surfaces and the parts were joined without any machining. Consequently, tolerances in the final part were reflective of normal solid castings, notwithstanding deviations imparted by the diffusion welding dies.

A. FABRICATION OF BLADE HALVES

The procedure for preparation of split blade halves and precision ceramic bonding dies is shown in Figure 62. A metal die for producing wax pattern for conventional transpiration-cooled airfoils was utilized. Two half-blades were made from epoxy tooling materials. The epoxy die inserts were cast "one-against-the-other" so that the faying surfaces perfectly matched. When each was inserted within the die in conjunction with a removable metal core, wax injection produced a pattern for each mating blade half. The injected wax patterns mated except for minor surface defects and warpage typical of such patterns. Using conventional foundry techniques, shell molds were made from the patterns. Thereafter, the parts were directionally cast using proprietary production processes. Mating as-cast blade halves are shown in Figure 63.

The lack of fit between split halves was measured by insertion of a plastic intermediary between the mating split halves which were then pressed together. As shown in Figure 64, the typical fit was quite good considering the warpage normally encountered in thin investment castings; maximum gaps were observed at the trailing edge tip and trailing edge-to-root fillet. Handworking of the wax pattern in this latter area, necessitated by a feather edge from the parting line location, contributed to deviations.

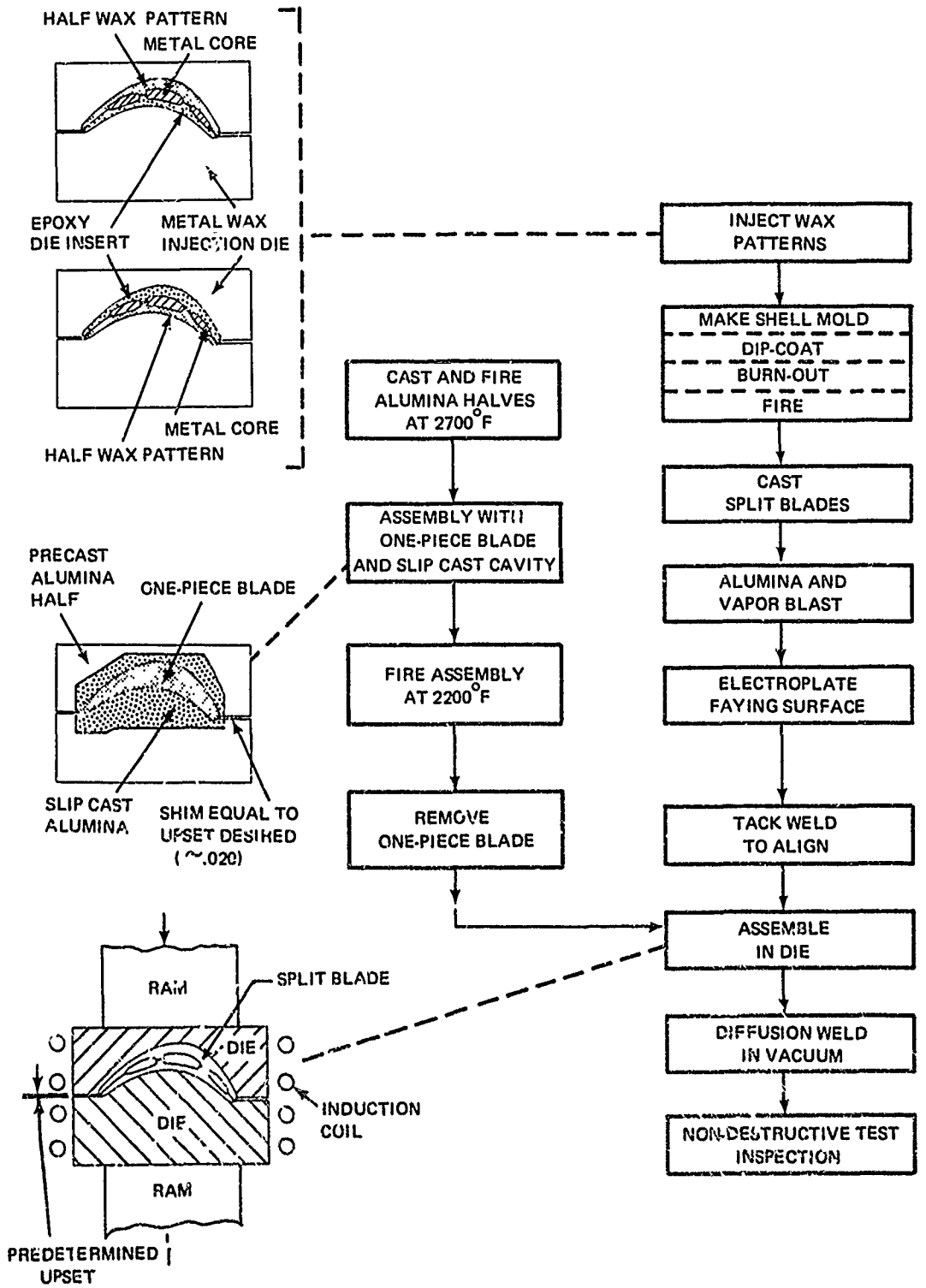

Figure 62 Split Blade Diffusion Welding Flow Chart

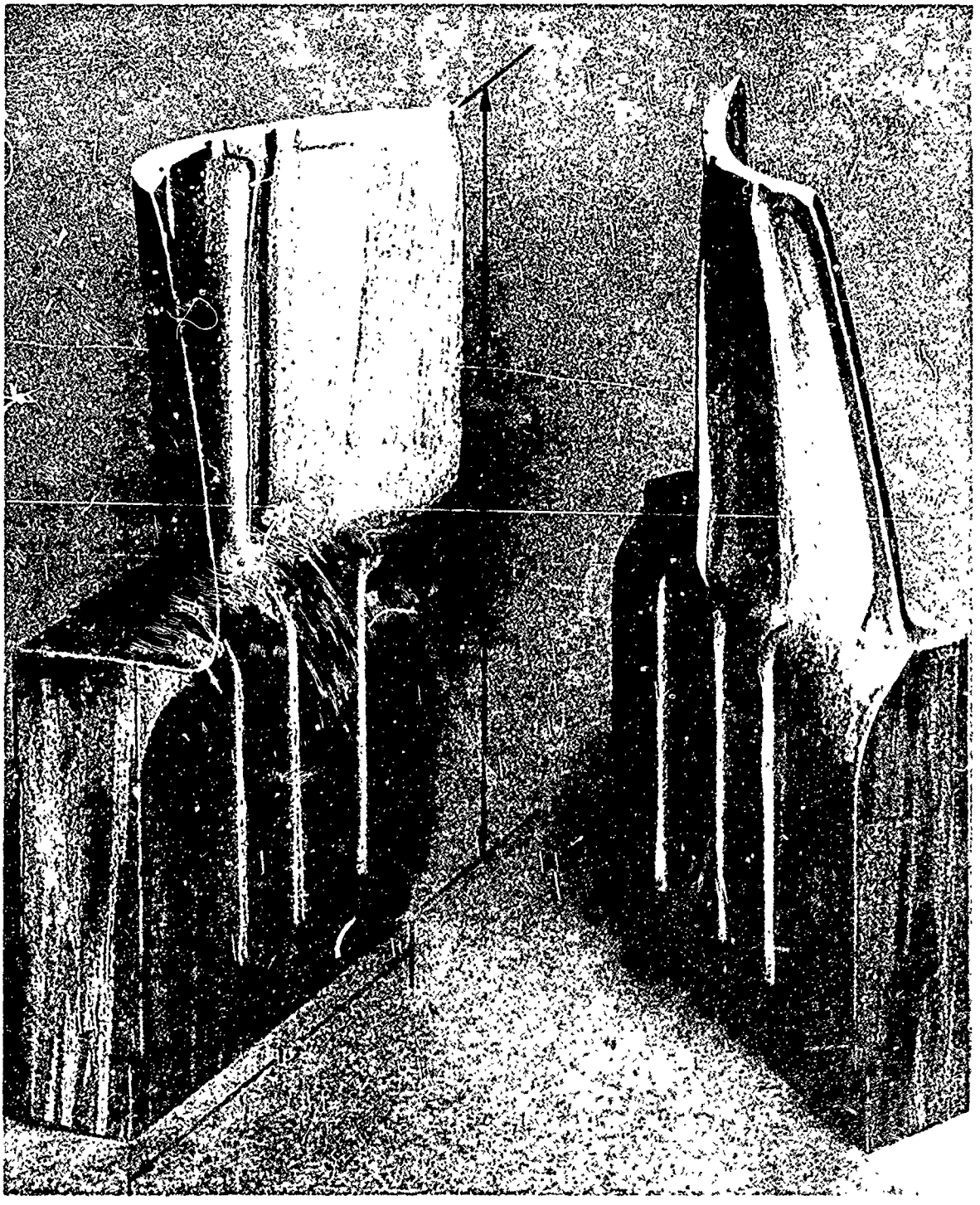

Figure 63 As-Cast, Alumina Blasted, and Etched PWA 1422 Blade Halves Which Were Welded Showing Surface Contour and Finish. The Heavy Root Section is Necessitated by the Directional Casting Process

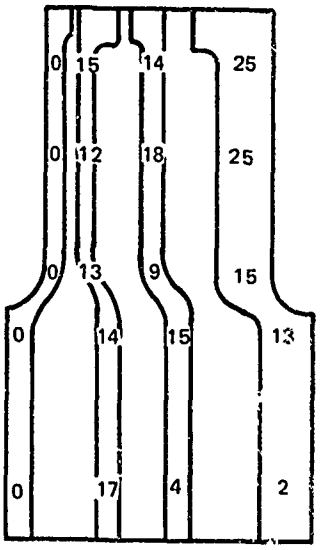

Figure 64 Lack of Fit (In Mils) Measured Between a Typical Pair of As-Cast Blade Halves

Ceramic diffusion welding dies were chosen for ease of fabrication, strength at temperature, and economy. The sequential steps in their fabrication are also shown in Figure 62. Rectangular die halves with a rough blade cavity larger than the actual blade half were slip cast against an epoxy pattern using an alumina silicate-bonded mixture. After firing at 2700°F, the mated shell halves were separated by a wax or metal shim equal to the desired upset (~ .020 inches). A solid (un-split) blade casting was placed in the cavity and alumina slurry slip cast around it. The assembly was then fired at 2200°F. In this way, the fired die conformed to the dimensions of a blade when both were at 2200°F, eliminating any lack of fit due to differential expansion. On cooling, the dies were parted and thereupon ready for insertion of the split halves to be diffusion welded. Split die halves are shown in Figures 65 and 66.

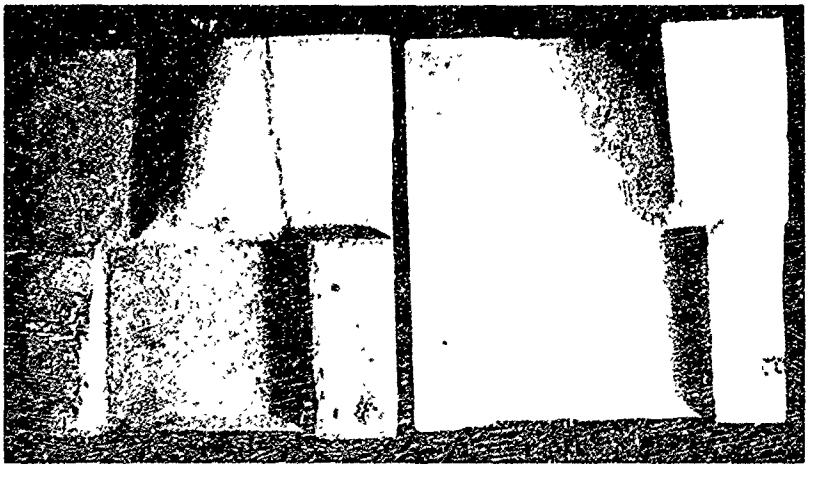

Figure 65 Cast and Fired Alumina Dies Used for Welding Split Blades

Figure 66 Split Blade Halves Set in Open Alumina Die Halves

B. WELDING BLADE HALVES

Thirteen split blades were diffusion welded using varying parameters and interlayers as shown in Table XVIII. Three systems were evaluated based on nickel-20 percent cobalt interlayers:

- 0.2 mil, since it had the best properties
- 0.2 mil + foil*, to determine the advantage of using a foil intermediary in overcoming lack of fit.
- 0.5 mil, since it had better accommodation to lack of fit than 0.2 mil and was easier to apply to the contoured joint than the foil.

As shown in Figure 67, the split blade was assembled in the die which was then placed within the welding press. Alignment of the parts was achieved by small tack welds at the root and tip; the ceramic dies or parts did not self-align. Direct heating by induction was chosen because it was felt that radiant heating through the low conductivity die would not heat the parts in a reasonable time. The irregular shape of the blade resulted in temperatures deviating as much as 50°F from the mean (a tendency for severe overheating was noted at the trailing edge-to-root transition). When the assembly reached the welding temperature, ram pressure was applied based on the nominal joint area of two square inches. Usually this was sufficient to bring the dies together within one hour. At the end of the welding cycle, the assembly cooled by radiation. Due to uneven loading or thermal stresses during cooling, it was not untypical for the dies to crack. Materials less susceptible to thermal shock than alumina would have been better chosen.

* Throughout Phase III, whenever "foil" is used, the reference is to 4.5 mil Hastelloy-X. This material was used since Foil B of the required size and thickness was not readily rolled.

The welding cycle was typically two hours; subsequently, the 0.2 mil interlayer joints were heat treated two additional hours at 2200°F; the 0.5 mil interlayer joints were exposed to 2200°F for 20 additional hours. All blades were given the normal subsequent heat treatment; 1975°F/4 hr + 1600°F/32 hr.

TABLE XVIII

SUMMARY OF SPLIT BLADE WELDING TRIALS

Blade	Ni-20Co Interlayer Thickness	Intermediary**	Welding Condition	Root Upset* mils	Comment
1	Unplated With 5 mil Foil	Yes	2100°F/3.5 ksi/0.5 hr.	45	Misaligned
2	1 mil + Foil	Yes	2120°F/6 ksi/1 hr.	55	Trailing Edge Melt
3	0.2 mil + Foil	Yes	2035°F/5.2 ksi/1 hr.	44	Good
4	0.5 mil	No	2050°F/7.5 ksi/1 hr.	24	Good, Some Airfoil Crack
5	0.5 mil	No	2140°F/5.8 ksi/2 hr.	36	Trailing Edge Melt
6	0.2 mil	No	2100°F/8 ksi/2 hr.	18	OK
7	0.2 mil	No	2075°F/9 ksi/2 hr.	13	OK
8	0.2 mil	No	2100°F/9 ksi/2 hr.	20	OK - Tip Misaligned
9	0.2 mil + Foil	No	2180°F/9 ksi/2 hr.	26	OK - Tip Misaligned
10	0.2 mil	No	2175°F/9 ksi/2 hr.	15	Inadequate Upset
11	0.2 mil + Foil	No	2160°F/9 ksi/2 hr.	13	OK - Base Misaligned
12	0.2 mil + Foil	No	2150°F/9 ksi/2 hr.	11	Trailing Edge Melt
13	0.5 mil	No	2075°F/9 ksi/2 hr.	16	Misaligned

*One measurement on root exterior. Blades 1-5 are not representative due to locally deviant dies.

**Foil is 4.5 mil Hastelloy-X with 0.1 mil Ni-20Co interlayer on each side.

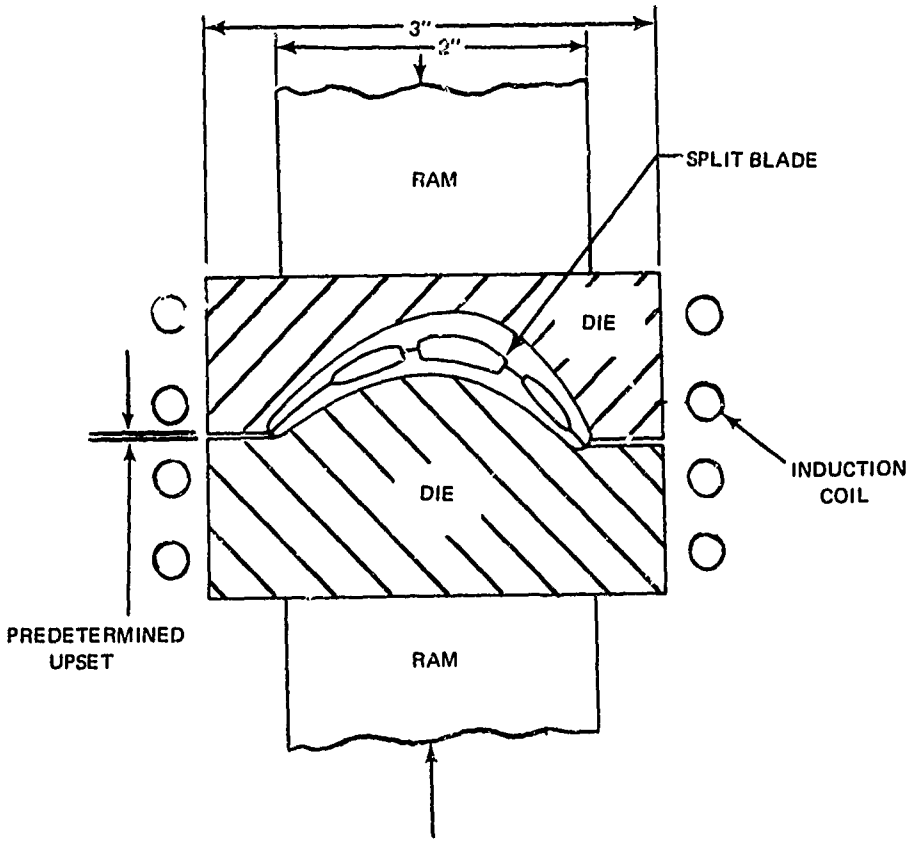

Figure 67 Schematic Diagram of Set-Up for Diffusion Welding Split Blades

Twenty mils upset was designed into the ceramic dies. Elaborate measurements were not taken on the dies or parts to determine actual local upset. After the welded blades were removed from the die the center of root section was measured for overall upset. This upset averaged 17 mils for blades (SB7-13) made with the better dies. A typical part is shown in Figure 68 after removal from the welding die. Because cast surfaces do not have sharp corners, notches were inevitable at the joint edges. These were removed by blending (typically removal of up to .030 inches) from the leading and trailing edges. Blended parts are shown in Figures 69 and 70.

C. INSPECTION OF WELDED BLADES

After welding and polishing, split blades were inspected visually, with fluorescent penetrant, and using ultrasonic contact through transmission. The ultrasonic method entailed the use of 5 MHz conical tipped transducers on opposite sides of the part. Transmission of sound indicated continuity; the absence of it indicated a gap. After non-destructive inspection, selected parts were sectioned and examined visually for joint continuity as shown in Figures 71 and 72. The correlation of these results with the non-destructive inspection method is indicated in Figure 73. Firm conclusions cannot be drawn as to the effectiveness of the limited inspection, especially in view of the subjectivity and narrow localization of the metallographic correlation.

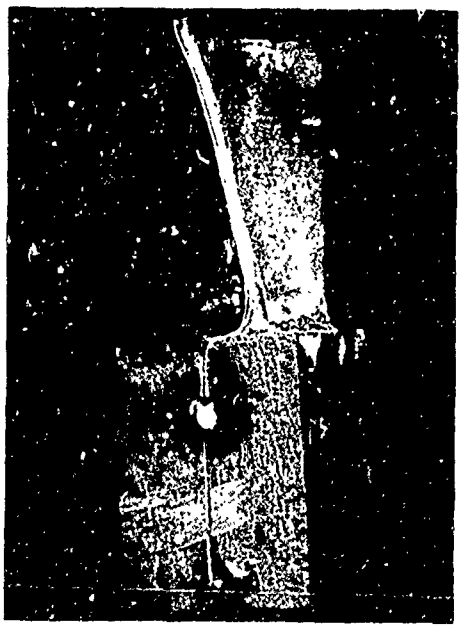

SB7 0.2 MIL Ni-20Co

Figure 68 Diffusion Welded Split Blade After Removal From Welding Die, Showing Tack Welds Used to Align Parts

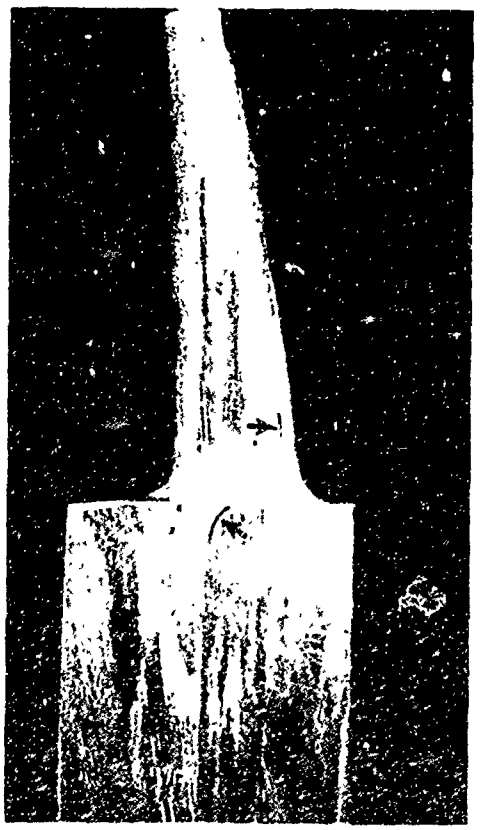

SB6 0.2 MIL Ni-20Co

Figure 69 Diffusion Welded Blade Etched to Show 0.2 Mil Ni-20Co Joint Defects Indicated By Arrows

Figure 70 Three Diffusion Welded PWA 1422 Split Blades

Figure 71 Tip End of Etched Diffusion Welded Blade Showing Lack of Fit at Trailing Edge. A 0.5 Mil Ni-20Co Interlayer Was Used.

Figure 72 Midsection of Diffusion Welded Blade Made With a 4 Mil Foil Intermediary and 0.2 Mil Ni-20Co Interlayer. Although Misaligned, Note How Design of Left Two Joints Contrasts With That of Right Two in Achieving a Joint.

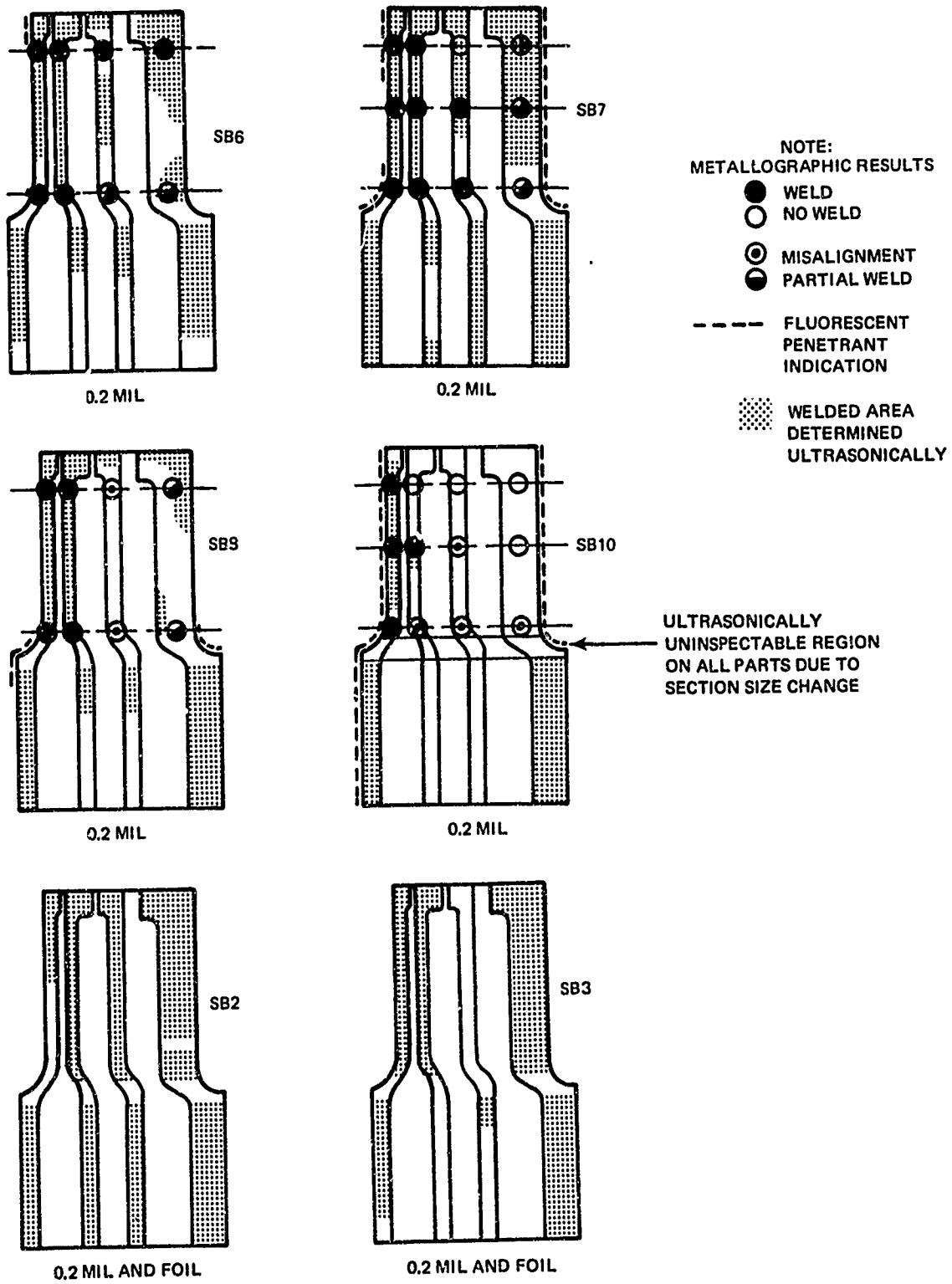

Figure 73 Correlation of Results of Non-Destructive Testing With Metallographically Observed Welding

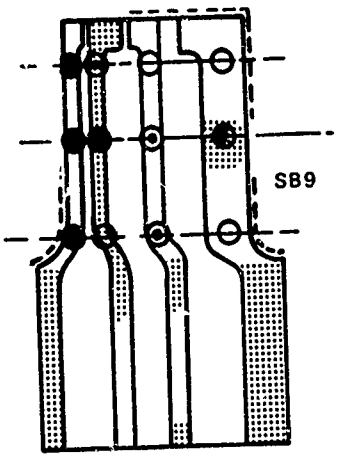

0.2 MIL + FOIL

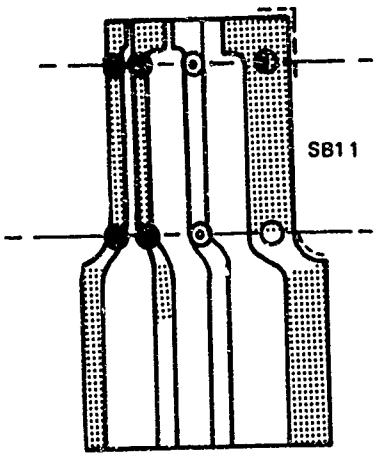

0.2 MIL + FOIL

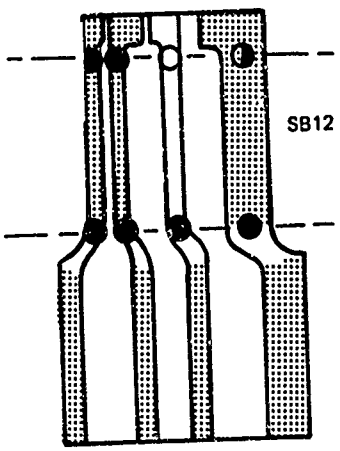

0.2 MIL + FOIL

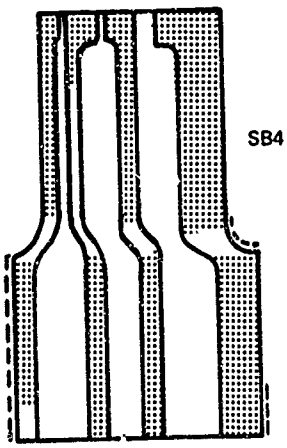

0.5 MIL

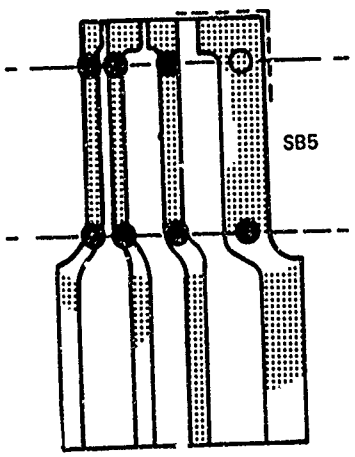

0.5 MIL

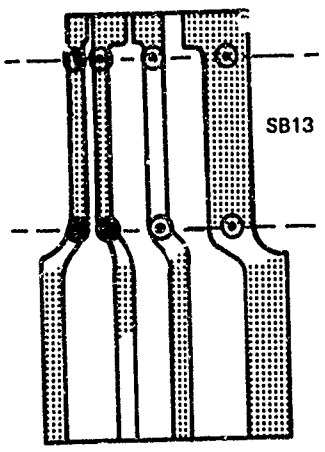

o.5 MIL

Figure 73 (Cont'd) Correlation of Results of Non-Destructive Testing With Metallographically Observed Welding

The predominant causes of defects were two-fold: (1) lack of contact at the trailing edge due to inadequate upset, and (2) misalignment of the ribs due to shifting. Subsidiary defects were localized trailing edge melting caused by induction heating and cracking of the parts along the longitudinal grain boundaries due to excess deformation. Typical defective parts are shown in Figure 74.

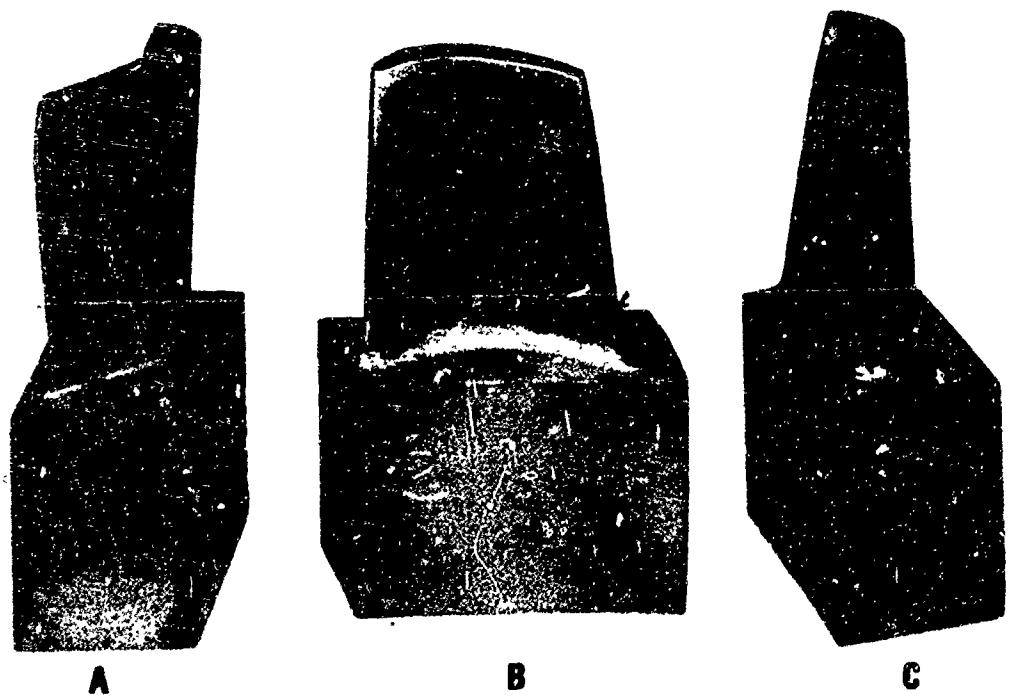

Figure 74 Defects in Diffusion Welded Split Blades: Lack of Fit (A and C) and Localized Melting at Trailing Edge (B).

The trailing edge was consistently defective, whereas the leading edge was nearly consistently joined. This can be attributed to the thicker leading edge section size, lack of warpage, and favorable joint design. Furthermore, the overall thinness of the trailing edge makes it evident that the die deviations here are much more critical. It seems apparent that the inadequate upset in the trailing edge could have been overcome through modification of the die.

Shifting of the parts relative to one another is also a deviation that can be overcome mechanically through part or die design. In retrospect, some simple method of keying the parts to one another surely would have yielded considerably better joint continuities. Conjunctively better joint design also may have overcome the effects of slight misalignment (See Figure 72). The contoured surface of the joint was determined by the design of the parting line in the

original wax pattern die. Small shifts in alignment produced substantial gaps measured in the direction of the upset (e.g., perpendicular to the part axis). This was particularly noticeable in the transition region from the root to the airfoil section. These aspects point up the obvious necessity of designing the part for diffusion welding.

If precision metal dies had been used, or further refinement of the induction heating process made, localized temperature variations which caused melting would have been overcome. The attractiveness of the ceramic dies lay in the economic precision fabrication. Cracking due to thermal shock would probably have been overcome by the choice of a silica based system of low expansion.

Cracking of the base metal generally occurred in those parts which had more severe misalignment but it does indicate a major problem-area when diffusion welding parts of inherent low elongation. Naturally, the amount of upset and consequent likelihood of cracking are related to the part design, lack of fit, and joining system. In this program 20 mils upset was arbitrarily chosen to attempt to ensure that there would be some upset everywhere. Based on the results of welding of the 1 x 1 inch ribbed and 1 x 3 inch shear specimens, adequate upset to achieve a good weld need not include base metal cracking. To achieve this when welding a blade requires careful design of the welding dies. The obvious advantage of using dies for welding in general is that all parts meet precise external dimension requirements.

D. THERMAL FATIGUE TESTING

Welded split blade airfoil sections were subjected to fluidized bed cycling between 1800°F and 70°F in a manner similar to that described previously for the thermal fatigue test specimens. The airfoil section was separated from the massive root block. Prior to testing, fluorescent penetrant joint discontinuities were recorded. These were especially prevalent at the trailing edge, and reflected the non-destructive inspection results for the specific blade sections shown in Figure 73. After 275 cycles, the airfoils were examined visually and with fluorescent penetrant.

The results, summarized in Table XIX, show that cracks tended to propagate in the marginally welded trailing edge region. Significantly, there was no indication of failure in well-joined areas such as the leading edge. The results reflect the varied quality of the split blade diffusion welds due to parameter variation, light outgassing from the ceramic welding dies, and inadequate upset at the trailing edge. While there was no measure of the nature or extent of strain at the joint, the total parting at the trailing edge of some of the poorer specimens showed the test was effective. However, as a measure of intrinsic weld strength the thermal fatigue tests in the prior Mechanical Properties Section were undoubtedly more meaningful. Based on those results and the performance of airfoil regions other than the trailing edge, it is likely that fully welded blade sections would have successfully passed thermal fatigue testing.

TABLE XIX

RESULTS OF FLUIDIZED BED THERMAL CYCLING BETWEEN 1800°F AND 70°F
(Airfoil Sections of Ni-20% Cobalt Diffusion Welded PWA 1422 Split Blades)

		Visual and Fluorescent Penetrant Indications	
Blade	Interlayer-Mils	Starting	After 275 Cycles
8	0.2	Substantial trailing edge porosity	Trailing edge separation
6	0.2	Substantial trailing edge prorsity	Partial trailing edge separation
5	0.5	Trailing edge partially welded	Minor propagation
13	0.5	Moderate trailing edge indications	Trailing edge separation
11	0.2 + foil	Major trailing edge indications	Trailing edge propagation at 190 cycles
12	0.2 + foil	Minor trailing edge indications	Some trailing edge propagation

E. CONCLUSIONS

Comparison of the three joining system variations used for welding the split blades is generally in conformance with previous observations. On the as-cast surfaces, at any given point where upset was marginal, the 0.5 mil interlayer gave a sounder (void-free) joint when compared to the 0.2 mil interlayer. Due to the limited number of tests and other variables previously described, no firm conclusions can be reached on the merits of using foil intermediaries. Due to the contoured shape of the joint, placement of the foil without buckling was difficult. Segmenting of the foil into two pieces overcame most buckling but the obvious future recourse would be pre-forming. It would seem implicit that foil intermediaries will be advantageous provided they are used with a properly designed joint. Naturally, to achieve better properties the composition of Foil B would have to be improved upon.

The results, based on the limited effort, indicate that it is feasible to fabricate airfoils by joining split blade halves. To construct parts in a reproducible manner meeting the requirements of hollow engine parts, considerable manufacturing development is required in the areas suggested above. Additional metallurgical development will be required if foil intermediaries are to be used, and it would be desirable to further evaluate and refine properties if interlayers between 0.2 and 0.5 mils are to be used.

VII
CONCLUSIONS AND RECOMMENDATIONS

A. CONCLUSIONS

- The nickel-cobalt interlayer system was effective in producing metallographically homogeneous joints in directionally solidified PWA 1422 nickel superalloy.
- Joints were relatively insensitive to parameter variation, but interlayer composition became more critical as thickness increased. Nickel-20 percent cobalt was the most satisfactory composition.
- Joints made with interlayers 0.2 mil thick had good tensile, stress rupture, and thermal fatigue properties compared to the base metal.
- Joints made with interlayers 0.5 mils thick were metallographically homogeneous but had lower properties than thinner interlayers.
- Joints made with soft alloy foil intermediaries had good accommodation to lack of fit in the joint, but joint properties were reduced by the composition of the foil.
- Controlled quaternary alloy platings could be made by the dispersion plating technique, however, the inherent tendency to entrap electrolyte in the deposited material made them unsatisfactory as interlayers.
- Variation in upset in diffusion welded specimens was due to the intrinsic variability in creep properties of cast superalloys near their incipient melting point.
- Mechanical interaction of specimens with dissimilar metal dies can result in fracture of the diffusion weld from thermal stresses at the completion of the welding cycle.
- Nickel-Cobalt diffusion welds can be made between as-cast surfaces provided preparation removes residual oxides and does not introduce sandblast particles.
- Hollow blades can be fabricated by using nickel-cobalt interlayers and foil intermediaries to join as-cast split blade halves with ceramic dies.
- Lack of weld, inadequate upset, and misalignment of faying surfaces observed in the fabricated blades were due to die and joint design problems, the resolution of which was beyond the scope of this program.

B. RECOMMENDATIONS

- Develop design and manufacturing technology to reproducibly join split airfoils. This would include design of airfoils specifically for diffusion welding with the aim of avoiding unfavorable joint configurations and, evaluation of alternate methods of forming blade halves and dies in an accurate and reproducible manner.

- Extensively evaluate the system interaction between metallurgical-joining, design, and manufacturing processes. This would include consideration of improved performance intermediaries and varying thickness interlayers as they were applicable, together with joining systems requiring less deformation.

- Evaluate actual airfoils with particular attention to the effects of diffusion welding on component performance.

APPENDIX

TABLE A-I

SUMMARY OF DIFFUSION WELDS ON 1-X 1 RIBBED SAMPLES WITH ELECTROPLATED INTERLAYERS OR NO INTERLAYER

Sample No.	Interlayer Composition	Interlayer Thickness mils/side	Temp. °F	Time Hrs.	Pressure ksi	Upset* in.	Comments on Joint Microstructure
24	A	–	2200	1	0.50	.002	Planar interface; intermetallic phases
153[a]	A	–	2130[b]	2	0.50	.006	Extreme lack of fit; planar interface
156[a]	A	–	2120[c]	4	0.75	.0095	Extreme lack of fit; planar interface
33	B	.1	2210	1	0.50	.005	
113	B	.2	2225	1	1.00	.024	Excess γ'; no contamination
121	B	.2	2130	1	1.00	.010	Excess γ'
23	B	.3	2200	1	0.50	.007	Excess γ'
8	C	.07	2200	1	2.2	.030	Homogeneous, severe cracking in channel
11	C	.07	2100	1	1.3	.011	Homogeneous
16	C	.07	2200	1	0.50	.002	Homogeneous; planar; little grain growth
29	C	.07	2190	1	0.50	.004	Excess γ'
46	C	.2	2195	1	0.75	.004	Excess γ'
50	C	.2	2210	1	1.0	.019	Excess γ'
68	C	.2	2115	1	1.0	.004	Notched; cracked on heat treat; evidence of contamination
35	C	.3	2200	1	0.5	.002	Excess γ'; contamination
38	C	.3	2180	1	0.72	.008	Homogeneous; contamination
80	C	.3	2220	1	1.0	.006	
83	C	.3	2180	1	1.0	.008	Chem-milled surfaces, many unwelded areas, severe contamination
84[a]	C	.3	2205	1	1.0	.028	Some unbonds; contamination
54	C	.3	2185	1	1.0	.006	Excess γ'
74	C	.3	2220	1	1.0	.011	Excess γ'
85	C	.5	2190	1	1.0	.020	γ' depletion
60	C	.5	2190	1	1.0	.006	Depleted
65	C	.5	2140	1	1.0	.002	Contamination
77	C	.5	2200	1	1.0	.007	Porosity; depleted.
63	C	.8	2200	1	1.0	.013	Depleted
71	C	.8	2200	1	1.0	.017	Porosity; depleted.

Note: See page 111 for explanatory notes.

TABLE A-I (Cont'd)

Sample No.	Interlayer Composition	Interlayer Thickness mils/side	Temp. °F	Time Hrs.	Pressure ksi	Upset* in.	Comments on Joint Microstructure
9	D	.07	2200	1	1.55	.021	Homogeneous
12	D	.07	2170	1	1.3	.015	Homogeneous; good grain growth
14	D	.07	2050	1	0.5	.004	Homogeneous; little grain growth
126	D	.2	2185[d]	2	0.5	.009	Homogeneous; trace of contamination
128	D	.2	2175[d]	2	0.5	.018	Excess γ'; no apparent contamination
139	D	.2	2160[e]	2	0.5	.007	Excess γ'; trace of contamination
167	D	.2	2160[f]	2	1.0	.003	Lapped surfaces; slight heterogeneity; trace of contamination; several PM cracks
141[a]	D	.5	2160[c]	2	0.5	.007	Several areas of lack of fit; slight PM cracking (homogeneous)
5	E	.07	2170	1	2.3	.014	Homogeneous
10	E	.07	2200	1	1.3	.007	Homogeneous
13	E	.07	2170	1	1.3	.004	Homogeneous; little grain growth
15	E	.07	2140	1	0.5	.005	Homogeneous; areas of good grain growth
28	E	.07	2160	1	0.5	.003	Homogeneous; contaminated
30	E	.07	2200	4	0.5	.004	Homogeneous
112	E	.1	2190	1	1.0	.007	Homogeneous; no apparent contamination
123	E	.1	2175	1	1.0	.002	Slightly cracked
137	E	.1	2140[e]	2	0.5	.004	Excess γ'; slightly cracked
20	E	.2	2170	1	0.3	.002	Depleted; contaminated
47	E	.2	2220	1	0.75	.006	Homogeneous; slight contamination
51	E	.2	2195	1	1.0	.006	Slight heterogeneity; contaminated
69	E	.2	2195	1	1.0	.005	Slight heterogeneity; contaminated
90	E	.2	2200	1	1.0	.003	Severe contamination due to unremoved plating smut
91	E	.2	2200	1	1.0	.005	Slight contamination; notched at periphery
92	E	.2	2190	1	1.0	.001	Severe cracking
93	E	.2	2200	1	1.0	.003	Severe cracking
98	E	.2	2240	1	1.0	.008	Contaminated due to unremoved plating smut; slight heterogeneity
99	E	.2	2180	1	1.0	.004	Heterogeneous; slight cracking
100	E	.2	2190	1	1.0	.007	Contaminated; no cracks

TABLE A-I (Cont'd)

Sample No.	Interlayer Composition	Interlayer Thickness mils/side	Temp. °F	Time Hrs.	Pressure ksi	Upset* in.	Comments on Joint Microstructure
101	E	.2	2200	1	0.5	.002	Cracked; contaminated
103	E	.2	2200	1	2.0	.015	No PM cracks
104	E	.2	2210	1	1.5	.015	No PM cracks; substantial contamination and heterogeneity
106	E	.2	2200	1	1.0	.009	Homogeneous; slight cracking from edge notch
107	E	.2	2200	1	1.0	.008	DS material; incipient melted
108	E	.2	2200	2	0.5	.008	No porosity or cracking; slight heterogeneity
109	E	.2	2190	2	0.5	.005	DS material; no cracks, contamination, or incipient melting
110	E	.2	2190	2	0.5	.004	Slight crack from notch; porosity; slight heterogeneity; contaminated
111	E	.2	2200	1	1.5	--	Contaminated; severe edge notching
114	E	.2	2225	1	1.0	.012	Contaminated; slightly depleted
122	E	.2	2195	1	1.0	.008	Slight contamination
124	E	.2	2200	1	1.0	.001	Contaminated
125	E	.2	2170[d]	2	0.5	.006	Contaminated
127	E	.2	2195[d]	2	0.5	.007	Thin ribbed sample; contaminated; severe PM cracking
129	E	.2	2225[d]	2	0.5	.007	Thin ribbed sample; contaminated; slight depletion; PM cracking
130	E	.2	2160[d]	2	0.5	.017	DS material; contaminated; slightly depleted
131[a]	E	.2	2165[e]	2	0.5	.012	Contaminated; slight heterogeneity
138	E	.2	2200[e]	2	0.5	.006	DS material; slight contamination
142[a]	E	.2	2120[g]	2	0.5	.004	Severe lack of fit; contaminated; slight PM cracking
150	E	.2	2155[e]	1	1.0	.003	Heterogeneous; slight contamination
151	E	.2	2190[e]	1	1.0	.009	Heterogeneous; slight contamination
152	E	.2	2170[e]	1	1.0	.009	Heterogeneous; slight contamination
162[a]	E	.2	2180	2	0.5	.007	DS material; poor edges; many voids
36	E	.3	2240	1	0.5	.010	Contaminated; depleted
39	E	.3	2240	1	0.7	.016	Slight depletion
55	E	.3	2180	1	1.0	.005	Contaminated; depleted; porosity
75	E	.3	2200	1	1.0	.009	Slightly depleted
81	E	.3	2190	1	1.0	.004	
161	E	.3	2150[h]	2	0.5	.001	Thin to std. web
164	E	.3	2165[h]	2	0.5	--	Thin to std. web; bad edges; many voids

TABLE A-I (Cont'd)

Sample No.	Interlayer Composition	Interlayer Thickness mils/side	Temp. °F	Time Hrs.	Pressure ksi	Upset* in.	Comments on Joint Microstructure
165	E	.3	2135[f]	2	1.0	.003	Thin to std. web; few voids; poor edges
168	E	.3	2120[f]	2	1.0	.001	Thin rib pair; poor edges; poor bond
61	E	.5	2215	1	1.0	.012	Cracked; depleted
67	E	.5	2200	1	1.0	.010	Contaminated; depleted; porosity
78	E	.5	2195	1	1.0	.008	Contaminated; depleted; porosity
64	E	.8	2185	1	1.0	.005	Depleted
72	E	.8	2185	1	1.0	.005	Depleted
17	F	.07	2200+				Overtemp. due to T/C failure
21	F	.07	2200	1	0.3	.002	Homogeneous; planar interface
105	F	.1	2200	1	1.0	.010	Contaminated; slight heterogeneity
144	F	.2	2170	1	1.0	.013	No visible contamination
145	F	.2	2200	1	1.0	.012	No visible contamination
146	F	.2	2130	1	1.0	.001	No visible contamination; edge notches
18	G	.07	2200+				Overtemp. due to T/C failure
22	G	.07	2190	1	0.3	.001	Homogeneous; planar interface; little grain growth
31	G	.07	2160	4	0.5	.001	Slight contamination
48	G	.2	2175	1	0.75	.005	Homogeneous; contaminated
70	G	.2	2190	1	1.0	.006	Slight heterogeneity; contaminated
37	G	.3	2190	1	0.5	.005	Homogeneous; contaminated
40	G	.3	2195	1	0.7	.006	Slight heterogeneity; slight depletion
56	G	.3	2210	1	1.0	.011	Slight heterogeneity; contaminated
76	G	.3	2190	1	1.0	.007	Slight depletion
82	G	.3	2230	1	1.0	.016	
62	G	.5	2150	1	1.0	.005	Contaminated; depleted
66	G	.5	2215	1	1.0	.008	Cracked; no notch; depleted
79	G	.5	2210	1	1.0	.014	Depleted; porosity and contamination in joint
73	G	.8	2170	1	1.0	.003	

TABLE A-I (Cont'd)

Sample No.	Interlayer Composition	Interlayer Thickness mils/side	Temp. °F	Time Hrs.	Pressure ksi	Upset* in.	Comments on Joint Microstructure
6	H	.07	2200	1	2.1	.025	Homogeneous
19	H	.07	2200+				Overtemperature due to T/C failure

*Upset is the average change in height of the internal channel.

PM - Parent Metal
A - None
B - Pure Ni
C - Ni-15% Co
D - Ni-20% Co
E - Ni-25% Co
F - Ni-30% Co
G - Ni-35% Co
H - Ni-40% Co

a - As cast mating surfaces
b - First 5 minutes at 2000°F/1.5ksi
c - First 5 minutes at 2000°F/2ksi
d - First 15 minutes at 2.0 ksi
e - First 5 minutes at 1.5 ksi
f - First 5 minutes at 2.0 ksi
g - First 5 minutes at 2050°F/2.0 ksi
h - First 5 minutes at 2100°F/1.5 ksi

TABLE A-II

SUMMARY OF DIFFUSION WELDS ON 1 X 1 RIBBED SAMPLES WITH DISPERSION PLATED INTERLAYERS

Sample No.	Interlayer Composition* % Co	% Cr	% W	Interlayer Thickness mils/side	Temp °F	Time Hr.	Pressure ksi	Upset in.	Comments on Joint Microstructure
7	28	9	21	.1	2200	1	2.1	.030	Slight heterogeneity
136	13	8	15	.1	2180[a]	5	0.5	.003	Notching; particles; homogeneous; slight BM cracking
148	13	8	15	.1	2195[b]	4	0.75	.012	Slight BM cracking
135	13	8	15	.3	2200[a]	5	0.5	.003	Notching; particles; homogeneous; slight cracking
143	13	8	15	.3	2165[c]	1.5	1.5	.004	Notching; particles at interface
147	13	8	15	.3	2155[b]	4	0.75	.010	Slight BM cracking
34	32	10	9	.5	2200	1	0.5	.004	Cracked
53	27	8	4	.5	2000/2200	1/1	1.4/0.75	.006	Cracked
58	27	8	4	.5	1950/2155	1/4	2.0/1.0	.010	Heterogeneous; particles at joint
42	21	4	13	.5	2200	1	0.75	.005	Cracked
52	21	4	13	.5	1800/2200	1/1	4.0/0.75	.003	Cracked
43	21	11	15	.5	2195	1	0.75	.004	Cracked
45	21	11	15	.5	2000/2200	1/1	1.4/0.75	.009	Cracked
87	27	8	4	.5	2230	4	1.0	.015	Depleted; particles at joint
88	21	11	15	.5	2215	4	1.0	.017	Depleted; particles at joint
89	21	4	13	.5	2190	4	1.0	.007	Slight cracking
96	21	11	15	.5	2180	4	1.0	.003	Depleted; particles at joint
97	27	8	4	.5	2180	4	1.0	.011	Depleted; particles at joint
134	13	8	15	.5	2130[a]	5	0.5	.002	Edge notches; particles; cracked
149	13	8	15	.5	2140[b]	4	0.75	.015	Slight BM cracking
157	13	8	15	.5	2180[b]	4	0.75	.011	As-cast, notches and cracks; depleted

a - First 5 minutes at 1.0 ksi
b - First 5 minutes at 2.0 ksi
c - First 30 minutes at 4.0 ksi

*Balance is nickel

TABLE A-III

SUMMARY OF DIFFUSION WELDS ON 1 X 1 RIBBED SAMPLES WITH FOIL INTERLAYERS

Sample No.	Foil	Foil Thickness mils	Base Metal Plate mils	Temp °F	Time Hr.	Pressure ksi	Upset in.	Comments on Joint Microstructure
41	I	3.5	.07Ni-20Co	1900/2200	0.5/1.0	1.0/1.0	.009	
49	I	4.5	.07Ni-20Co	1820/2215	1/1	4.0/0.75	.006	
44	I	3.5	.07Ni-20Co	1990/2200	1/1	1.4/0.75	.009	Good weld; little contamination
57	I	4.5	0.1Ni-15Co	1890/2115	1/1	2.0/1.0	.006	
32	I	2.5	0.2Ni-25Co	2200	1	0.5	.010	Good weld; little contamination
132	I	2.5	0.2Ni-25Co	2175[a]	2	0.5		As-Cast surfaces; poor accommodation
26	II	3	.07Ni-30Co	2190	1	0.5	--	
27	II	2	.07Ni-30Co	2200	1	0.5	.004	
86	III	30	0.1Ni-35Co	1950	2	4	--	
25	IV	4	.07Ni-30Co	2140	1	0.5	--	
59	IV	4	0.1Ni-15Co	1880/2075	1/1	2.0/1.0	.004	
133	V	4.5	0.2Ni-25Co	2170[a]	2	0.5	.004	Homogeneous except for large γ' in foil
140	V	3.5	0.2Ni-25Co	2190[b]	2	0.5	.007	As-Cast surfaces; very good accommodation; homogeneous except for large γ'
155	VI	6	0.1Ni-15Co					Homogeneous; little γ' in foil; clean interfaces
154	VI	2	0.2Ni-20Co	2185[a]	2	0.5	.006	Crack at plating interface
163	VI	8	0.2Ni-25Co	2150[a]	2	0.5	.002	As-Cast surfaces; voids and contamination; poor appearance
166	VI	6.5	0.2Ni-25Co	2175[c]	2	1.0	.011	As-Cast surfaces; severe PM cracking; contaminated; good edges and weld.
158	VI	8	0.5Ni-20Co	2170[b]	4	0.75	.027	As-Cast surfaces; fair accommodation; slightly depleted

I - Foil A: no plate
II - Foil A: 0.1Ni-30Co plate
III - PWA 1422: no plate
IV - PWA 1422: 0.1Ni-30Co
V - Foil B: no plate
VI Foil B: 0.1Ni-25Co

a - First 5 minutes at 1.5 ksi
b - First 5 minutes at 2.0 ksi/2150°F
c - First 5 minutes at 2.0 ksi